„Dunarea de Jos” University of Galați
Doctoral School for Mechanical and Industrial Engineering

DOCTORAL THESIS

EXTENDED ABSTRACT

THE BEHAVIOUR OF MULTIAXIAL GLASS FIBRE COMPOSITES UNDER LOW-VELOCITY IMPACT

PhD Student Iulian PĂDURARU

Scientific Coordinator
professor eng. Lorena DELEANU, PhD

Series I 6: Mechanical Engineering No. 69
Galati
2023

„Dunărea de Jos" University of Galați
School for Mechanical and Industrial Engineering

DOCTORAL THESIS

EXTENDED ABSTRACT

THE BEHAVIOUR OF MULTIAXIAL GLASS FIBRE COMPOSITES UNDER LOW VELOCITY IMPACT

PhD Student Iulian Păduraru

President	**Prof. phys. Luminița MORARU, PhD** "Dunărea de Jos" University of Galati
Scientific Coordinator	**Prof. eng. Lorena DELEANU, PhD** "Dunărea de Jos" University of Galati
Scientific referees	**Prof. eng. Anton HADĂR, PhD** "Politehnica" University of Bucharest
	Prof. eng. Simion HARAGÂȘ, PhD Technical University of Cluj-Napoca
	Prof. phys. Gabriel MURARIU, PhD "Dunărea de Jos" University of Galati

Series I 6: Mechanical Engineering No. 69

Galați
2023

The series of doctoral theses defended publicly in ”Dunărea de Jos” University of Galati, starting with October 1, 2013 are:

Field **ENGINEERING SCIENCES**

Series I 1:	**Biotechnologies**
Series I 2:	**Computers and Information Technology**
Series I 3:	**Electrical Engineering**
Series I 4:	**Industrial Engineering**
Series I 5:	**Material Engineering**
Series I 6:	**Mechanical Engineering**
Series I 7:	**Food Engineering**
Series I 8:	**Systems Engineering**
Series I 9:	**Engineering and Management in Agriculture and Rural Development**

Field **ECONOMICS**

Series E 1:	**Economy**
Series E 2:	**Management**

Field **HUMANITIES**

Series U 1:	**Philology-English**
Series U 2:	**Philology-Romanian**
Series U 3:	**History**
Series U 4:	**Philology-French**

Field **MATHEMATICS AND NATURE SCIENCES**

Series C:	**Chimistry**

ACKNOWLEDGEMENT

I would like to express my sincere thanks to those who supported and guided me during the elaboration of my PhD thesis.

When I started on this academic journey to complete my PhD thesis on "The behaviour of Multiaxial Glass Fibre Fabric Composites under Low -Velocity Impact", I could not have anticipated that I would have the privilege of working under the supervision of prof. eng. Lorena Deleanu, PhD. Today, at the end of this remarkable stage of my life, I would like to express my most sincere thanks.

In special, I want to express my gratitude for your constant support, wisdom and professional guidance. With your passion and dedication to the field of research, you have been able to inspire and guide me throughout the entire journey of this PhD thesis. With patience and confidence, you understood the direction I wanted to go with this study and you were always there to offer me invaluable advice and motivational encouragement. The successful completion of this thesis in one year is mostly due to your support, and for that I am deeply grateful.

I would also like to express my sincere thanks to the distinguished official referees prof. eng. Anton Hadăr, PhD, prof.eng. Simion Haragâș, PhD, prof. phys. Gabriel Murariu, PhD, prof. phys. Luminița Moraru, PhD as well as all the members of the mentoring committee, whose expertise and advice contributed significantly to the development of this PhD thesis: associate prof. Constantin Georgescu, PhD and associate prof. Daniel Ganea, PhD.

I would like to mention the collaboration and support offered by the Polytechnic ''Politehnica''University of Bucharest through the collaboration with lecturer eng. Horia Petrescu, PhD, the National Institute for Aerospace Research "Elie Carafoli" - INCAS Bucharest and INAS Craiova for their recommendations on modelling in Ansys Explicit Dynamics. Without the support and resources provided by these educational and research institutions, this study would not have been possible.

I would also like to express my sincere thanks to eng. George Ghiocel Ojoc, PhD, for his continuous help and support throughout the project. Our collaboration was essential to the success of this research and his presence was an important source of inspiration. Thank you to lecturer phys. Alina Cantaragiu Ceoromila for the outstanding images obtained with the scanning electron microscope of "Dunărea Jos" University.

I cannot end without mentioning the support of my family, who have been with me throughout this academic journey and have encouraged me to keep going through the difficult times.

I hope that the results of this study will make significant contributions to the field of composites research.

Galati,
September 2023

Iulian Păduraru

Cuprins

Acknowledgement *5*
Summary *6*

Chapter 1 Recent trends in the application and testing of low velocity impact stressed glass fibre composites ***7***
1.1 Composites for low velocity impact..... *7*
1.2. Classification of fibres and fabric types..... *8*
1.3. Aspects of low speed impact glass fibre composites..... *9*
1.4. Applications of glass fibre composites *11*
1.5. Conclusions on glass fibre composites..... *11*
1.6. Research directions..... *12*

Chapter 2. Thesis structure ***13***

Chapter 3. Simulation of the behaviour of a composite at low velocity impact ***14***
Introduction..... ***14***
3.2. Concepts of constitutive material models..... *14*
3.3. Key issues for simulation in Ansys Explicit Dynamics..... *14*
3.4. The layered panel impact model - hemispherical impactor..... *15*
3.5. Simulation results and discussion..... *17*
3.5.1. Equivalent stress distribution analysis on the two-layer panel *17*
3.5.2. Comparative analysis of main wire failure using simulation images and equivalent stress distribution for the two impactors used in the experimental tests *18*
3.6. Conclusions on the evaluation of the low velocity impact simulation *21*
3.7 Conclusions on impact simulation results.....*30*

Chapter 4. Manufacturing process of multiaxial glass fibre composites..... ***31***
4.1. Test plan for testing quadriaxial fabric composites with epoxy resin..... *31*
4.2. Materials used in composite testing *31*
4.2.1. Glass fibre fabric *31*
4.2.2. Epoxy resin matrix *33*
4.3. Laboratory technology for panel production *34*
4.4. Characterisation of the developed panels *36*
4.5. Test procedures and test machine *36*
4.6. Conclusions on panel production..... *38*

Chapter 5. Interpretation of experimental results and investigation of failure mechanisms..... ***39***
5.1. Parameters measured in the low speed impact test.....*39*
5.2. Experimental results on INSTRON CEAST 9340 impact machine..... *41*
5.2.1. Influence of number of layers on impact parameters *41*
5.2.2. Influence of impact energy and impact velocity on impact parameters *42*
5.3. Investigation of failure mechanisms..... *44*
5.4. Summary of experimental results and conclusions *49*
Chapter 6. Personal contributions and conclusions *53*
6.1. Importance of the thesis..... *53*
6.2. Final conclusions on the low velocity impact strength of the author's panels *53*
6.3.Personal contributions..... *56*
6.4. Research perspectives.....*57*

List of the author's scientific works..... *58*
Bibliography *60*

Cuprins

Mulțumiri *5*
Cuprins *6*
Capitolul 1 Tendințe recente în aplicarea și testarea compozitelor cu fibră de sticlă solicitate la impact de viteză mică *7*
1.1. Compozite destinate impactului de viteză mică *7*
1.2. Clasificarea fibrelor și tipuri de țesături *8*
1.3. Aspecte ale compozitelor cu fibră de sticlă la impact de viteză mică *9*
1.4. Aplicații ale compozitelor cu fibre de sticlă *11*
1.5. Concluzii privind compozitele pe bază de fibră de sticlă *11*
1.6. Direcții de cercetare *12*
Capitolul 2. Structura tezei ***13***
Capitolul 3. Simularea comportării unui compozit la impact de viteză mică ..... ***.14***
3.1. Introducere *14*
3.2. Conceptele de modele constitutive ale materialelor *14*
3.3. Aspecte-cheie pentru simularea în Ansys Explicit Dynamics *14*
3.4. Modelul impactului panou stratificat – impactor semisferic *15*
3.5. Rezultate ale simulării și discuții *17*
3.5.1. Analiza distribuției de tensiuni echivalente pe panoul cu două straturi *17*
3.5.2. Analiza comparativă a cedării firelor principale cu ajutorul imaginilor din simulare și a distribuției de tensiuni echivalente pentru cele două impactoare folosite în testele experimentale *18*
3.6. Concluzii privind evaluarea simulării impactului de viteză mică *21*
3.7 Concluzii asupra rezultatelor simulării impactului…… *30*
Capitolul 4. Procesul de fabricație al compozitelor multiaxiale din fibră de sticlă ***31***
4.1. Planul de teste destinat încercării compozitelor cu țesătură cuadriaxială și rășină epoxidică *31*
4.2. Materialele utilizate în realizarea probelor de compozit *31*
4.2.1. Țesătura de fibre de sticlă *31*
4.2.2. Matricea de rășină epoxidică *33*
4.3. Tehnologia de laborator pentru obținerea de panouri..... ..... *34*
4.4. Caracterizarea panourilor elaborate *36*
4.5. Proceduri de testare și mașina de testare *36*
4.6. Concluzii privind realizarea panourilor *38*
Capitolul 5. Interpretarea rezultatelor obținute experimental și investigația mecanismelor de cedare ***39***
5.1. Parametrii măsurați la testul de impact la viteză mică ..... *.....39*
5.2. Rezultate experimentale pe mașina de impact INSTRON CEAST 9340 ..... *41*
5.2.1. Influența numărului de straturi asupra parametrilor impactului *41*
5.2.2. Influența energiei și a vitezei de impact asupra parametrilor impactului *42*
5.3. Investigarea mecanismelor de cedare *44*
5.4. Sinteza rezultatelor experimentale și concluzii *49*
Capitolul 6. Contribuții personale și concluzii ***53***
6.1. Importanța tezei *53*
6.2. Concluzii finale asupra rezistenței la impact de viteză mică a panourilor realizate de autor *53*
6.3. Contribuții personale *56*
6.4. Perspective de cercetare *57*

Lista lucrărilor științifice ale autorului *58*
Bibliografie *60*

Chapter 1. Recent Trends in the Application and Testing of Glass Fibre Composites under Low-Velocity Impact

1.1. Composites Intended for Low-Velocity Impact

Composite materials are widely used in various industries due to their outstanding advantages such as high stiffness and relatively low weight. These innovative materials offer a unique combination of properties that make them the most preferred choice in a variety of applications [13]. Composites are materials obtained by combining two or more component materials to create new materials with improved properties. In low-velocity impact applications, such as automotive bumpers and sports equipment, composites provide additional advantages over traditional materials like metallic alloys or plastics.

Low-velocity impact typically ranges between 1 m/s and 10 m/s, depending on the impacting mass and the stiffness of the target. When the impact velocity is below 5 m/s, the response is primarily controlled by the impacting element rather than the impact velocity itself. Damages caused by low-velocity impact often remain undetectable through visual inspection, thereby compromising structural stability. Common failure modes of long-fibre reinforced composites include matrix cracking, delamination and fibre breakage. Various experimental observations and numerical models have been developed to comprehend composite responses to this type of impact [38].

The damages resulting from an impact depend on numerous factors, such as the shape of the impacting element, impact velocity and the layer architecture of a composite material [9]. Furthermore, fibre-reinforced composite materials exhibit various modes of failure, including fibre breakage, matrix cracking, delamination, exfoliation etc. These distinct modes of failure manifest simultaneously under impact loading [26]. During the impact, damages within laminates propagate around the impact area [44], diminishing the stiffness and strength of the composites. The majority of the impactor's kinetic energy is absorbed in the elastic and plastic deformation of the target material prior to perforation (break of the components: layers, matrix, fibres, yarns), attributed to the target rigidity.

Hosseini et al. [21] discussed the development of a hybrid composite material comprising E-glass fibre, basalt fibre and graphene nanoparticles for aviation industry applications. The addition of graphene significantly enhances the material strength and impact resistance while simultaneously reducing its weight. Impact testing was conducted with an impactor mass of 1.926 kg, and the impacting element had a total weight of 9.34 kg, featuring a hemi-spherical shape, with a diameter of 12.7 mm. The impact test demonstrated improved material strength with the inclusion of 2% graphene. Specimen testing was also carried out at a impact velocities of 1.5 m/s and 3 m/s, at room temperature. The study indicates that the addition of graphene nanoparticles enhances fibre-matrix bonding and limits the damage through microcracking.

The paper [49] discusses the use of glass fibres as ductile fibres in polymer-reinforced hybrid composites to enhance their impact resistance. The authors found that incorporating layers of glass fibres into the composites can significantly enhance their impact strength.

The study presented by Lei et al. [27] explores the impact resistance of carbon fibre twill weave laminates, glass fibre laminates and hybrid carbon/glass fibre laminates, subjected

to low-velocity impact. The authors also investigated the effects of incorporating glass fibres into woven carbon fibre laminates to enhance impact resistance. Prepreg glass fibre twill fabrics with a fibre content of 55% were used to manufacture glass fibre laminates with epoxy resin. The glass fibre-reinforced composite was cured by thermal treatment, at a temperature of 160°C and a pressure of 0.6 MPa, for a curing time of 70 minutes. Low-velocity impact tests were conducted using an Instron 9340 testing machine, following the ASTM D7136/D7136M-15 (Standard Test Method for Measuring the Damage Resistance of a Fibre-Reinforced Polymer Matrix Composite to a Drop-Weight Impact Event). A hemi-spherical impacting element with a diameter of 16 mm was utilized. The behaviour of the laminates under low-velocity impact was investigated through impact tests with incident energies ranging from 2.5 J to 30 J.

1.2. Classification of Fibres and Fabric Types

Reinforcements for composites can be long fibres, in various weaves or in unidirectional arrangement, particles, or whiskers (short fibres). The role of fibres in a composite structure is extremely important, as they bear a significant part of the applied load. Fibres can be made of glass, carbon, polymers, metallic alloys or ceramics. Thermosetting resins are suitable as matrix bases for advanced fibre-reinforced composites. Fibres are the main load-bearing constituents, providing strength and rigidity to the composite. The most commonly used fibres are glass, carbon, and polymer fibres, with aramid fibres being representative for ballistic impact resistant applications. Carbon fibres are extensively used in the aircraft industry and many structural applications due to its highest values of strength and stiffness. However, it is also the most brittle, with a strain at break of 0.5% to 2.4%. Glass fibres have lower strength and stiffness, but are less expensive than carbon fibres. The mechanical properties of aramid fibre are between those of carbon fibres and glass fibres.

Fibres can be classified into two categories [20]: synthetic fibres and natural fibres.

Glass fibres. Glass has a long history of use in various forms. As a structural material, glass was introduced in the 17th century and gained widespread popularity in the 20th century with advances in plain glass technology. Glass fibres were later developed as a substitute for metals, leading to their use in both commercial and military applications. The development of formulations with controlled properties and the ability to draw molten glass into continuous filaments through pultrusion processes opened the way for the use of glass fibres as reinforcement. This development has opened up a wide range of applications in the aerospace and high-performance structural industries. Today, glass continues to be used in many aerospace and commercial applications due to its high performance characteristics. The versatility and reliability of glass fibres as a structural material has made them a preferred choice in various industries.

For structural applications, the most commonly used glass product forms are fabrics, fibres, cables and unidirectional tapes, created by twisting the fibres. "E" Glass, initially designed for electrical applications, is the most versatile type of glass fibre in terms of application diversity. It offers a wide range of filament diameters, ranging from 3.5 μm to 13 μm, allowing the production of components with intricate, very thin shapes. On the other hand,

S-2 glass fibres are renowned for their high strength and are available in a single filament diameter.

Although woven rovings could be a form of textile product, they hold substantial importance in military applications. Moreover, there are other forms of glass products serving as complementary items for advanced structures, including chopped fibres and short fibres. Glass fibre composites exhibit high strength and stiffness, along with good resistance to corrosion and fatigue.

Another classification of various glass fibres used in impact applications is provided in [2] as follows. Glass fibres have been categorized based on their characteristics and specific uses in composite materials. There are several types of glass fibres, such as:

E-Glass: it is the most common and is used in a wide range of applications. It is known for its mechanical strength, corrosion resistance and chemical stability.

S-Glass: it is a type of glass fibres with superior properties as compared to E-Glass. It has higher tensile strength and is used in applications requiring exceptional performance, such as ballistic protection and impact resistance.

C-Glass: this glass fibre contains more calcium and possesses improved chemical and thermal properties. It is particularly used in industrial applications that involve corrosion resistance and thermal insulation.

A-Glass: it has a higher aluminium content and is primarily used in applications requiring high mechanical strength and low thermal conductivity.

D-Glass: it is used in special applications, such as fire protection. It possesses properties of high temperature resistance and flame resistance.

These types of glass fibres offer diverse options for composite materials, enabling the development of products tailored to specific needs, in various industries, such as constructions, automotive, aviation and defence.

To enhance the mechanical properties of composites, they are commonly reinforced with fabrics or semi-finished products containing unidirectional fibres, which are arranged parallel to the warp direction and the weft direction. The characteristics of these fabrics, whether woven or non-woven, involve factors, such as the fibre architecture (2D or 3D), fibre nature, number of filaments/fibres in a yarn, warp and weft yarn count per cm^2, specific density (density per unit area) and fabric thickness [7].

There are several types of weaves used in composite materials subjected to low-velocity impact. These weave types are employed in composites to achieve specific properties concerning impact resistance and overall material performance.

1.3. Specific Aspects of Glass Fibre Composites under Low-Velocity Impact

In composite structures, impact creates internal damages that often cannot be detected through visual inspection. This internal deterioration can lead to significant reduction in strength. Therefore, the effects of object impact on composite structures need to be understood, and appropriate measures must be taken in the design and manufacturing processes [1]. Concerns regarding the impact effect on the performance of composite structures have been a factor limiting the utilization of composite materials.

Impact energy, E_i and energy absorbed by the composite, E_a, are two important parameters for assessing the impact response and strength of composite structures. Impact energy is defined as the total amount of energy introduced into a composite material sample. *Absorbed energy* is the energy absorbed by the composite specimen through its internal changes (strains, cracks, breaks etc.) [3].

Low-velocity impacts can lead to hidden delamination in composite laminates, resulting in reduced stiffness and potential structural integrity issues over time. Impact damages, especially delamination, significantly diminish the compressive strength and fatigue resistance of composite structures. Consequently, extensive experimental and analytical investigations have focused on the low-velocity impact behaviour of glass fibre-reinforced laminates. Various studies have examined the impact behaviour of glass/epoxy resin laminates, considering factors such as fibre orientation, laminate thickness and temperature [43].

The response of composite materials to impact depends on the constituent materials, geometry, impact velocity, and mass and shape of the impacting element. This suggests that the type of fibre used in the composite material could play a crucial role in its impact response [24].

Authors Mathivanan et al. [33] conducted impact tests on composite laminates with an epoxy matrix reinforced with woven glass fibres, using an impact testing machine in accordance with standards. Impact tests were carried out to observe the type and extent of laminate damage for different thicknesses and impact velocities. As the impact energy increased, the specimens experienced one of two types of damages: either cracking from the laminate centre to the edge or significant damage characterized by a localized dent in the region directly contacting the impactor.

By overlaying force-displacement curves, changes in the material response to impact, at different velocities, can be observed. This technique allows for a comparative analysis of the force-displacement relationship and provides insights into the material behaviour under various impact conditions. By examining the overlaid curves (Fig.1.1), trends and patterns can be identified, revealing the material response to increasing impact velocities.

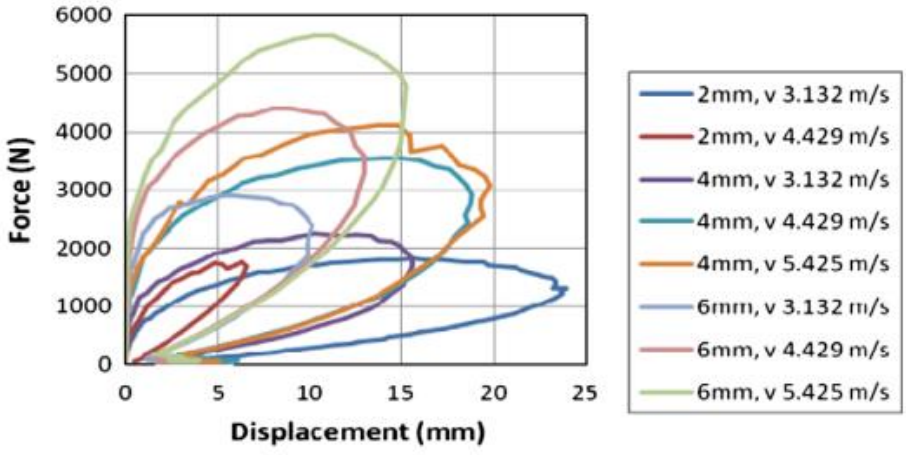

Fig. 1.1. Overlaying of curves force – displacement for different impact velocities and composite thicknesses [33]

1.4. Applications of Glass Fibre Composites

Fibre-reinforced composite materials find applications in various industries with a high level of technology, such as the aerospace, automotive and energy sectors (especially wind energy). The significant market demand drives a continuous increase in the production of composite materials or structures. This growth is strongly supported by their exceptional mechanical strength, low density, as well as productivity and the intricate shaping complexity of structures specific to composites, when compared to metallic materials [8].

Composite materials have widespread use in the automotive industry, particularly for low-velocity impact applications. The paper [22] focuses on the low-velocity impact performance of automotive structures, which can significantly impact structural safety and shorten the service cycle of components.

Composite materials, especially those with glass fibres, find use in the maritime industry for low-velocity impact applications, such as boat hulls, decks, and superstructures. Composites provide impact resistance against floating debris, collisions with docks, while also offering corrosion resistance and reduced weight.

Composite materials with glass fibres and epoxy resin matrices are utilized across a diverse range of applications, including the aerospace, maritime, automotive, and building industries. They are valued for their superior mechanical properties such as tensile strength, stiffness, and durability, as well as their low specific weight and corrosion resistance. Glass fibre composite materials, in general, hold significant potential for integration into highway infrastructure and are already employed in bridge decks, railings and other structural components [24].

1.5. Conclusions Regarding Glass Fibre Composites.

Glass fibre-reinforced composites with epoxy resin matrices exhibit significantly greater impact strength and durability than monolithic materials. However, their behaviour under impact is influenced by several factors, such as fibre and yarn geometry, orientation, density, distribution, impact velocity and energy. Numerical simulations have been successfully employed to assess composite behaviour under impact and optimize their design [31], particularly when constitutive material models are experimentally determined.

Glass fibre composites exhibit excellent impact resistance, rendering them ideal for applications where protection against low-velocity impact is necessary. They can absorb and distribute impact energy, aiding in failure prevention and maintaining structural integrity. The study [32] concludes that the behaviour of glass fibre-reinforced polyamide composites under low-velocity impact is influenced by the fibre volume fraction and impact energy. The authors discovered that including glass fibre in polyamide decreases the absorbed energy in composite plates when subjected to low-velocity impact.

Khan Z. et al. [24] suggest that glass fibre composite materials generally offer numerous advantages over traditional materials, such as a high strength-to-weight ratio, excellent corrosion resistance and durability. Two distinct impact responses have been observed: elastic deformation without significant damage, and the initiation and propagation of major damages under elastic and plastic strain (Fig. 1.2).

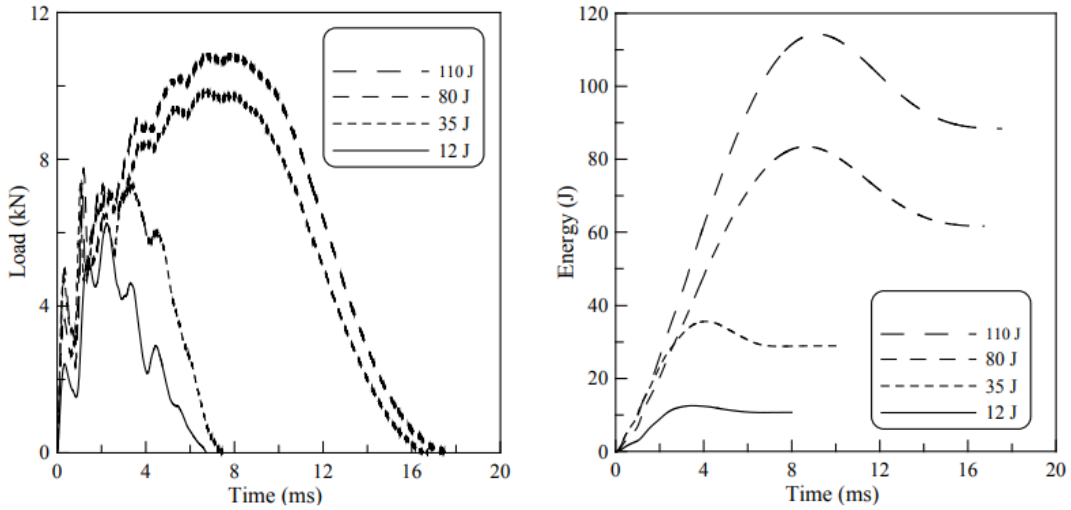

a) b)

Fig. 1.2. Comparative analysis of glass fibre-reinforced composite laminate performance at various impact energies [24]: a) force-time curves, b) energy-time curves

1.6. Research Directions

Research on glass fibre composites may involve future investigations at multiple scales, considering the behaviour of composites at various dimensional levels. This includes the study of the composite's microstructure, fibres, yarns and matrix, as well as the overall macroscopic response to low-velocity impact. Multi-scale modelling (micro, meso or macro) and experimental techniques could provide a comprehensive understanding of composite behaviour and offer solutions for enhancing the performance of these materials.

For this research study, the research directions are as follows:

- conducting a recent and critical literature review in the field of low-velocity impact-resistant composites based on glass fibre fabrics,
- formulating a laboratory process and recipe for producing composite panels,
- designing a comprehensive testing plan to highlight the influence of various factors on impact resistance (impact velocity, panel thickness, shape and size of the impactor etc.),
- modeling and simulating a low-velocity impact between an impactor and a composite using the finite element method, correlating the model with experimental data using validation criteria, and applying the model to other components that need to withstand similar impact conditions,
- obtaining experimental data on composite panels to determine the influence of the impactor shape, impact velocity and panel thickness for the same glass fibre fabric and matrix,
- investigating the failure mechanisms of composites in this impact process, as it provides valuable insights for optimizing the composite and/or the component made of the composite,

Chapter 2. Thesis Structure

The main objective of this PhD thesis is to investigate and characterize the response of multi-axial glass fiber fabric composites to low velocity impact. It involves conducting experimental tests to measure and analyse parameters, such as maximum impact force, energy absorbed by the composite, modelling and simulation of impact response and failure mechanisms. Figure 2.1 shows the structure of the thesis and the main aspects of modelling and testing this family of composites.

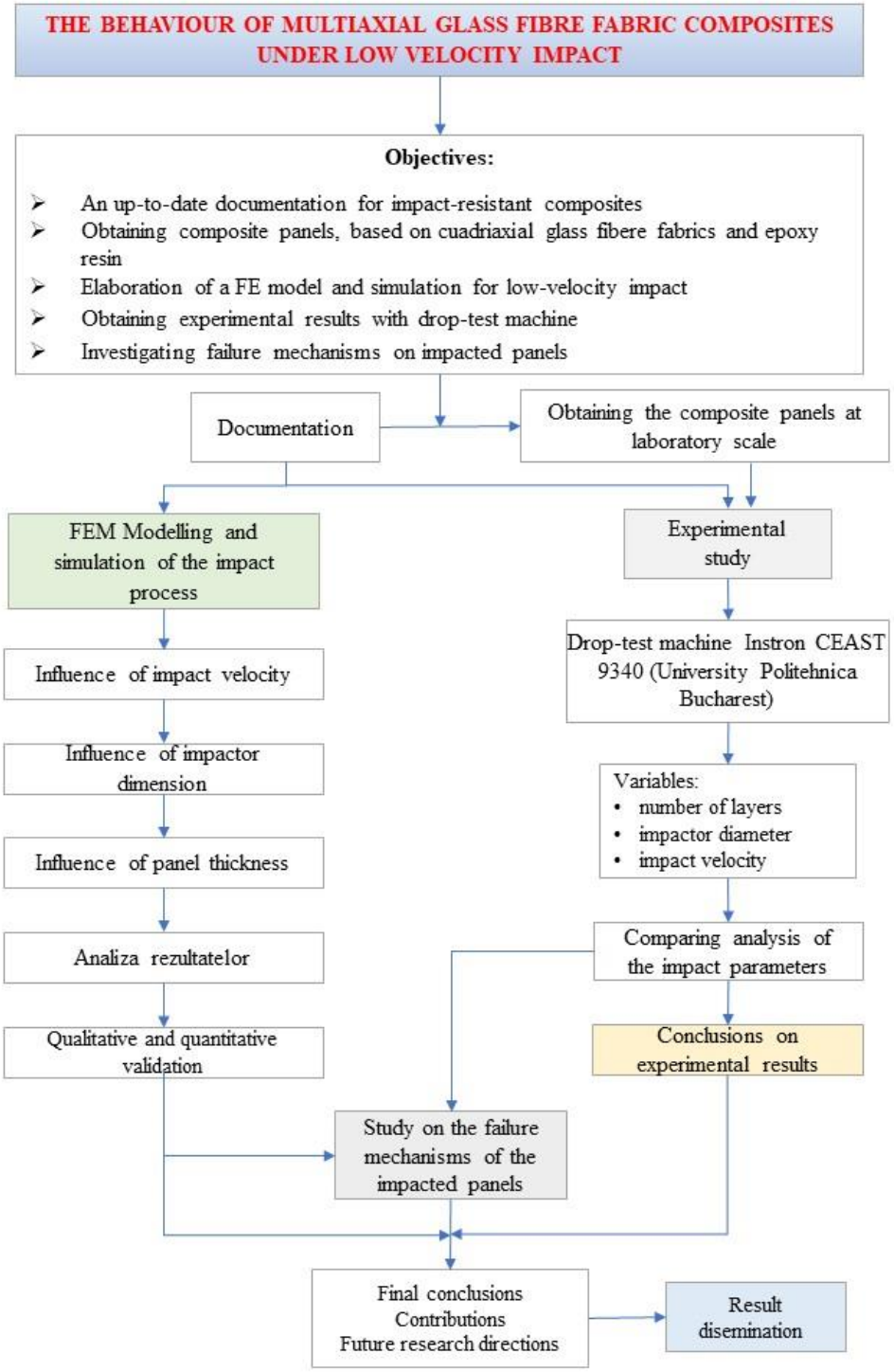

Fig. 2.1. Diagram of the general organization of the PhD thesis

Chapter 3. Simulation of the Behavior of a Quadriaxial Fabric Composite under Low-Velocity Impact

3.1. Introduction

Materials exhibit complex behavior under dynamic loads, necessitating the modeling of various processes specific to impact [4], [11], [18]. These processes include nonlinear response to loading, strengthening (hardening) during loading, the influence of strain rate, changes in mechanical properties due to thermal softening, volume and mass change through compaction (for porous materials), orthotropic response (for composites, especially those with long fibers), crushing failure (e.g., in ceramics), reactions involving chemical energy release during the process (e.g., explosions), failure behavior and phase changes (solid to liquid or gas transition and vice versa) [1], [5], [36].

Modeling these characteristic impact processes involves three main components: the equation of state, the models of the involved materials and their failure criteria [50].

3.2. The Concepts of Constitutive Material Models and Yield Criteria

In simulations using dynamic explicit codes, the temperature-dependent behavior of elastic and elastoplastic properties is not directly available. In these cases, a single value is used for each property without considering temperature variation. The solver will use these fixed values, defined for properties during the numerical resolution [34].

The isotropic bilinear hardening model is a suitable choice in analyses involving large deformations. For using this model, two important values are required: the yield strength and the tangent modulus, specific to the material in question. The material elastic modulus corresponds to the first slope of the curve, while the tangent modulus is associated with the second slope [46].

The model for impact plate - hemispherical body, developed in this study, was implemented using Explicit Dynamics software (Ansys) [50]. The time step used is determined by the stability and consistency condition imposed by the Courant-Friedrichs-Lewy (CFL) criterion. This criterion is a measure to ensure that the selected time step is small enough to accurately capture wave propagation and rapid changes in the analysis [12]. In general, the time steps used in simulations has on the order of milliseconds, and thousands of calculation cycles (time steps) need to be performed in order to obtain a realistic solution.

3.3. Aspects for Simulation in Ansys Explicit Dynamics

Within the field of low-velocity impact, determining the friction coefficient can be simpler and easier as compared to high-speed or ballistic impact. At low velocities, the influence of friction (as a function of loading and relative velocity between bodies) may be less significant, confirming the hypothesis that this friction coefficient may be considered constant under certain simulation conditions, as strain rates and contact stresses vary relatively slowly. For this model, a constant COF of 0.1 was considered.

Definition of Connections. In the Ansys documentation, surface-to-surface interaction is also referred to as surface contact. To minimize or avoid hour glassing in finite element analyses, specific techniques and algorithms are used, such as re-meshing methods, mesh adaptation or erosion of elements with excessive deformations [30], [50].

Discretization network. In numerical analyses, the use of uniform discretization networks is preferred as it brings benefits in terms of efficiency, accuracy and solution stabilization [28].

Regarding boundary conditions, the Explicit Dynamics solver relies on time as a reference and, therefore, is sensitive to inertia. This allows for the detection ("visualization") of failure mechanisms that can only be observed on real specimens as a result at the end of a test [17].

3.4. Model of the Impact Layered Panel - Hemispherical Body

In this model, although the fibers are made of isotropic material, as seen in the simulation images, due to the arrangement of fibres at orientations 0°, +45°, 90°, and -45°, there exists an anisotropic character of the panel and the distribution of stresses and strains is in a diamond pattern relative to the impactor axis. Figure 3.1 presents the front and back of a plate (60 mm × 60 mm), impacted by the 10 mm hemispherical impactor, at v_3=4 m/s, where the stretching of the fibers in the four directions of the yarns can be noticed.

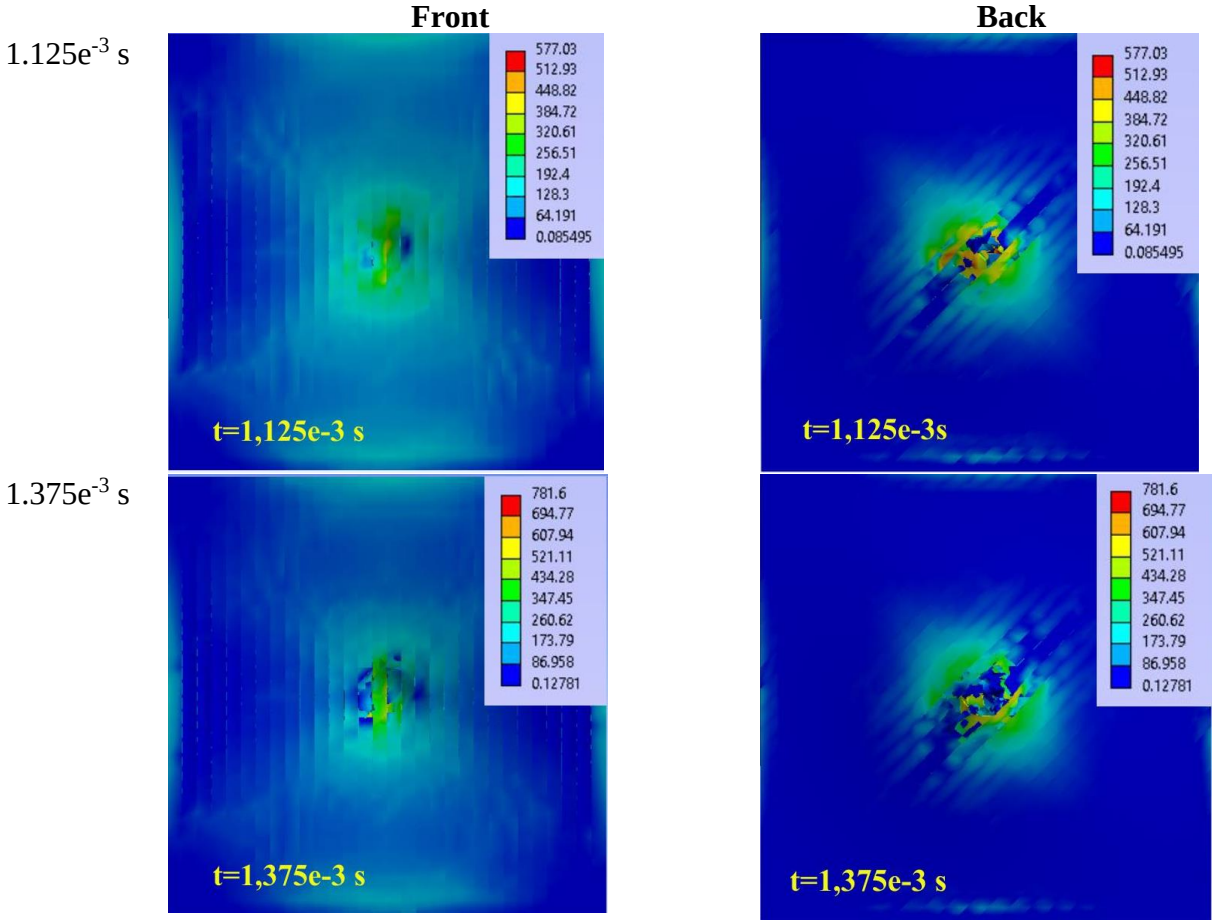

Fig. 3.1. Influence of yarn architecture (in 8 substrates) on equivalent stress distribution (in MPa)

The model consists of several bodies (265 bodies of which 264 are yarns) and a hemispherical impactor: sublayers with yarn orientations 0^0 and 90^0 have 30 yarns each, and sublayers with yarn orientations $+45^0$ and -45^0 have 36 yarns each.

The number of nodes in this model is 107017 and the number of elements is 40496. In Fig. 3.2a, a few yarns from each sublayer were intentionally left visible to illustrate the architecture of a quadriaxial fabric layer, which is composed of 4 sub-layers of unidirectional fibres, differently oriented.

In Fig. 3.2b, an overview of the discretization network of the model is provided. In Fig. 3.2c, the discretization network is shown on a main yarn and on the impactor. Considering the multitude of yarns, a discretization network consisting of two elements across the width of the yarn was chosen.

The model includes symmetry planes, but a reduction of the model was not chosen because, regardless of the fineness of the discretization network and the accuracy of the dynamic model, the breaking of yarns does not occur symmetrically, as it happens in reality, too.

In the model, the interaction between bodies or between resulting fragments is with friction, the friction coefficient being considered constant, set at COF=0.1.

The chosen model is isothermal for two reasons. Firstly, the Explicit Dynamics software does not support adiabatic models [50]. Secondly, specialized literature has indicated that in the range of impact velocities between 1 m/s and 400 m/s, the influence of the thermal field can be considered negligible in simulating damage processes.

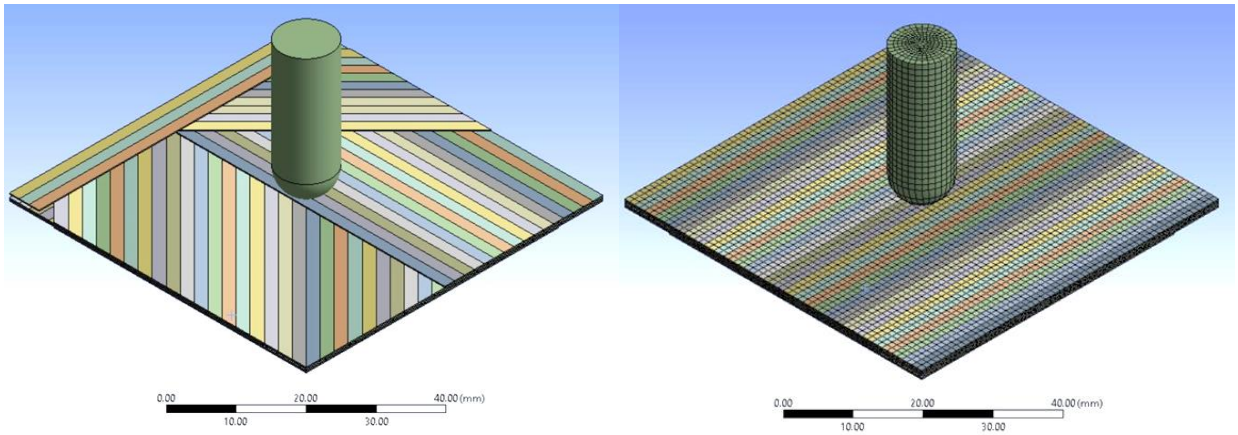

a) b)

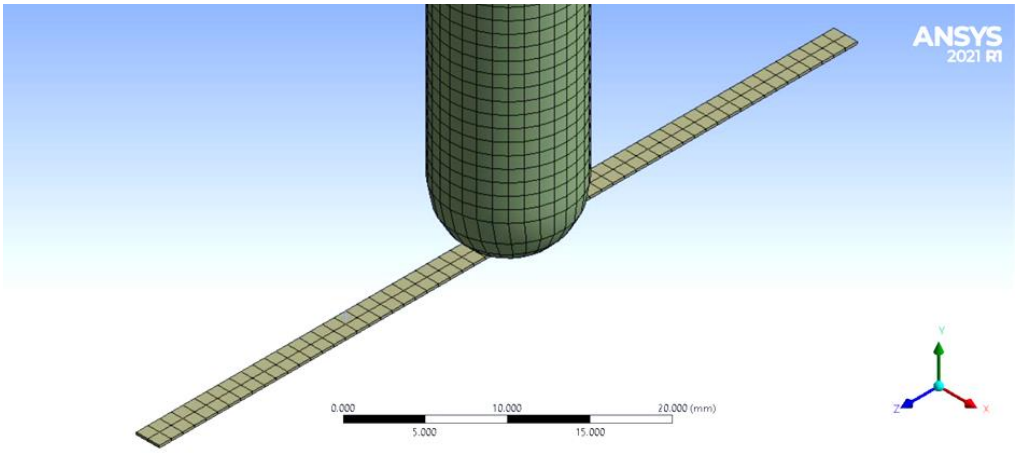

c)

Fig. 3.2. Geometric model and discretization network for impactor and yarn

Each yarn is fixed on its lateral edge section to prevent displacement. The model is structured as follows: 8 layers of unidirectional yarns with orientations of 0^0, $+45^0$, 90^0, and -45^0. The yarns have a thickness of 0.2 mm, and the width of each yarn is 2 mm. The study [14] analyzes the effect of the cross-sectional shape of the yarn on resin flow through the gaps between yarns in textile reinforcements, with one of the variants closely resembling a rectangle, as in this study

Figure 3.3 depicts the constitutive material model used for the yarn (yield strength in tension and compression is 400 MPa, elastic modulus E=10 GPa, tangent modulus 4 GPa, Poisson's ratio 0.306), while the impactor is considered rigid. [35] The matrix is assumed to have zero thickness, like the cohesive zone model with zero thickness [10], [19], but the detachment of nodes from adjacent yarns occurs at certain values of tensile and/or shear stress, characteristic of a high-quality epoxy matrix. The failure criterion for the yarn is the maximum equivalent plastic strain at break (EPS), with a value of 0.06 (or 6%), a typical value for glass fibres.

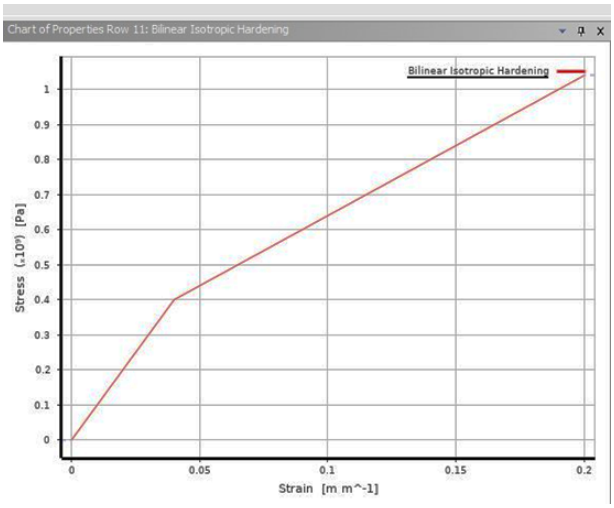

Fig. 3.3. Constitutive material model for yarn

The parameters for node detachment, introduced with the "stress criteria" command and capable of modeling delamination, in this case, between the fibres on the composite sublayers. These parameters are used in simulations to characterize the behavior of composite materials and delamination. The tensile limit is 60 MPa, and the shear stress detachment limit is 40 MPa, values that are plausible for characterizing a good quality epoxy resin.

3.5. Simulation Results of Impact and Discussions

3.5.1. Analysis of Equivalent Stress Distribution on the Two-Layered Panel

The simulations were run to highlight the following:

−the possibility of modeling impact at a mesoscale level, considering the behavior of unidirectional yarns with isotropic characteristics, an acceptable simplification since the architecture of yarns in quadriaxial oriented substrates (0°/45°/90°/-45°) imparts some degree of mechanical uniformity, at least in the plane of the fabric, and consequently, in the composite as well, so that, based on validation criteria, the model can be used to assess low-velocity impact resistance for certain ranges of parameter variations, such as the modeled panel area, number of layers, impact velocity and energy, in comparison to the panels that have already been tested,

−the validation criteria for the model can encompass both quantitative and qualitative aspects; qualitative criteria involve the geometric shape of the impactor penetration hole or the shape of the impactor imprint in case of partial penetration, the shape of delamination, while quantitative criteria may pertain to the number of broken sublayers, dimensions of the imprint or penetration hole (diameter, depth), size of delamination (or separation of layers and sublayers), which are observable in the simulation through virtual cross-sectional analysis of the model.

In Fig. 3.4, simulation images of the panel are presented, showing the front side (top) and back side (bottom), alongside real images of the 2-layer panel – front side (top), back side (bottom) – subjected to impact with a Ø 20 mm impactor, at a velocity of v_3=4 m/s. These simulation and real images provide detailed insights into the behaviour of the 2-layer panel during and after the impact with the 20 mm impactor, at a velocity of 4 m/s. From the run simulations, it can be observed that the impact duration aligns with the duration recorded on the impact testing machine, which is on the order of 10^{-3} seconds (a few milliseconds).

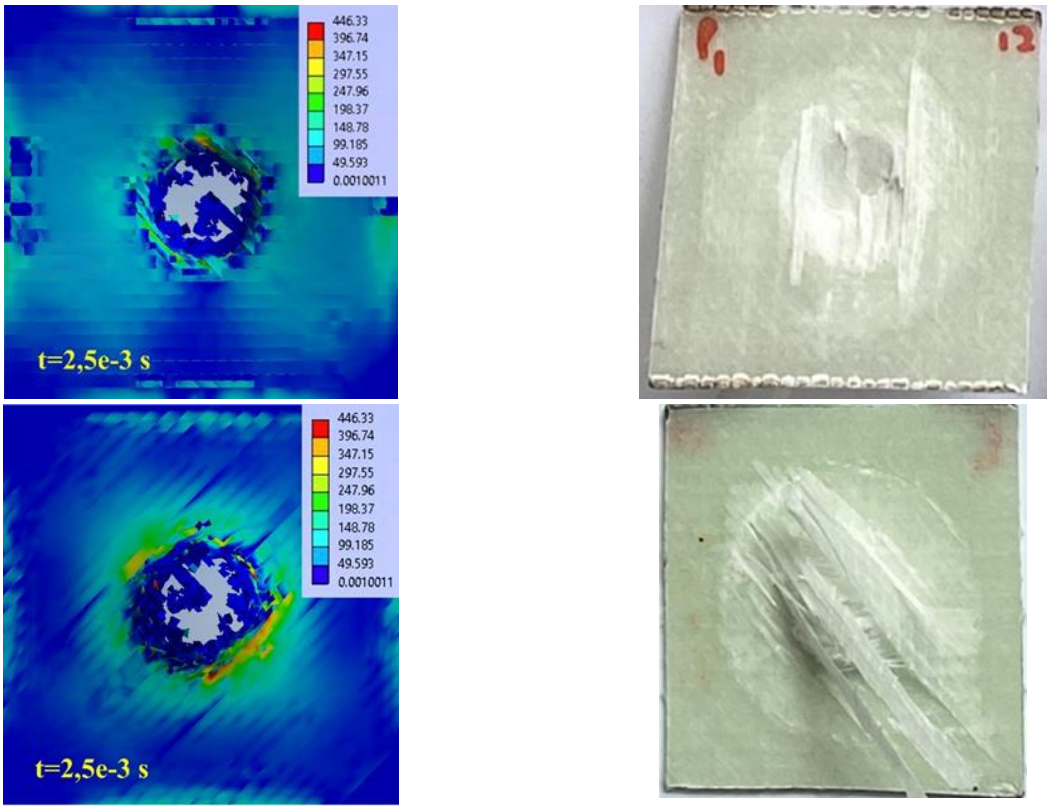

a) b)

Fig. 3.4. Images: Column a) Simulation images of the panel – front side (top), back side (bottom); b) Real images of the 2-layer panel – front side (top), back side (bottom) – tested with a Ø 20 mm impactor, at a velocity of v_3=4 m/s.

3.5.2. Comparative Analysis of Main Yarn Failure Using Simulation Images and Distribution of Equivalent Stresses, for the Two Hemispherical Impactors

The coding of the analyzed main yarns is retained in this chapter (Fig. 3.5). Main yarn 1, adjacent to the symmetry plane of the impactor axis, is considered, and the substrate number on which the yarn is located has been added.

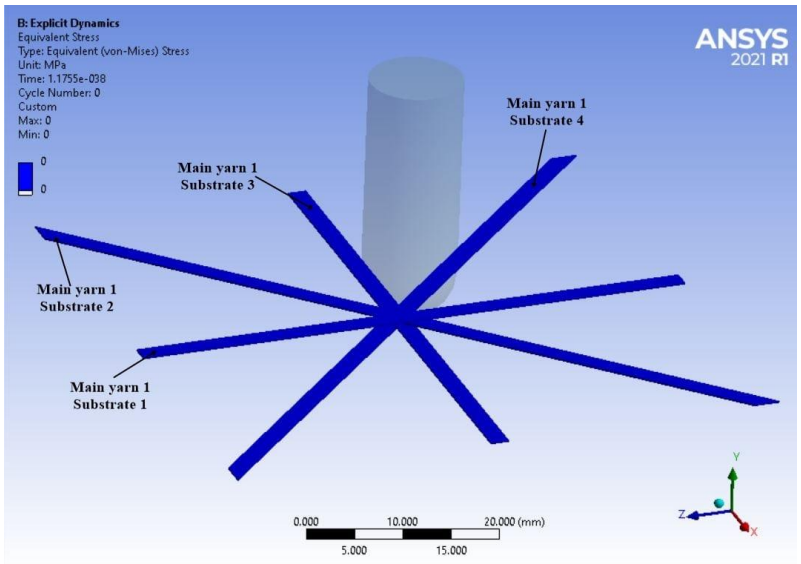

Fig. 3.5. Codes of the analyzed main yarns, for the analysis of equivalent stress distributions along yarns

Figures 3.6-3.9 depict, at different time moments of the simulation, an image displaying the distribution of equivalent stresses on the main yarns (in MPa), showcasing a yarn from each substrate. Additionally, graphs representing the distributions of equivalent stresses on the straight main yarns (parallel to the plate sides) and on the diagonal main yarns are presented. Each virtual image of the main yarns features its own color scale for equivalent stress, also measured in MPa.

From the run simulations, it is evident that the impact duration falls within the timeframe recorded by the impact testing machine, approximately in the order of 10^{-3} seconds (a few milliseconds). The simulations were run for 2.5×10^{-3} seconds, and it can be observed that for both simulations, at this time moment, the equivalent stresses are below 60...80 MPa. Consequently, these values are not likely to cause matrix break or detachment from the yarns at this stress value.

In the graphs, the break of a yarn is depicted by a sharp decrease in equivalent stress to zero. Subsequently, any fragments resulting from yarn breakage can experience compression as they are driven on the impactor head or crushed on the first sublayer that has not failed or has only partially failed.

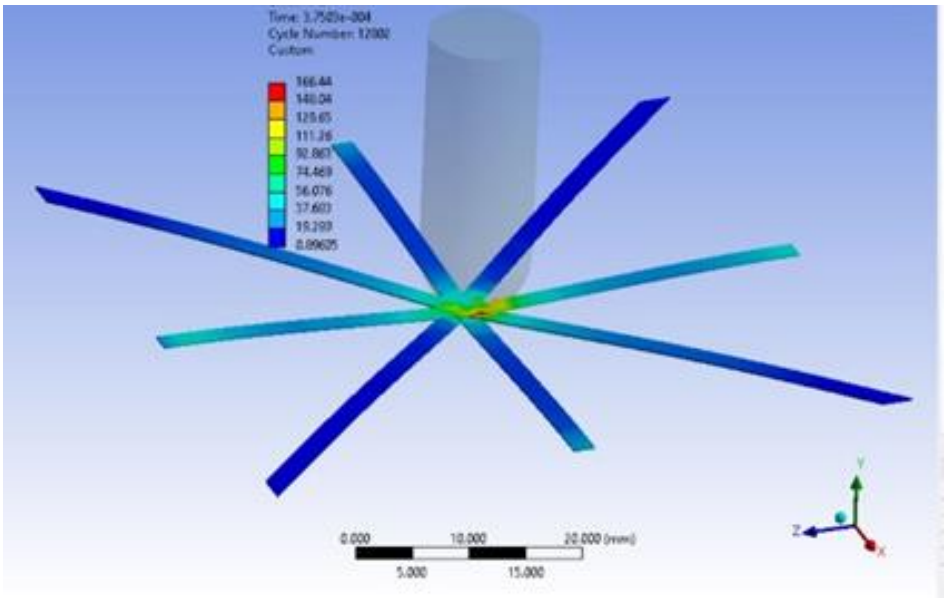

a)

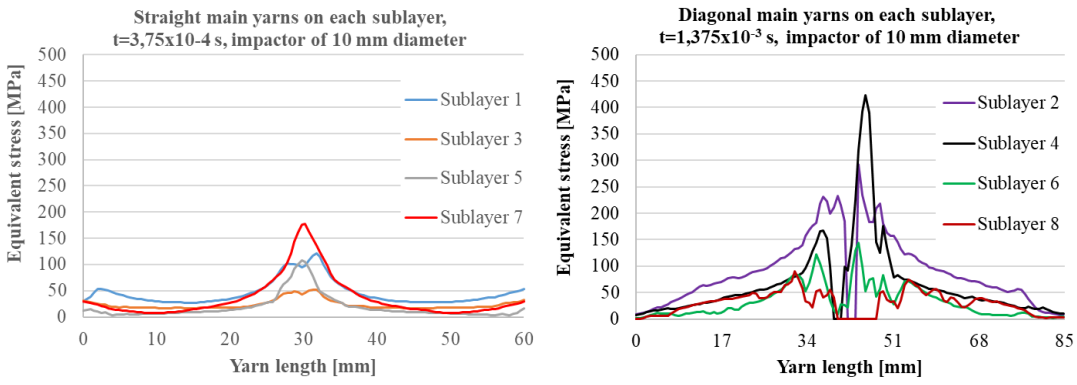

b) c)

Fig. 3.6. Simulation for the Ø 10 mm impactor and v_3= 4 m/s, at the time t= 3.75×10^{-4} s;
a) Main analyzed yarns (other bodies of the 2-layer panels are invisible) and the distribution of equivalent stress for: b) straight main yarns; c) diagonal main yarns

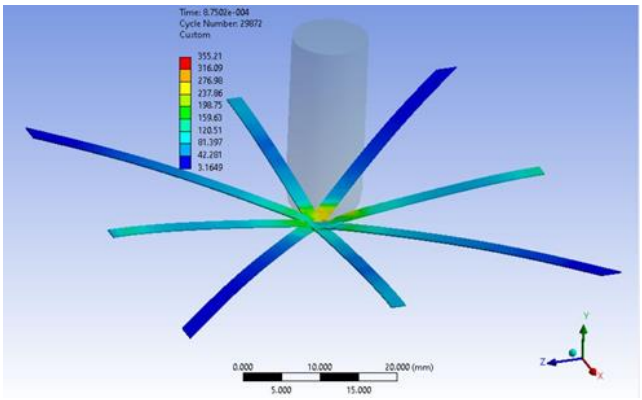

a)

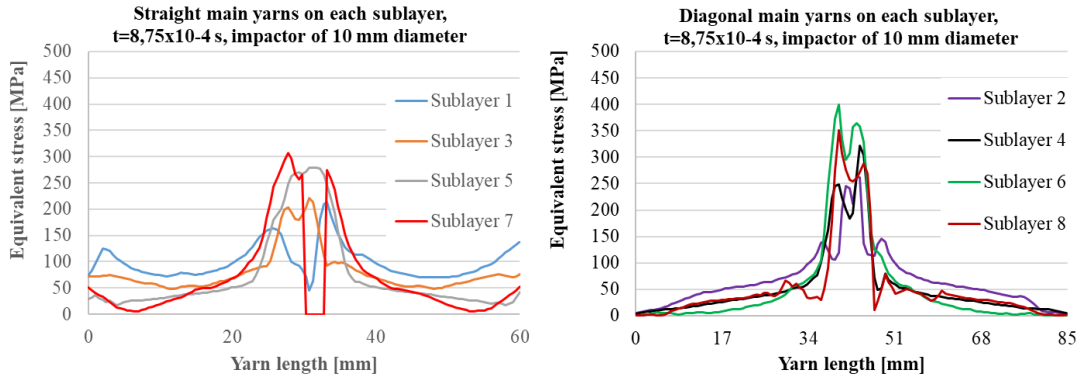

b) c)

Fig. 3.7. Simulation for the Ø 10 mm impactor at v_3 = 4 m/s, at the time t = 8.75 × 10^{-4} s; a) Main analyzed yarns (other bodies of the 2-layer panels are invisible) and the distribution of equivalent stress for: b) straight main yarns; c) diagonal main yarns.

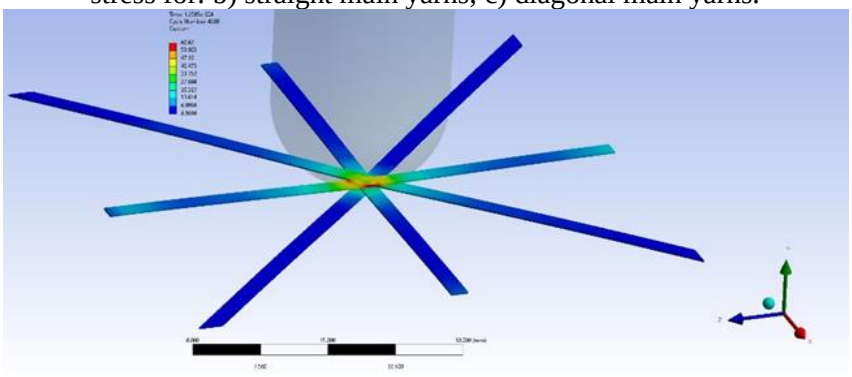

a)

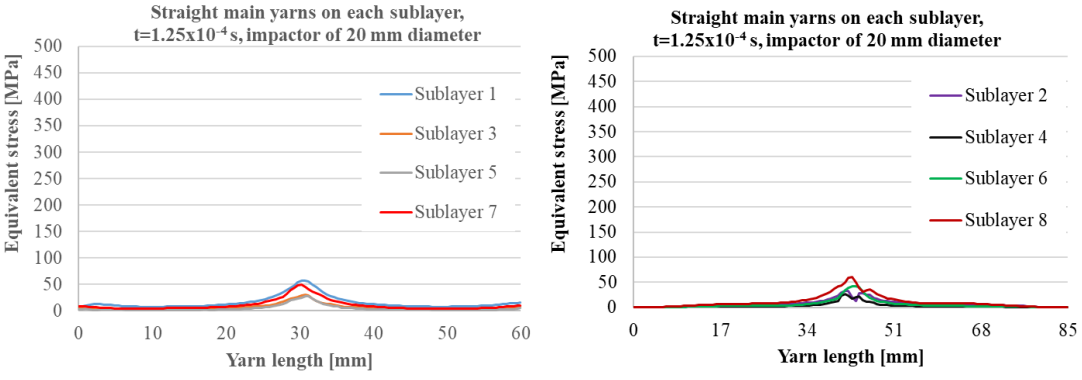

b) c)

Fig. 3.8. Simulation for the Ø 20 mm impactor at v_3=4 m/s, at the time t = 1.25×10^{-4} s; a) View of the analyzed main yarns (other bodies of the 2-layer panels are invisible) and the distribution of equivalent stress for: b) straight main yarns; c) diagonal main yarns

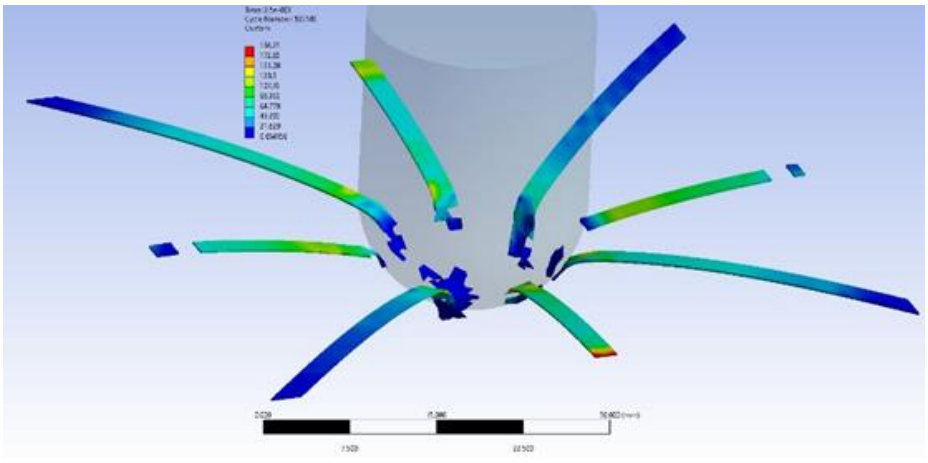

a)

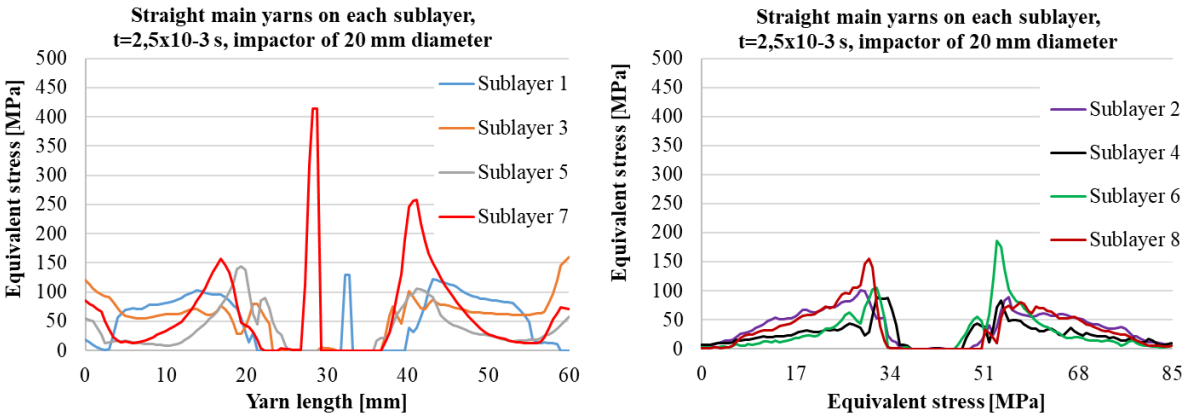

b) c)

Fig. 3.9. Simulation for the Ø 20 mm impactor at v_3=4 m/s, at the time t=2.5×10^{-3} s; a) View of the analyzed main yarns (other bodies of the 2-layer panels are invisible) and the distribution of equivalent stress for: b) straight main yarns; c) diagonal main yarns

The obtained results have led to the following conclusions.

1. The material model of the yarn, although simplified to a bilinear isotropic hardening model, yielded valid results in accordance with available experimental data from the literature. This was demonstrated through the validation of the number of broken layers damaged in the case of partially penetrated panels and the size of delamination on the back of the panel.
2. The analysis of equivalent stresses, at different time moments and on various sublayers, allowed for distinguishing the impact stages, both for complete penetration and partial penetration.

3.6. Conclusions Regarding the Evaluation of Low-Velocity Impact Simulation

For complete penetration (2-layer panel with 10 mm impactor), the observed stages from the model simulation are as follows:

- the loading of sublayers without breaking yarns is a very short stage, on the order of 10^{-4} s to 10^{-3} s, a longer interval than in a high-velocity ballistic impact (100 to 800 m/s), which is on the order of 10^{-6} seconds [37]. However, the equivalent stress values reach high levels, close to the breaking limit of the yarns, and the strains approaches the value of the failure criterion (equivalent plastic strain at brake). Additionally, the first substrate (implicitly the main yarns) is strongly compressed,

- from the moment the value set by the program for the failure criterion is reached (in this case, the equivalent plastic strain at break – denoted as EPS), the breaking of the yarns and delamination between substrates is initiated. A more significant delamination or detachment is observed between the last substrates due to their higher deformations,

- stage in which all yarns are successively broken (it is worth noting that the breaking of one or more yarns can occur between the selected simulation moments, and therefore, the graphs of equivalent stresses on the yarns may have values lower than the limit at break),

- stage in which the stresses on the analyzed main yarns are lower than the stress limit at break of the yarns, but still have values that can detach adjacent yarns and yarns from neighboring substrates, values that exceed the strength of the composite matrix, simulated through node detachment conditions (in this study),

- stage in which the values of equivalent stress decrease below values that trigger matrix failure, no more failures occur, and the impact process can be considered concluded.

It is worth emphasizing that the detachment of yarns, either from each other or from different substrates, can occur locally when exceeding the conditions for node separation, at stress levels much lower than the yarn limit at break.

Table 3.1 presents the moments at which the brake of each yarn occurred. It becomes evident when the first yarn breaks and when the last one does. For the 10 mm impactor, the first broken yarn to brake is the yarn located on substrate 7 (straight yarn), while for the 20 mm impactor, both the yarn on substrate 1 and the one on the last substrate (8) brake simultaneously.

The duration of yarn destruction is slightly longer for the larger diameter impactor.

Table 3.1. Breaking moments of main yarns

10 mm Impactor										
Time	**1.25**	**3.75**	**6.25**	**8.75**	**1.125**	**1.375**	**1.625**	**1.875**	**2.125**	**2.5**
Yarn	**[x10^{-4} s]**				**[x10^{-3} s]**					
1										
2										
3										
4										
5										
6										
7										
8										
20 mm Impactor										
	1.25	**3.75**	**6.25**	**8.75**	**1.125**	**1.375**	**1.625**	**1.875**	**2.125**	**2.5**
Yarn	**[x10^{-4} s]**				**[x10^{-3} s]**					
1										
2										
3										
4										
5										
6										
7										
8										

Straight Yarn Diagonal Yarn

- for the **10 mm diameter impactor**, the yarns break in the order: 8, 6, 4, 1, at the moment $t=1.375\times10^{-3}$ s, all yarns are broken.
- for the **20 mm diameter impactor**, at the moment $t=1.375\times10^{-3}$ s, only yarn 8 is broken; at $t=1.625\times10^{-3}$ s, the main yarn 4 is still intact, but it can be observed that in the next moment of simulation, $t=1.875\times10^{-3}$ s, it is also broken.

On the diagonal yarns, the stress increases at a faster rate and is more localized under the impactor. The stress reduction rate is faster and at much lower values for the 10 mm impactor. The 20 mm impactor produces higher equivalent stresses due to the bending process of the yarns, when the impactor is moving, values which are favourable for the further production of delaminations between the substrates and between the yarns on the same sublayers.

At this stage, when yarns are no longer damaged and the composite can only be considered as stressed,

- for the 10 mm impactor, delamination or matrix failure is only possible until the moment $t=1.625\times10^{-3}$ s, and that too only for yarn 4. In this stage, the equivalent stresses do not exceed the detachment values of the nodes, so the substrates and, implicitly, the yarns no longer detach except perhaps locally, as seen in an SEM image,
- for the 20 mm impactor, significant stress distributions appear (which can lead to the detachment of nodes between yarns and matrix) from substrates 6 and 8.

Figures 3.10 and 3.11 compare the distribution of equivalent stresses on the main yarns for the 10 mm and 20 mm impactors. Only a few significant moments have been selected for the impact process. It can be observed that, for both impactors, until $t=6.25\times10^{-4}$ s, no yarns in the composite have been broken.

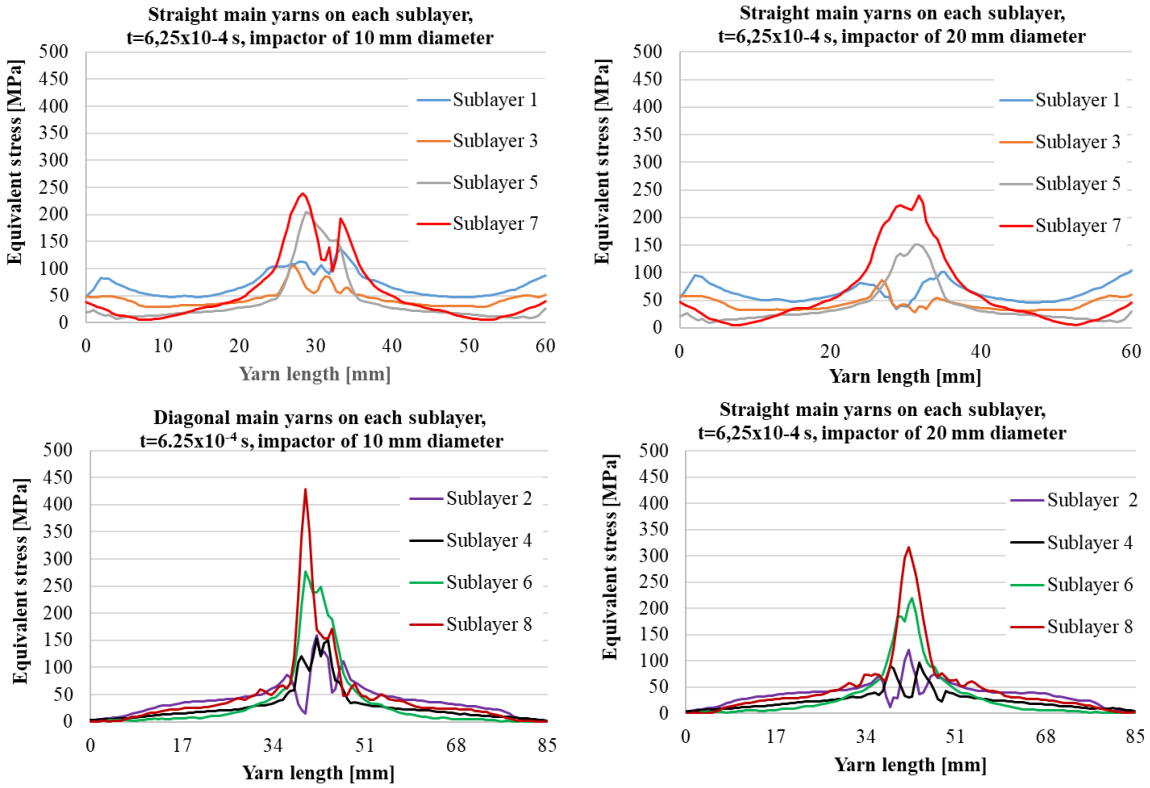

Fig. 3.10. Equivalent stress distribution (in MPa) on straight main yarns (on substrates 1, 3, 5 and 7) and on diagonal main yarns (on substrates 2, 4, 6 and 8) just before first yarn breakage, for 10 mm impactor (left column), for 20 mm impactor (right column)

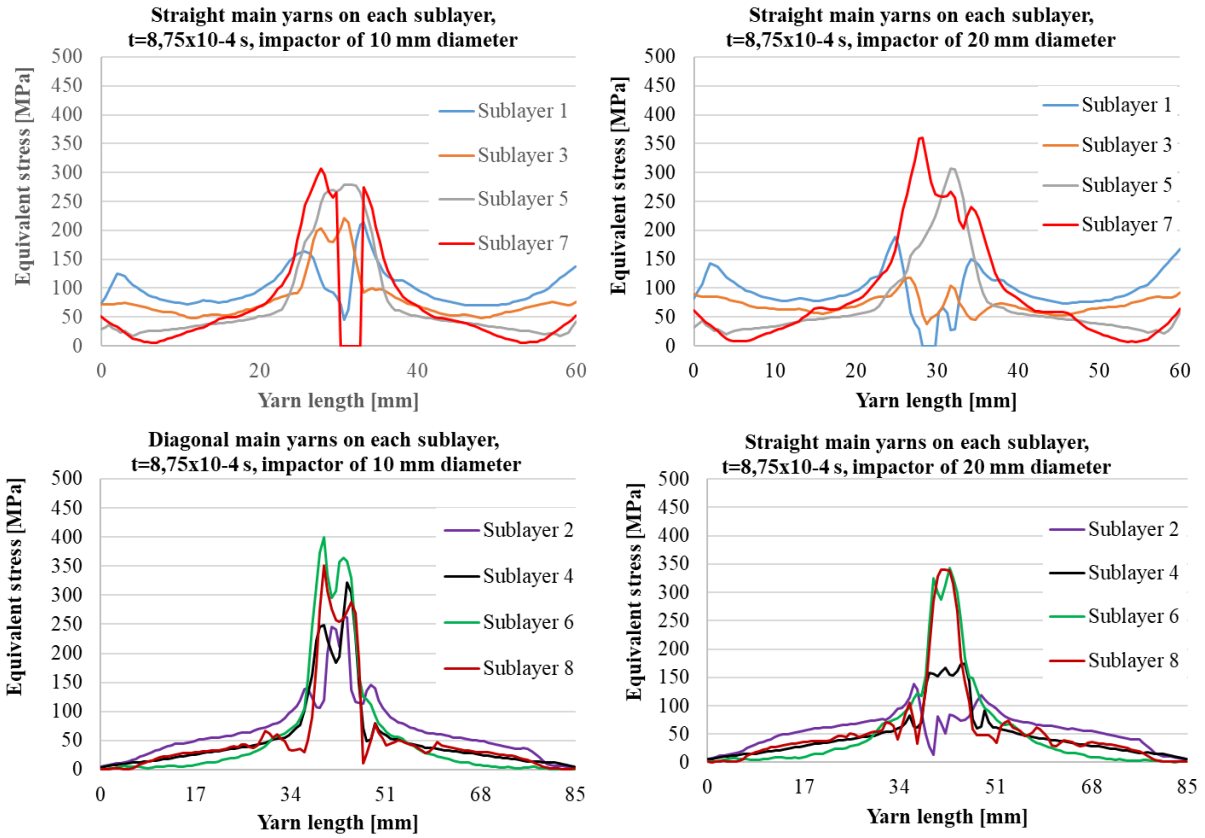

Fig. 3.11. The distribution of equivalent stresses on the main yarns at the moment $t=8.75\times10^{-4}$ s

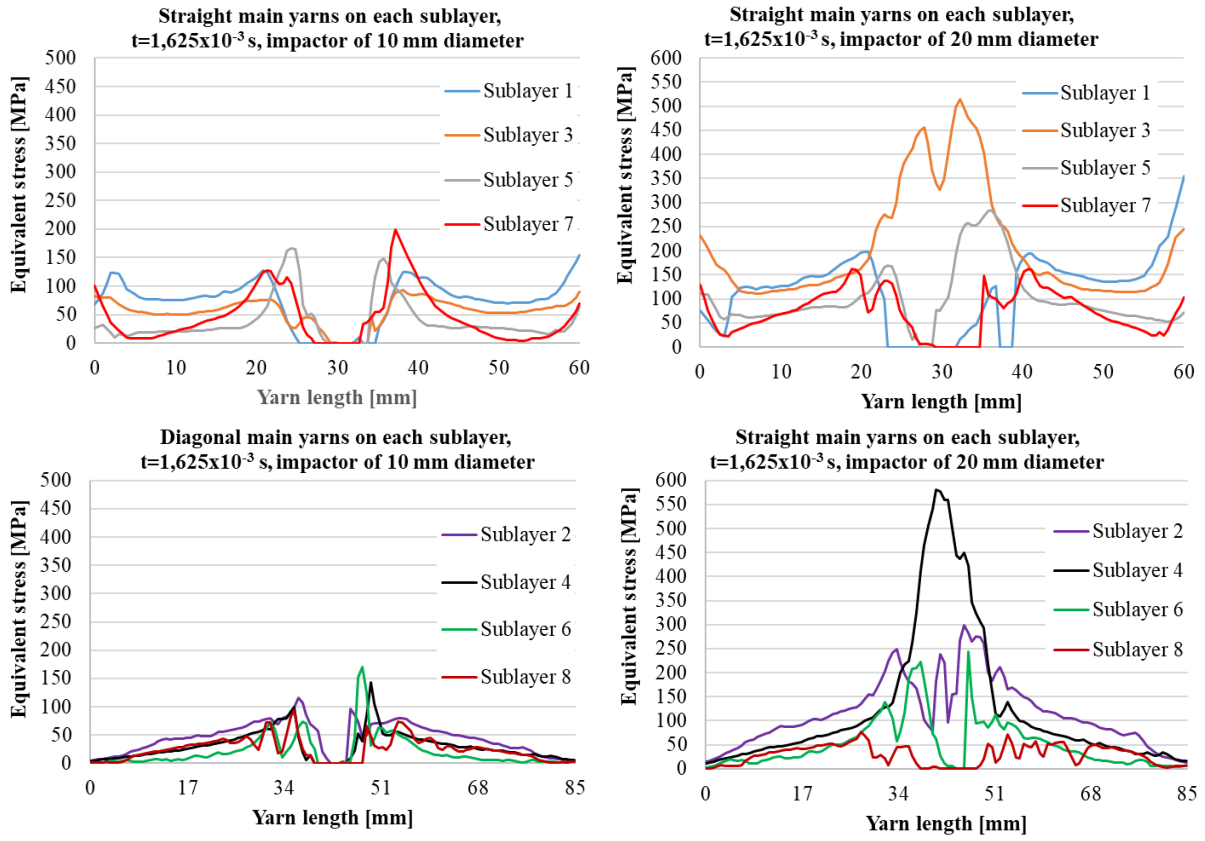

Fig. 3.12. The distribution of equivalent stresses on the main yarns at the moment $t=1.625\times10^{-3}$

The second stage in which the main yarns break, in the case of the 10 mm diameter impactor, lasts from $t=8.75\times10^{-4}$ s (Fig. 3.11), when the straight yarn on substrate 7 breaks, to $t=1.625\times10^{-3}$ s (Fig. 3.12), when all analyzed main yarns are broken. In the case of the 20 mm diameter impactor, at this moment, yarn 3 and yarn 4 are still intact, but highly stressed and strained. For the impact with the 20 mm diameter impactor, the diagonal yarns are not yet broken, with those in the middle of the composite being much less stressed. For the 20 mm diameter impactor, the breaking of the yarns ends at $t=1.875\times10^{-3}$ s (Fig. 3.13).

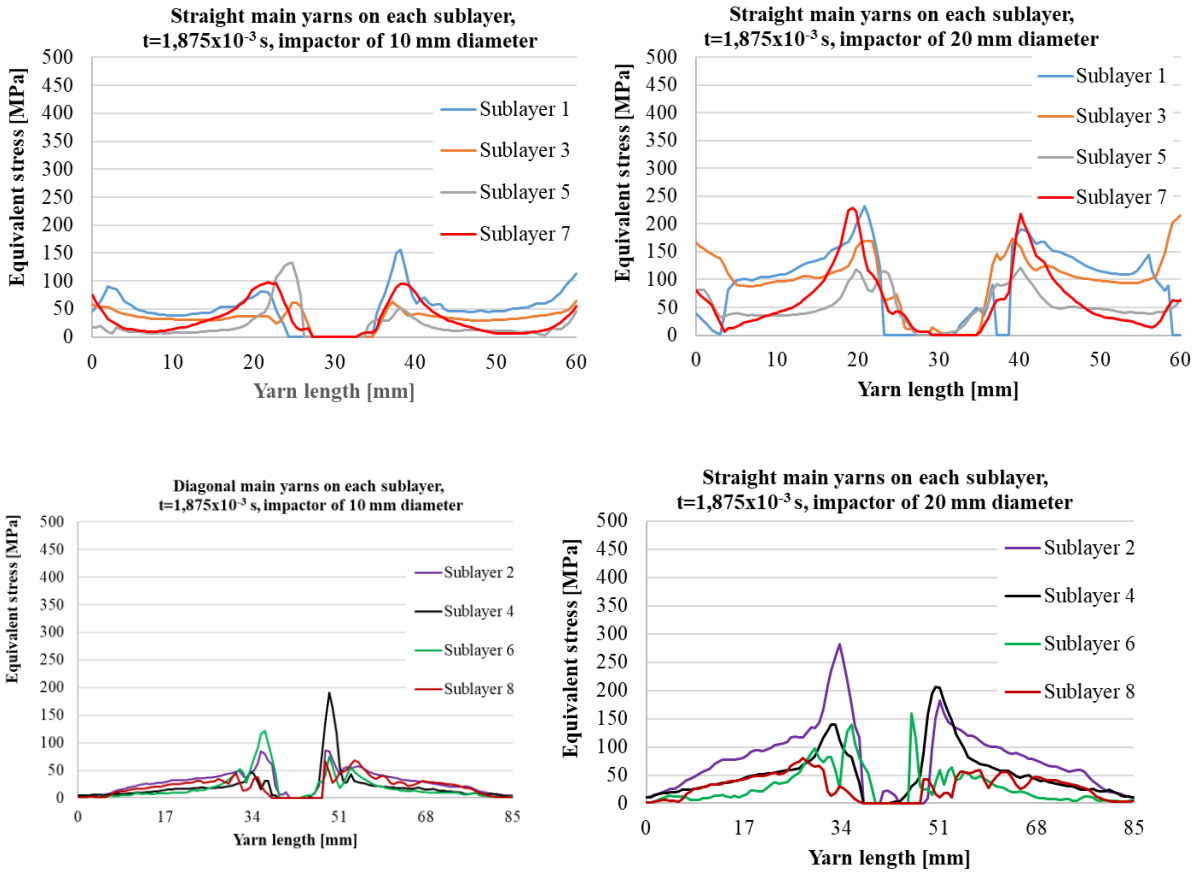

Fig. 3.13. Distribution of equivalent stresses on the main yarns, at the time $t=1.875\times10^{-3}$ s.

In the third stage, where the yarns are no longer breaking, but there are still under significant stresses to "unlock" the connections between the yarns (the common nodes between yarns). Thus, there is a region within the composite, particularly around the direct contact area with the impactor, where the stress limits for tensile and/or shear stresses that "unbind" these nodes are exceeded. From the graphs in Figure 3.14, it can be observed that delamination is less intense for the composite impacted by the 10 mm diameter impactor, and more intense, spreading over a larger area, for the composite impacted by the 20 mm diameter impactor. This observation is also supported by macro photographs of the actual panels, tested under the same conditions (Fig. 3.14). SEM images from Fig. 3.14b show the asymmetrical break of several yarns, for the panel of 2 quadriaxial layers. Additionally, it is noticeable that delamination is more pronounced (visible through colour differences) on the backside of the panels. Due to the different orientations of yarns in the substrates, delamination does not exhibit a circular shape.

The impact simulation was conducted until the time $t=2.5\times10^{-3}$ s (Fig. 3.15).

10 mm Impactor

20 mm Impactor

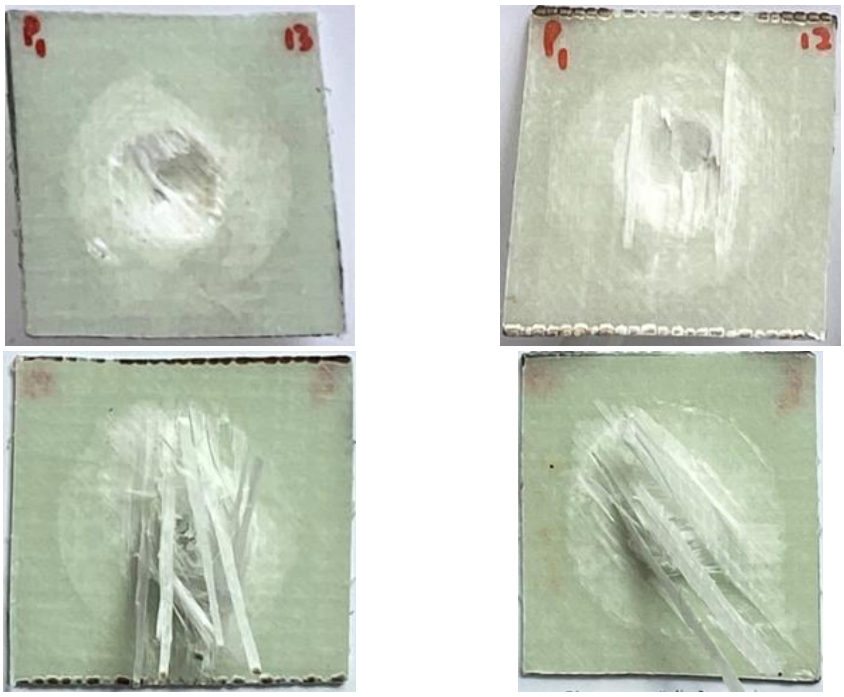

Fig. 3.14. Images of the plates tested under the same conditions as the simulated cases (v_3=4 m/s, plates of 60 mm×60 mm

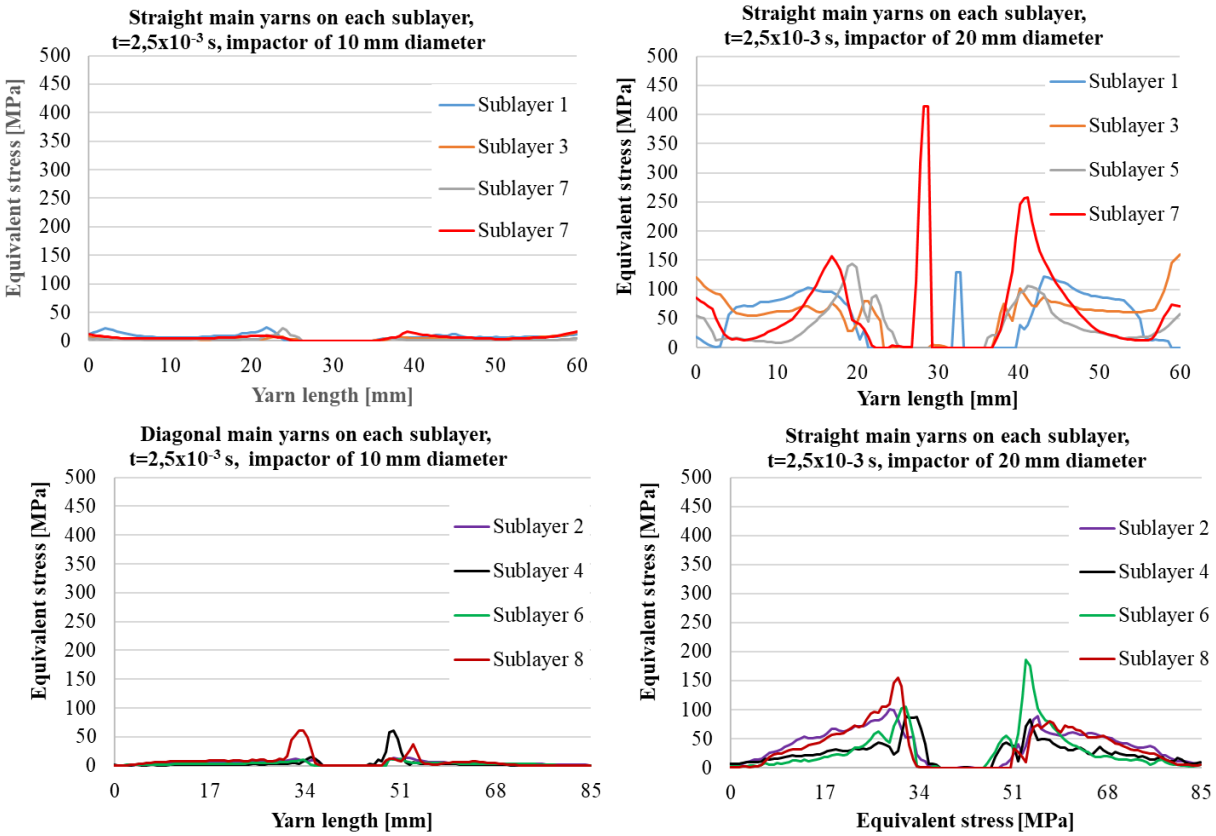

Fig. 3.15. Comparative evolution of equivalent stress (in MPa) for diagonal yarns: for the 10 mm diameter impactor (left column), for the 20 mm diameter impactor (right column).

Figures 3.16 and 3.18 show the equivalent stresses along the length of the main yarns, only for yarns 1, 2, 7, and 8, which are heavily loaded and break first, for the 10 mm diameter impactor, for all time steps in the simulation.

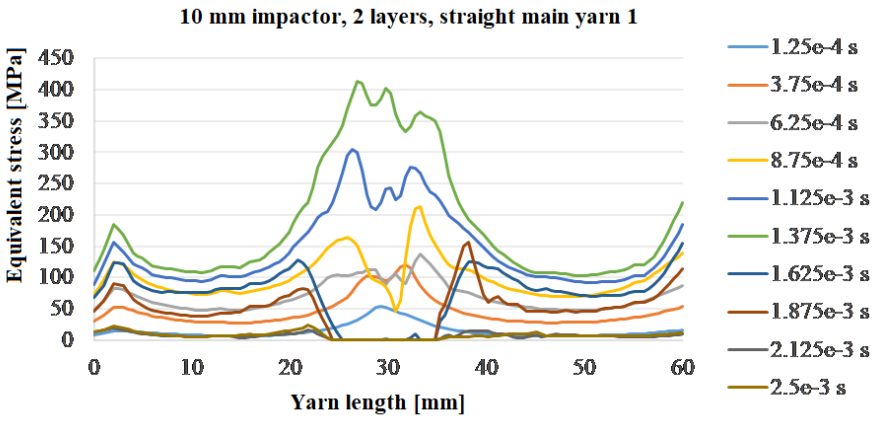

The straight main yarn on sublayer 1 breaks between $t=1.375\times10^{-3}$ and $t=1.65\times10^{-4}$ s. The breaking of the yarn occurs in two points, with the resulting central fragment being compressed on the other sublayers. The minimum value at $t=8.75\times10^{-4}$ is the result of local plastic deformation of the yarn, causing a reduction in equivalent stress.

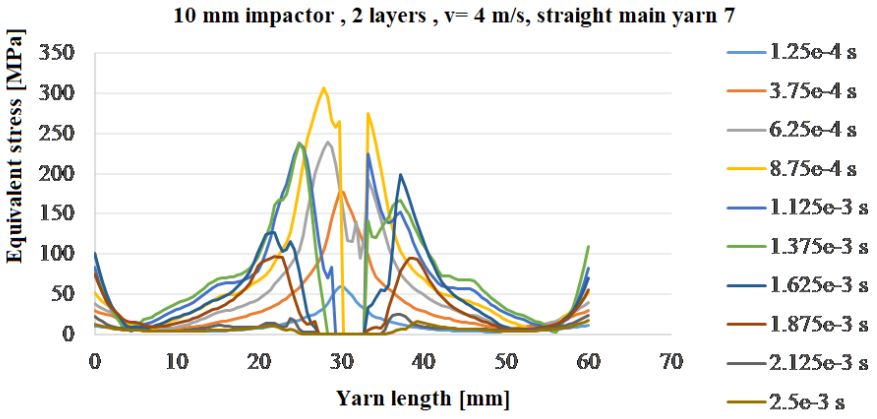

The straight main yarn on sublayer 7, breaks between $t=6.25\times10^{-4}$ s and $t=8.75\times10^{-4}$ s. High equivalent stresses appear at the broken ends of the yarn due to their bending as the impactor passes through the composite (especially with the cylindrical part of the impactor).

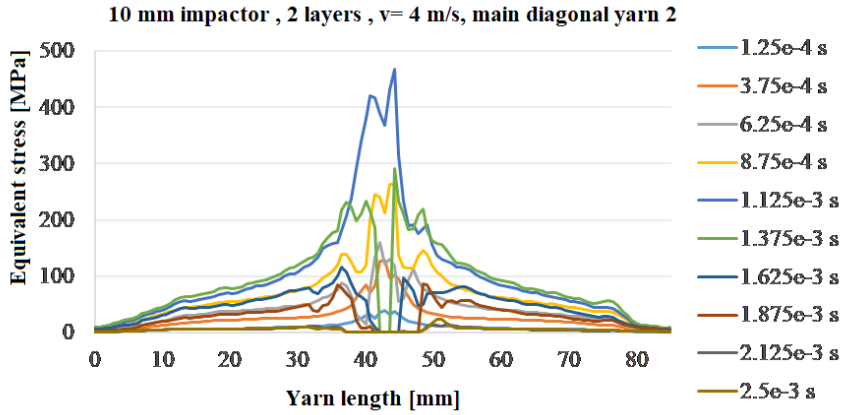

The breaking of the diagonal main yarn on sublayer 2 occurs between the moments $t=1.375\times10^{-3}$ s and $t=1.625\times10^{-3}$ s in the simulation.

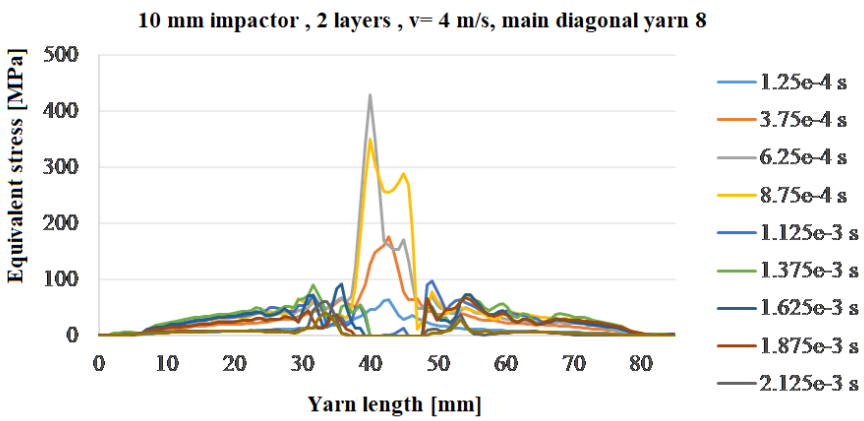

The diagonal main yarn on sublayer 8 breaks between the moments $t=8.75\times10^{-4}$ s and $t=1.125\times10^{-3}$ s. The breaking occurs towards the edge of the impactor contact. After the break, the yarn is pushed by the impactor, but the equivalent stresses are low, below 100 MPa.

Fig. 3.16. The distribution of equivalent stress on diagonal main yarns, for 10 mm diameter impactor

Only the first two main yarns (from sublayer 1 - straight yarn and from sublayer 2 - diagonal yarn) and the last two main yarns (from sublayer 7 - straight yarn and 8 - diagonal yarn) were chosen, from all 8 main yarns selected, one on each sublayer of the model, for analysis presented in the thesis.

Figure 3.17a depicts the exit hole for the plate impacted by a 10 mm diameter impactor. Determining the initial orientation of the yarns is more challenging due to one of the yarns being heavily bent and because its break occurred on one side of the impactor's axis. Additionally, the strongly bent portion of the yarn was long enough to pass through the orifice formed by the impactor in the composite.

In Figure 3.17b, the localized and asymmetric break of several main yarns from the first substrates is easily visible. In this context, A represents the straight main yarn from sublayer 1 (0°), B corresponds to the -45^0 inclined main yarn from sublayer 2, C denotes the main yarn, perpendicular to yarn A from the first sublayer (90°), and D represents the $+45^0$ inclined diagonal main yarn on sublayer 4. It may be noticed that the equivalent stress distributions suggest the fragmentation of main yarns, implying the break of each yarn at two points along its length, as deduced from the stress distribution graphs resulting from simulation. These fragments can be carried away from the plate by the impactor head if complete penetration occurs, or they can remain compressed (crushed, cracked) on the substrates where the yarns are still intact. On SEM images, such fragments are difficult to be observed, unless they remain caught within unbroken yarns, as the samples are blown with air jets to remove glass fiber fragments that might clog the vacuum chamber filter of the electron microscope.

Figure 3.18 depicts the analysis of equivalent stresses for the main yarns on substrates 1, 2, 7, and 8, in the case of simulating the impact with a 20 mm diameter impactor, at a velocity of 4 m/s, on the same composite plate consisting of 2 layers of quadriaxial fabric (8 sublayers of glass fiber yarns).

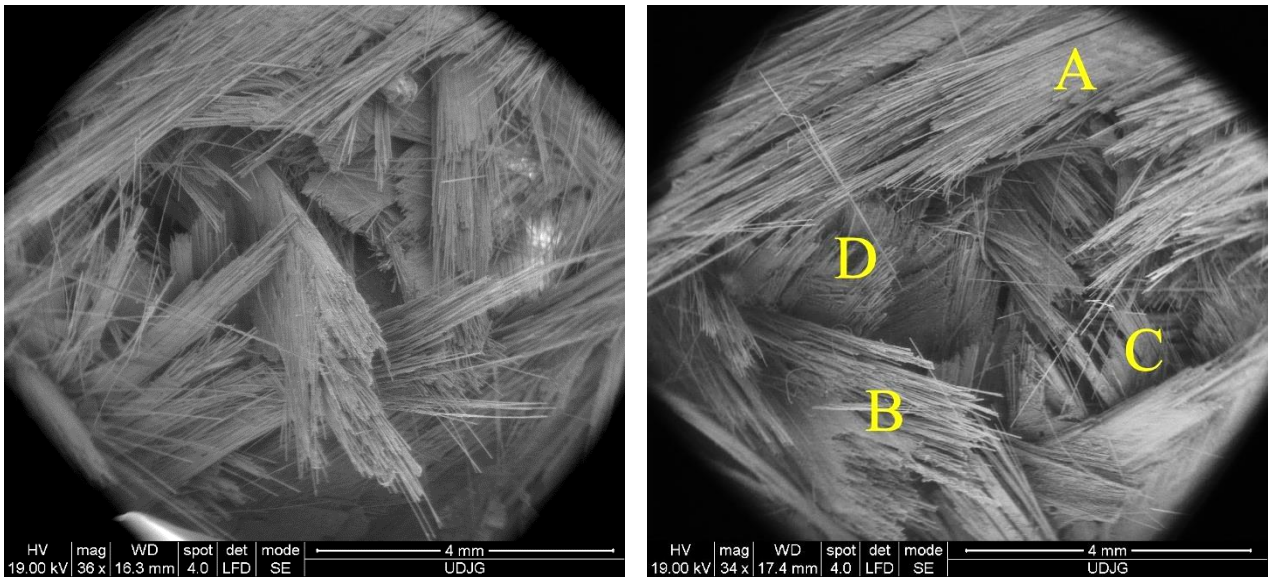

a) 10 mm Impactor b) 20 mm Impactor

Fig. 3.17. The local asymmetric break of the main yarns on substrates, for a sample impacted at a velocity of 4 m/s (view from the back of the plate)

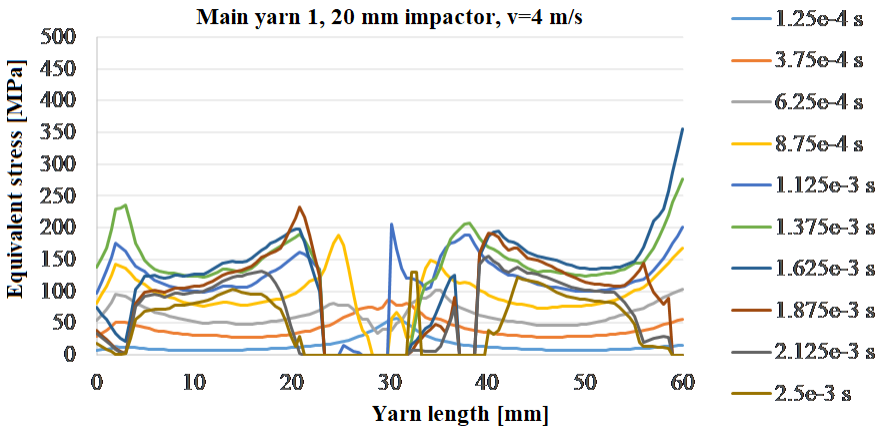

The main straight yarn on sublayer 1 brakes between the simulation moments of $t=6.25\times10^{-3}$ s and $t=8.75\times10^{-4}$ s. This time interval indicates the moment when the yarn can no longer withstand the load and fails under the applied stress.

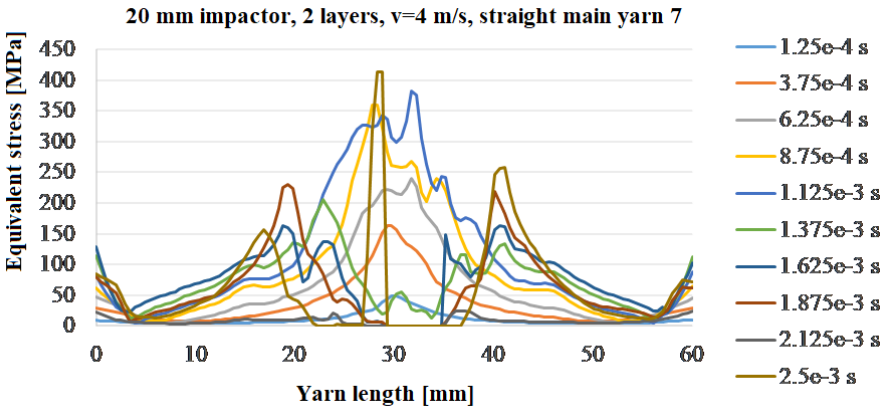

Main yarn on sublayer 7 breaks between $t=1.375\times10^{-3}$ s and $t=1.625\times10^{-3}$ s. High equivalent stresses appear on the broken ends of the yarn, indicating that they are subject to bending when the impactor passes, especially with its cylindrical part.

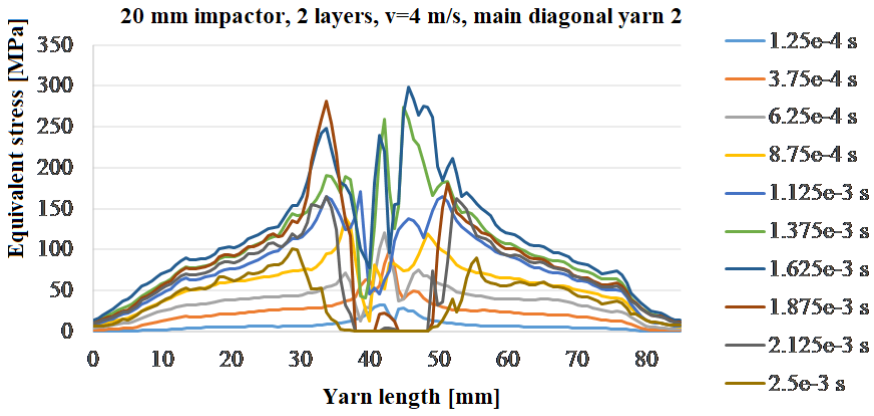

The diagonal main yarn on sublayer 2 breaks in two locations, between the simulation moments of $t=1.625\times10^{-3}$ s and $t=1.875\times10^{-3}$ s.

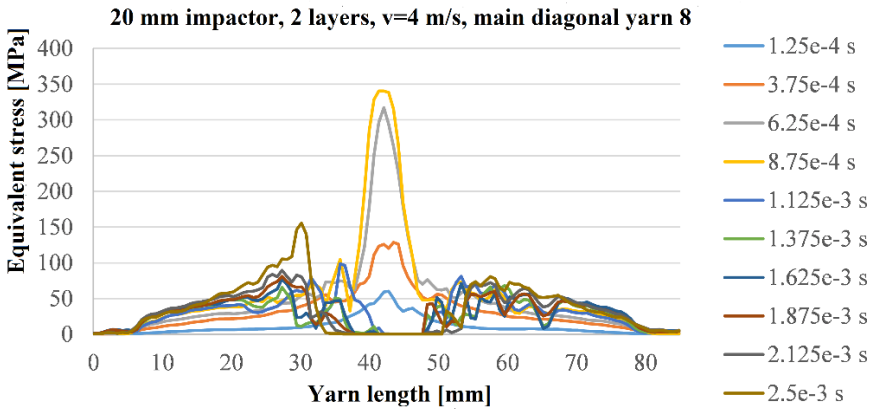

The diagonal main yarn on sublayer 8 breaks between the simulation moments of $t=8.75\times10^{-3}$ s and $t=1.125\times10^{-3}$ s.

Fig. 3.18. The distribution of equivalent stresses on diagonal main yarns, 20 mm diameter impactor.

3.7. Conclusions Regarding the Impact Simulation Results

The evaluation of the low-velocity impact simulation reveals that the destruction of the panels is similar for both impactors (one with a diameter of 10 mm and the other with 20 mm). However, the detachment model between yarns and between layers could be enhanced by introducing the zero-thickness cohesive zone model (CZM). The influence of yarn orientation has been highlighted, but the characteristics of yarn detachment might be overestimated. To further advance the research, it is proposed to determine the resin and composite characteristics through experiments in order to acquire the necessary parameters for applying the zero-thickness cohesive zone model [10], [19]. This step aims to refine the simulation model and provide more accurate predictions of the behavior of composite materials under low-velocity impact.

The model was run for the sample area of 60 mm×60 mm, but the panel geometry can be modified for larger area panels, close to those of the real application.

The model can be used for an initial estimate of the thickness for which the panel withstands a given impact, characterised by the velocity, shape and mass of the impactor.

Analysing the equivalent stress plots along the length of the main yarns (straight and diagonal), the local asymmetric break is confirmed by the SEM images in Fig. 3.17, in which a relatively small scale of magnification (×40, ×50) was chosen, so that the whole impactor orifice and the yarn breakage can be seen.

Chapter 4. Manufacturing Process of Multiaxial Glass Fibre Composites

4.1. Test plan for Testing Epoxy Resin Quadriaxial Fabric Composit

Analysis of technological solutions for multi-axial glass fiber woven and unidirectional composites, at low velocity impact has been investigated in several studies [16], [32], [43], [45]. Balasubramaniam K. et al. [6] proposed non-destructive testing based on calorimetric analysis to identify and locate impact damage barely visible in glass fiber reinforced polymer structures. Following impact, a subtile change in the thermal properties of the material occur, which can be detected and analysed to identify and locate barely visible damage. Rajan, B. G. et al. [41] analysed the impact resistance of hybrid carbon fibre and glass fibre composite pipes and found that the impact resistance decreases with increasing yarn orientation angle.

Fig. 4.1 details the test plan performed in this thesis. As can be seen, each test characterized by (number of layers, impactor, impact velocity) is repeated 3 times.

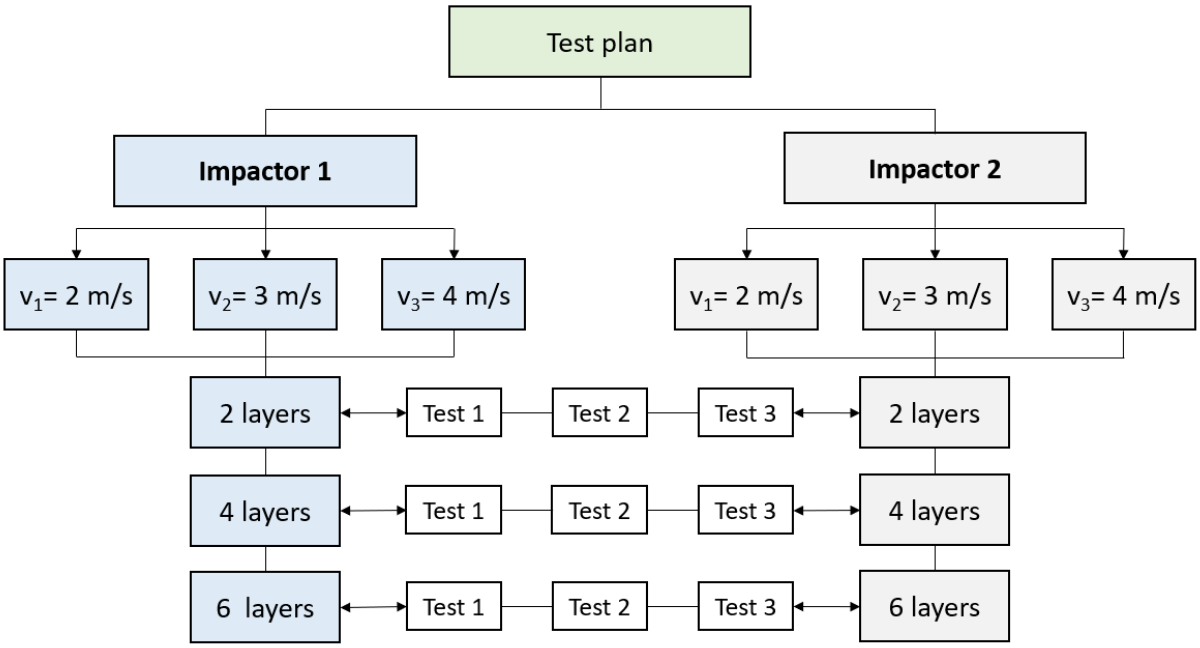

Fig. 4.1. Test plan performed in the thesis

4.2. Materials for in Manufacturing Composite Samples

4.2.1. Glass Fibre Fabric

The study used a fabric layered in four sublayers, with yarn orientation (0°/+45°/90°/-45°) (as shown in Fig. 4.2 where a) fabric view, b) one yarn and c) fibres in one yarn, with measured cross-section diameter), which provides quasi-isotropic properties. This fabric has the trade name "1200 g/m2 Quatriaxial Glass Cloth (0°/+45°/90°/-45°) 127" and is made of E-glass fibres [55]. The product was purchased from Castro, under the codes WTVQX1200-1 E-glass and Q1200E10Q [51].

Table 4.1 shows the elemental composition of glass fibres (average values) obtained by the EDX method.

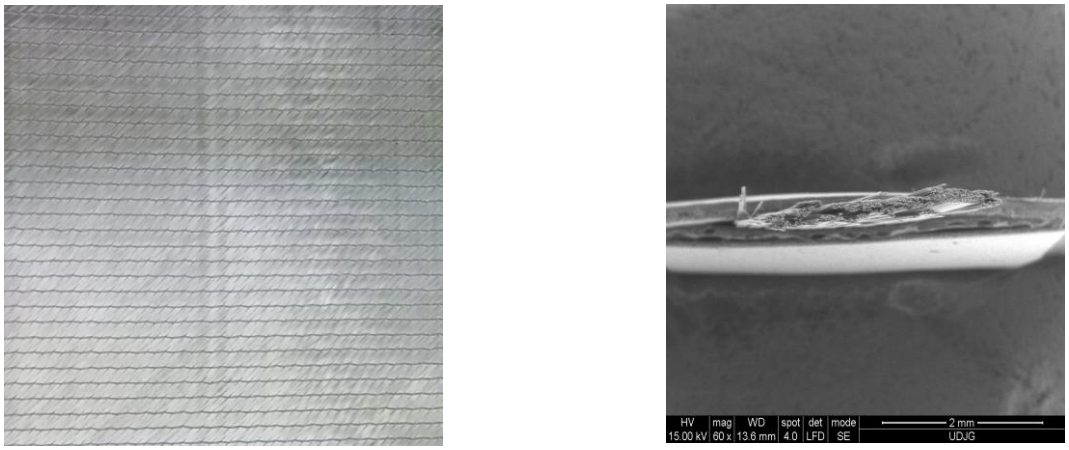

Fig. 4.2. Macro and micro images of quadriaxial fabric

By combining this fabric with the selected resin, superior performance composite panels can be produced for a wide range of applications, from bulding and marine domains to aerospace and sports equipment.

Table 4.1. Multiaxial glass fibre fabric architecture

No. of sublayer	Fibre orientation on the substrate	Weight of unit area (g/m^2)
1	0^0	283
2	45^0	300
3	90^0	307
4	-45^0	300
5	Auxiliary yarn	10
Total	-	1200(±3%)

Table 4.2. Analysis of the chemical composition of the glass fibre used (average values) [37]

Wt%													
B	**C**	**O**	**Na**	**Mg**	**Al**	**Si**	**S**	**Cl**	**K**	**Ca**	**Ti**	**Fe**	**Zn**
Fibre cross-sections													
29,39	24,75	9,03	0,38	0,42	3,55	14,21	1,75	0,20	0,22	8,88	0,50	2,19	4,43
Cross sections through the sheath													
30,81	24,11	10,34	0,48	0,74	3,61	13,21	1,61	0,22	0,48	9,07	0,88	2,82	6,69

4.2.2. Epoxy Resin Matrix

Biresin® CR82 resin [52] is an epoxy resin with outstanding performance, superior mechanical properties and excellent adhesion to glass fibres. This resin offers high resistance to mechanical load and a high degree of durability, making it ideal for use in applications with high strength and durability requirements [56]. CH80-2 hardener is a curing agent compatible with Biresin® CR82 resin, which imparts chemical and mechanical properties to the finished composite. This hardener improves impact strength and adhesion between resin and fibres, ensuring uniform resin distribution in the composite and anadequate curing reaction. The combination of Biresin® CR82 resin and CH80-2 hardener provides a highly effective bicomponent system for manufacturing glass fibre composites [54]. The choice of this resin is based on the advantages it offers in terms of mechanical properties, impact strength and adhesion to reinforcement, all of which being crucial for achieving high-quality composite panels.

For optimum results, it is important that the mixing ratio specified in the Biresin® CR82 resin data sheet with the CH80-2 hardener is precisely preserved. Deviations from this ratio may lead to reduced performance of the resulting composite.

Table 4.3. shows the mechanical and thermal properties of the already formed and thermally treated epoxy resin.

Tabelul 4.3. Mechanical and thermal characteristics of the resin used in this study [37], [52]

Mechanical properties for resin (after curing and thermal treatment)			
Resin **Biresin® CR82** (A)	With hardener **Biresin®** (B)		**CH80-2**
Tensile strength at break	SR EN ISO 527	MPa	90
Tensile elasticity modulus	SR EN ISO 527	MPa	3000
Deformation at break	SR EN ISO 527	%	5,6
Bending strength	SR EN ISO 178	MPa	130
Bending elasticity modulus	SR ENISO 178	MPa	3200
Compressive strength	SR EN ISO 604	MPa	105
Density	SR EN ISO 1183	g/cm^3	1,14
Shore hardness	SR EN ISO 868	-	D 85
Impact strength	SR EN ISO 179	kJ/m^2	66
Thermal characteristics for fully cured resin			
Resin **Biresin® CR82** (A)	With hardener **Biresin®** (B)		**CH80-2**
Temperature of thermal deformation	SR EN ISO 75-1	°C	83
Glass transition temperature	SR EN ISO 11357	°C	90

By using the CH80-2 hardener, the resulting resin has a fairly high tensile strength for this group of resins. With the CH80-1 hardener the resulting resin would have a tensile strength only 5% higher than that obtained using the CH80-2 hardener. The latter was chosen for component A because of the shorter processing time, but sufficient to press fit the developed layed-up composite. The choice of the CH80-2 hardener seems to be appropriate in this research, since the exothermal process and subsequent cooling were carried out within a reasonable time (about 1 hour after laying-up), allowing a proper curing (natural and artificial ageing) and maintaining the integrity of the composite.

For this study, it was chosen to keep the samples at 60°C, for 6 hours, in an oven with controlled parameters (time and temperature). Before treatment, the samples were allowed to be naturally aged for 7 days, at 23°C, in laboratory environment.

4.3. Laboratory Technology to Obtain Panels

The objective of the technology designed by the author was to obtain laboratory-level composite panels with multiaxial (quadriaxial) glass fibre fabrics, which will then be tested at low velocity impact.

The workshop was organised in two stands:

- stand I for cutting fibre glass fabrics,
- stand II for the manufacture of panels, including laying-up, pressing and work table for cutting and control.

The operations for producing the composite panels involve the following steps: cutting the quadriaxial fabric sheets (Fig. 4.3) with dimensions of 400 mm × 400 mm, weighing the stacks of 2 sheets, 4 sheets and 6 sheets, waxing the mold for easier panel removal, preparing the resin mixture by combining the two components in the recommended ratio by the manufacturer, applying resin to the fabric sheets (Fig. 4.4), pressing the composite in a press and maintaining pressure for 12 hours, removing from the press, inspecting and smoothing the edges, natural ageing in the laboratory atmosphere for seven days, artificial ageing and stabilization by heat treatment (6 hours at 60°C in a controlled temperature oven), quality checking of the panels, measuring certain characteristics (thickness at four points, weight, calculation of the fabric-to-composite mass ratio), marking 60 mm × 60 mm specimens for testing (Fig. 4.5), cutting them with a high-speed milling cutter in dry mode (Fig. 4.3), and finally, labeling them.

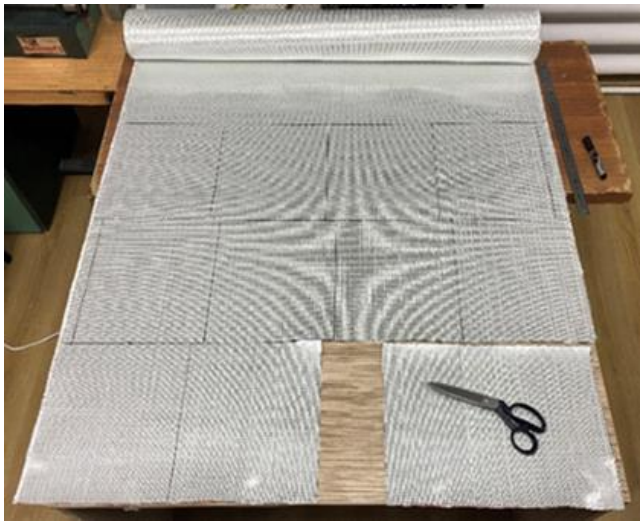

Fig. 4.3. Manufacturing the quadriaxial fabric sheets

Fig. 4.4. The press in which the sheets were placed

Fig. 4.5. Marking the test samples on the formed composite panels

The formed panels were placed inside the metal press and kept under load for a period of 12 hours.

After the pressing process was completed, the panels were removed and required the finishing of their edges. Once this process was finished, the final product was inspected, its thickness was measured at four points, and its weight was recorded.

Fig. 4.6. Cutting the samples from the composite panel

Figure 4.5 depicts the tracing process on the formed composite panels. In this stage, the composite panels are marked and delineated with areas, from which samples will be cut. These samples will subsequently undergo low-velocity impact tests. The 400 mm × 400 mm composite panel was divided into smaller panels of dimensions 60 mm × 60 mm.

4.4. Characterisation of the Produced Panels

The following composite panels were developed: 2 panels of 2 layers of quadriaxial fabric, 2 panels of 4 layers and 2 panels of 6 layers. For each set the characteristics in Tables 4.4, 4.5 and 4.6 were measured and calculated.

Table 4.4. Characteristics of 2-layer panels

No Crt.	Fabric weight	Panel weight	Resin weight *	Fabric/plate weight ratio **	Surface density ***	4-point thickness				
						1	2	3	4	average
	[g]	[g]	[g]		[kg/ m^2]	[mm]				
0	1	2	3	4	5	6	7	8	9	10
Panel 1	221.5	316	94.5	0.700	3.511	1.65	1.61	1.65	1.70	1.6525
Panel 2	221.5	316	94.5	0.700	3.511	1.65	1.70	1.6	1.6	1.6375
Average	**221.5**	**316**	**94.5**	**0.7**	**3.511**	**1.65**	**1.65**	**1.625**	**1.65**	**1.6425**
Max	221.5	316	94.5	0.7	3.511	1.65	1.70	1.65	1.7	1.6525
Min	221.5	316	94.5	0.7	3.511	1.65	1.61	1.6	1.6	1.6375

Table 4.5. Characteristics of 4-layer panels

No Crt.	Fabric weight	Panel weight	Resin weight*	Fabric/plate weight ratio **	Surface density ***	4-point thickness				
						1	2	3	4	average
	[g]	[g]	[g]		[kg/ m^2]	[mm]				
0	1	2	3	4	5	6	7	8	9	10
Panel 1	439.5	608.5	169	0.722	6.761	3.35	3.34	3.4	3.45	3.385
Panel 2	440	603.5	163.5	0.729	6.7	3.4	3.45	3.6	3.5	3.4875
Average	**439.75**	**606**	**166.25**	**0.7255**	**6.7305**	**3.375**	**3.395**	**3.5**	**3.475**	**3.436**
Max	440	608.5	169	0.729	6.761	3.4	3.45	3.6	3.5	3.4875
Min	439.5	603.5	163.5	0.722	6.7	3.35	3.34	3.4	3.45	3.385

Table 4.6. Characteristics of 6-layer panels

No Crt.	Fabric weight	Panel weight	Resin weight *	Fabric/plate weight ratio **	Surface density ***	4-point thickness				
						1	2	3	4	average
	[g]	[g]	[g]		[kg/ m^2]	[mm]				
0	1	2	3	4	5	6	7	8	9	10
Panel 1	664	897	233	0.740	9.966	5	4.5	5.5	5	5
Panel 2	662	883.5	221.5	0.749	9.816	5.6	5.7	5.8	5.7	5.7
Average	**663**	**890.25**	**227.25**	**0.744**	**9.891**	**5.3**	**5.1**	**5.65**	**5.35**	**5.35**
Max	664	897	233	0.749	9.66	5.6	5.7	5.8	5.7	5.7
Min	662	883.5	221.5	0.740	9.816	5	4.5	5.5	5	5

4.5. Test Procedure and Test Machine

Two different diameters of hemispherical, hardened steel impactor were used, impactor 1 being 10 mm in diameter, while impactor 2 is 20 mm in diameter. This is the only difference between the two types of impactors. The impactor velocity varies between 2 m/s and 4 m/s, with three different tested values, for each impactor size: v_1= 2 m/s, v_2= 3 m/s, v_3= 4 m/s.

The impact tests were performed at room temperature, using the Instron CEAST 9340 pneumatically controlled drop tower impact machine (maximum impact energy range 0.3-405 J, impact velocity range 0.77-4.65 m/s, impactor weight between 1 kg and 37.5 kg and drop height adjustable to achieve the desired impact energy), as shown in Fig. 4.7.

Figure 4.8 shows the graphs versus time of the parameters analysed in this paper, as obtained using the dedicated Instron CEAST 9340 impact testing machine software [57] and processed in Excel. It is a concrete example of tests performed with the same parameters and it is observed that the variation of the shape of the curves and the parameters of interest is very small compared to the measured values. This indicates a very good repeatability of the experiments and the thesis contains the representation of all tests performed in the Appendix with experimental data.

Fig. 4.7. Instron CEAST 9340 low velocity impact testing machine - [57] during testing

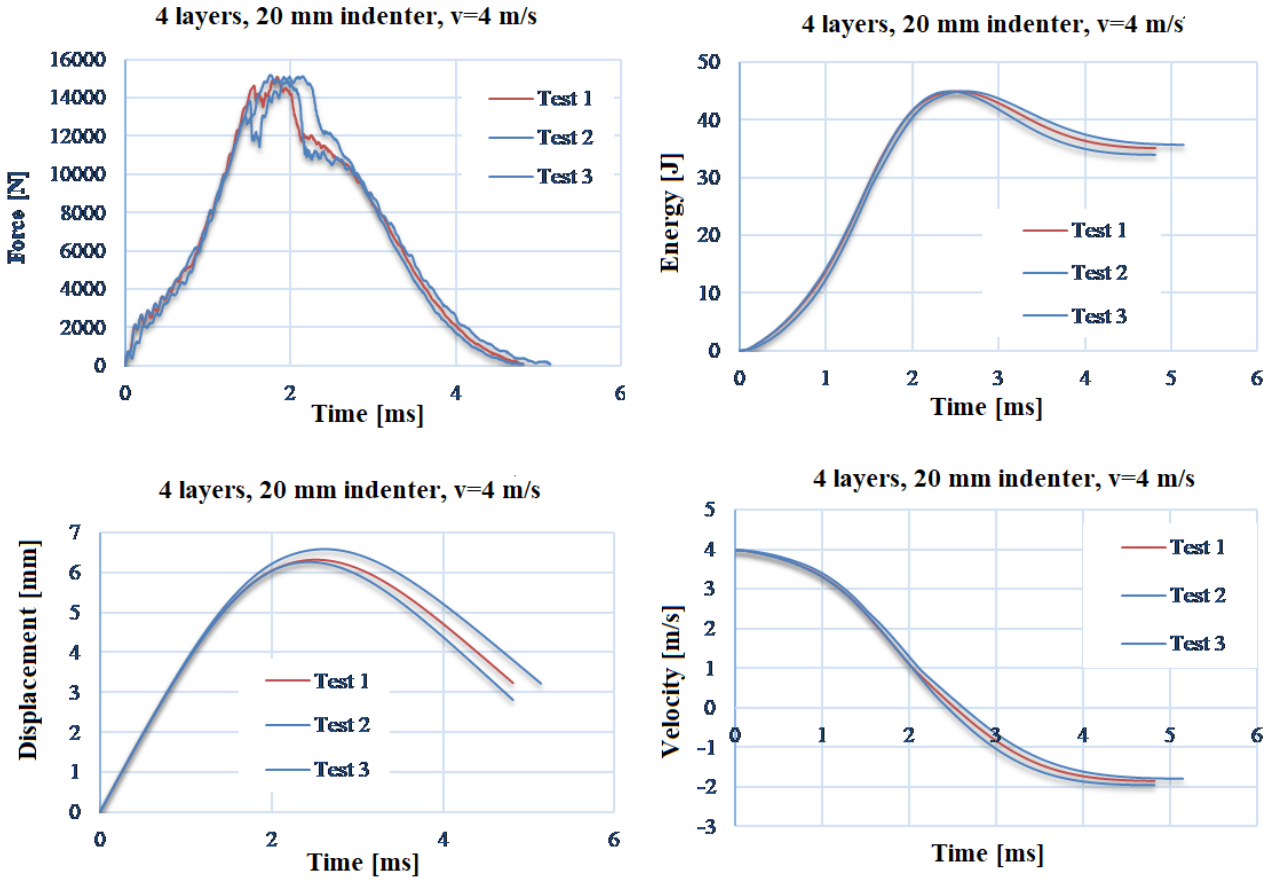

Fig. 4.8. Repeatability graphically exemplified, for tests on 4-layer panels, hit with the 20 mm impactor

4.6. Conclusions on the Manufacturing of the Panels

The characteristics of the composite panels developed for this study, are shown in Table 4.7. Note the ratio of the weight of the fabric to the weight of the panel, which has a mean of 0.723, with a standard deviation of 0.018, for all the panels. If the ratio of the standard deviation to the mean value of this panel characteristic is calculated as a percentage, 2.49% is obtained, reflecting a very good quality of the produced composite panels.

Table 4.7. Characteristics of developed panels

Panel code (number of layers)	**Thickness average**	**Weight**	**Density surface area**	**Weight ratio fabric/plate**
	[mm]	[g]	[kg/m^2]	-
S2	1.6425	316	3.511	0.700
S4	3.436	606	6.733	0.725
S6	5.25	890.25	9.891	0.744

Depending on the results of the impact tests, the technology can be improved for the selected thicknesses in order to reduce the production and inspection time, based on the experience gained in manufacturing these panel sets.

Chapter 5. Interpretation of Experimental Results and Investigation of Failure Mechanisms

5.1. Parameters in Low-Velocity Impact Test

This doctoral thesis has involved significant efforts in investigating the response of multiaxial glass fibre fabric composites to low-velocity impact, using advanced experimental methods, as also reported in [16], [42].

The low-velocity impact tests using the Instron CEAST 9340 impact machine allow the determination of parameters that characterize the behaviour of multiaxial glass fibre fabric composites under dynamic loading. Three tests were conducted for each set of testing parameters (number of layers, impact velocity, impactor diameter).

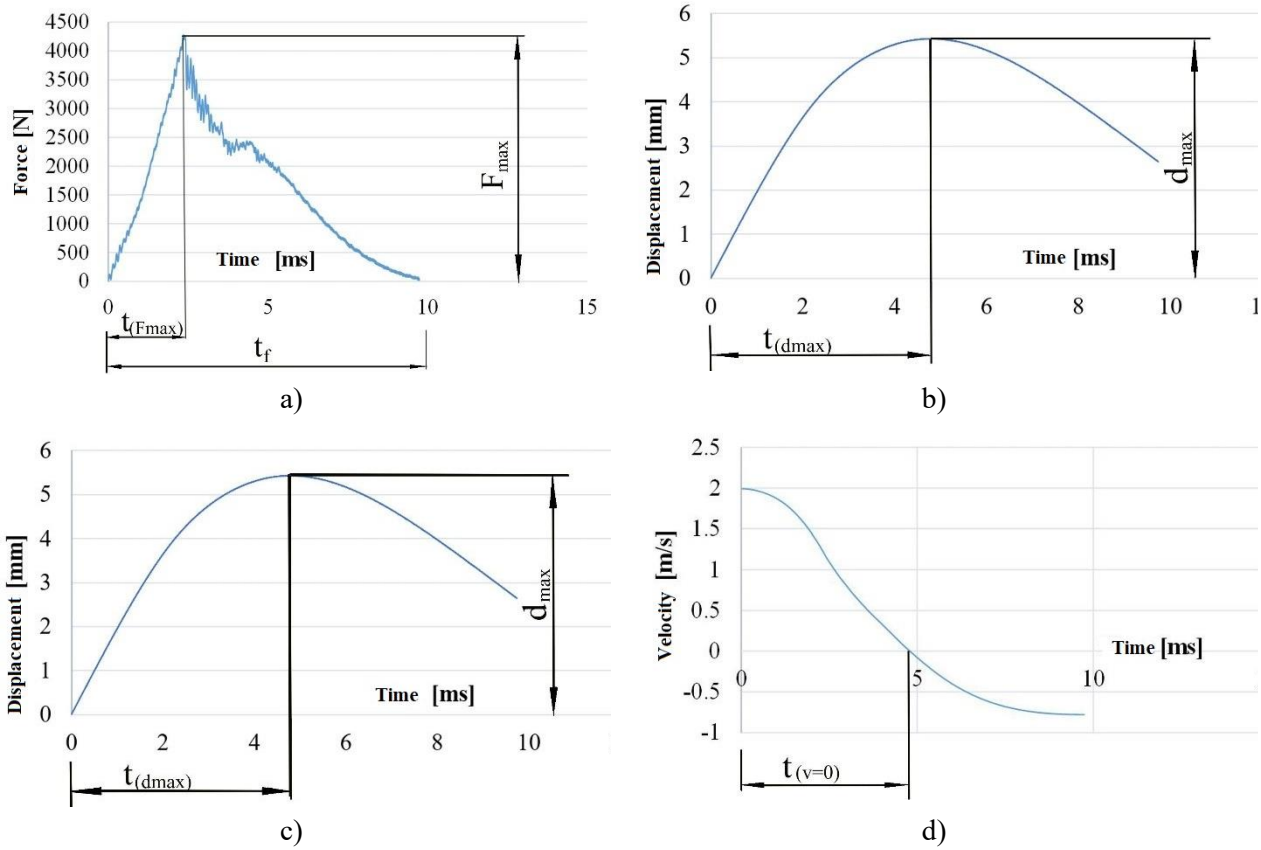

- **Fig. 5.1.** Significance of the analysed parameters

On the graphs obtained on the droptest machine it is possible to identify the stages of the impact process: stress in the elastic and elasto-plastic range up to the maximum force, an impact destruction stage, differentiated if the impactor is rejected (partial penetration) or if it passes through the plate (total penetration). Figure 5.1 shows the parameters of interest for characterizing the impact response of each sample. The notations have the following meanings:

g_p – panel thickness, mm,
F_{max} – maximum force, N,
$t_{(Fmax)}$ – time from the beginning of the impact to the maximum force value (F_{max}), ms,
t_f – time from beginning of impact to zero impact force (F=0), ms,
E_{max} – maximum energy, J,
$t_{(Emax)}$ – time from the beginning of the impact to the maximum value of absorbed energy (E_{max}), ms,
$t_{(v=0)}$ – time from the beginning of the impact to zero value of the impactor velocity (v=0), ms,

d_{max} – maximum displacement, mm,
$t_{(dmax)}$ – time from the beginning of the impact to maximum displacement, ms,
v_1 ,v_2, v_3 – nominal impact velocity, m/s (v_1=2 m/s, v_2=3 m/s and v_3=4 m/s).

Table 5.1 is an example of how these parameters are presented. The results of all performed tests are presented in the Appendix of the thesis. Figure 5.1 shows the time evolution of impactor force, displacement, velocity and shape of the impactor, energy absorbed by the specimen for three tests.

Table 5.1. Example of test results presentation, for tests performed with 10 mm impactor, with v_1=2 m/s, for the set of 3 panels made of 6 layers of quadriaxial fabric

Layers	**Test**	**Thickness**	**F_{max}**	**$t_{(Fmax)}$**	**t_f**	**$t_{(v=0)}$**	**E_{max}**	**$t_{(Emax)}$**	**d_{max}**	**$t_{(dmax)}$**
		[mm]	**[N]**	**[ms]**	**[ms]**	**[ms]**	**[J]**	**[ms]**	**[mm]**	**[ms]**
6	1	3.600	6611.047	2.105	4.619	2.265	10.902	2.265	2.647	2.265
	2	3.700	6143.685	2.097	4.760	2.330	10.903	2.330	2.667	2.239
	3	3.540	6435.433	1.809	4.172	2.055	10.884	2.055	2.300	2.055
Average		**3.613**	**6396.722**	**2.004**	**4.517**	**2.217**	**10.896**	**2.217**	**2.538**	**2.186**
Max		3.700	6611.047	2.105	4.760	2.330	10.903	2.330	2.667	2.256
Min		3.540	6143.685	1.809	4.172	2.055	10.884	2.055	2.300	2.055
SD		0.066	192.753	0.138	0.251	0.117	0.009	0.117	0.168	0.093
SD%		1.826	3.013	6.884	5.548	5.294	0.080	5.294	6.639	4.275

Max – maximum value of the determined/calculated parameter for all three tests, Min – minimum value of the determined/calculated parameter for all three tests, SD –standard deviation of a parameter obtained for all three values, SD% – standard deviation, expressed as a percentage, for the ratio between SD and the respective parameter mean value.

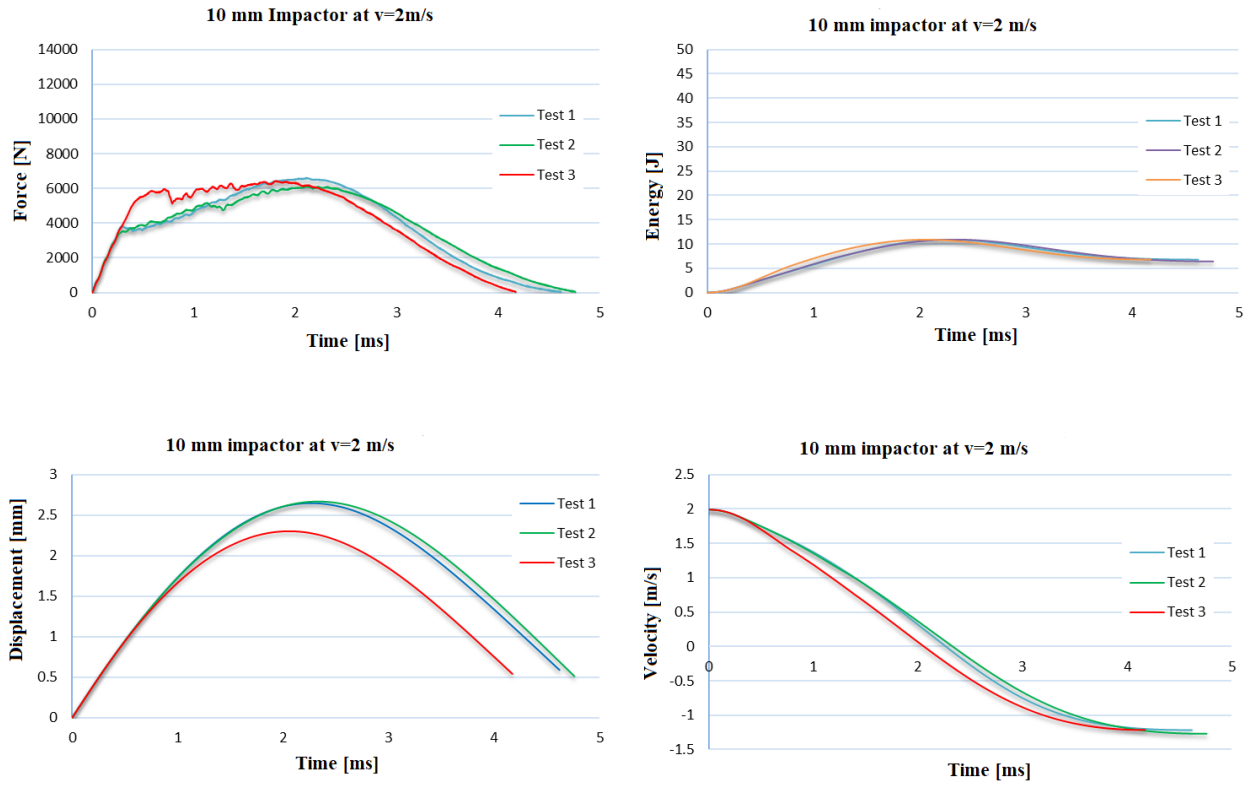

Fig. 5.2. Panels composed of 6 layers of glass fibre fabrics, tested with a 10 mm diameter impactor, at a velocity of 2 m/s

It is observed that the moment when E_{max} is recorded coincides with the moment when the impact velocity becomes zero (v=0), physically reflecting that the kinetic energy of the impactor was completely absorbed by the panel at that moment ($t_{(Emax)}= t_{(v=0)}$). Recoil of the impactor in the case of partial penetration is due to the elastic component of the panel deformations. In the case of total penetration, the impactor goes through the panel but retains a residual velocity, indicating that its entire initial kinetic energy was not absorbed by the panel.

5.2. Experimental Results on Instron CEAST 9340 Impact Machine

5.2.1. Influence of the Number of Layers on Impact Parameters

In this sub-chapter, experimental results obtained by performing impact tests with the Instron CEAST 9340 impact machine, on multiaxial glass fibre fabric composites are presented and analysed.

In Fig. 5.3, force-time graphs are given for the performed tests. Only one of the three tests was considered here, the one with an average evolution between the other two tests.

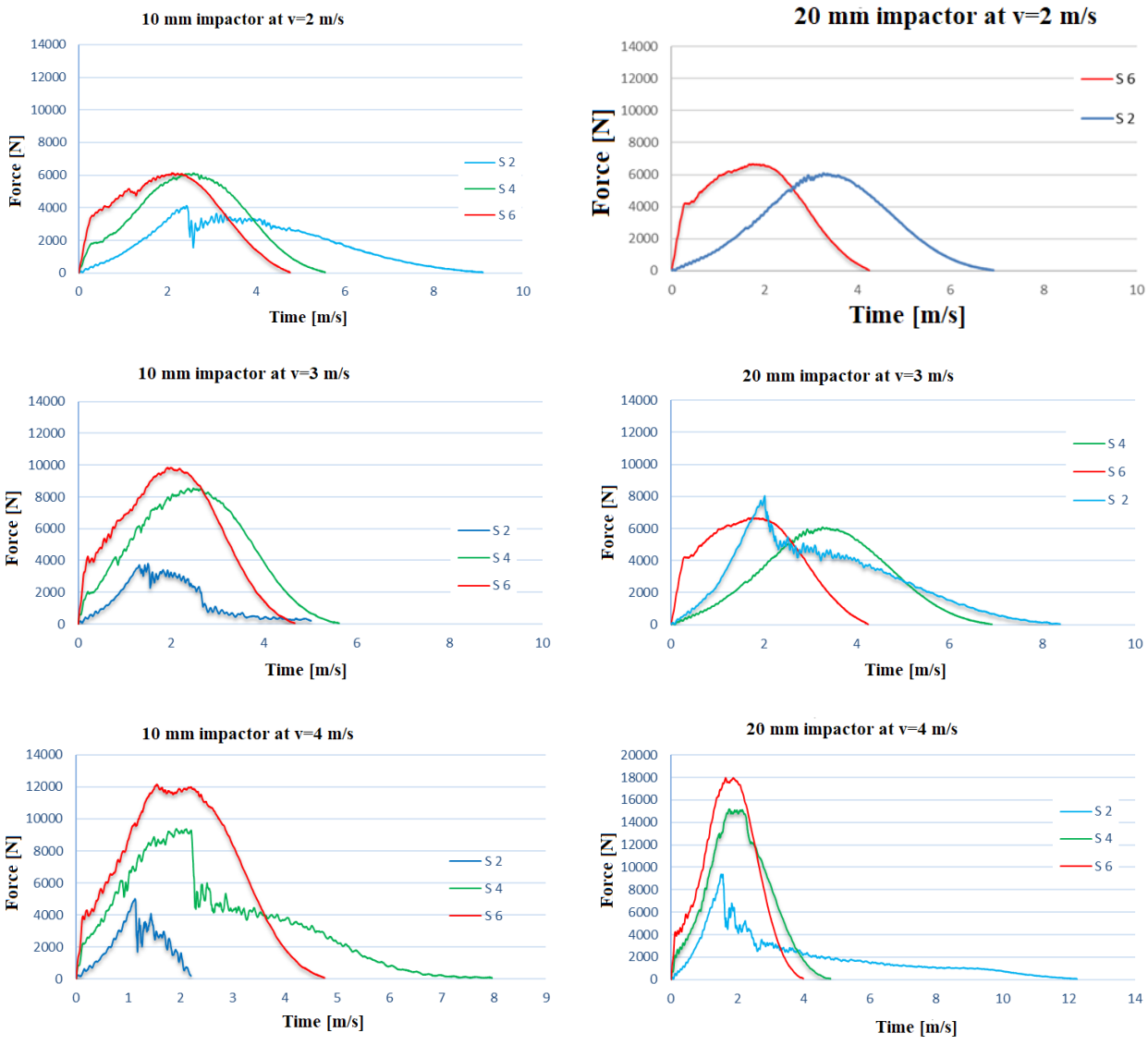

Impactor Ø 10 mm Impactor Ø 20 mm

Fig. 5.3. Influence of the number of layers on the force-time curve (s represents the number of layers)

By testing the material at different impact velocities, researchers can estimate strength and energy absorption capacity under extreme conditions.

In the left column of Fig. 5.3 are the graphs of the tests performed with the Ø 10 mm impactor and in the right column are the graphs of the tests performed with the Ø 20 mm impactor.

At the lowest impact velocity, v_1=2 m/s, it may be seen that F_{max} is obtained on the 6-layer panel, around 6000 N. Increasing the velocity to v_2=3 m/s causes the force to increase, reaching F_{max}=10000 N.

At Ø 20 mm impactor, also for the 6-layer quadriaxial fabric panel, F_{max} is 18000 N. The larger the radius of the impactor, the higher the force.

At the highest test velocity, at the Ø 10 mm impactor, F_{max} is 12000 N, while with the Ø 20 mm impactor, F_{max} is 18500 N, also on the 6-layer panel.

For the 2-layer panel F_{max} is obtained at 4000 N for v_1 and at 4500 N for v_2.

With the Ø 10 mm impactor, F_{max} occurs at v_1=2 m/s for the 6-layer panel and for the other panels the values of this parameter are close.

At v_2=3 m/s, F_{max} occurs more rapidly on the thin 2-layer panels and the longest time $t_{(Fmax)}$ is obtained for the 4-layer panel and close to the 6-layer panel.

With the Ø 10 mm impactor, at v_3=4 m/s, F_{max} occurs at the lowest time at the thinnest panel.

$$F_{max\,(2s)} < F_{max\,(4s)} < F_{max\,(6s)} \tag{5.1}$$

The same goes for the Ø 20 mm impactor.

The impact time until force cancellation is longer for thin panels with 2 layers of quadriaxial fabric ($t_f = 10$ ms) and increasingly lower on panels with more layers.

The deterioration that occurs in the panels can be explained by the fact that the impactor slows down and prolongs the duration of the impact, and thus the compressive stress.

5.2.2. Influence of Impact Energy and Impact Velocity on Impact Parameters

This analysis provides a comprehensive view of how the composite reacts to impact of different different velocities or energies and provide important information about energy absorption and deformation of the structure in critical situations.

Figure 5.4 shows the thickness of the panels as a function of the number of layers. The evolution is almost linear, suggesting the same glass fibre content (in mass percentage). The quality of the panels is reflected by the very low thickness variation.

Figure 5.5 presents absorbed energy - time curves.

The force-time and energy-time graphs indicate that, in the case of panels with partial penetration, the impactor comes to a stop within the panel, and the impactor's entire kinetic energy is absorbed by the panel. The form of the curves indicates that the energy increases over time until reaches a maximum (E_{max}), and then gradually decreases when the impactor is rebounded on the panel and comes to

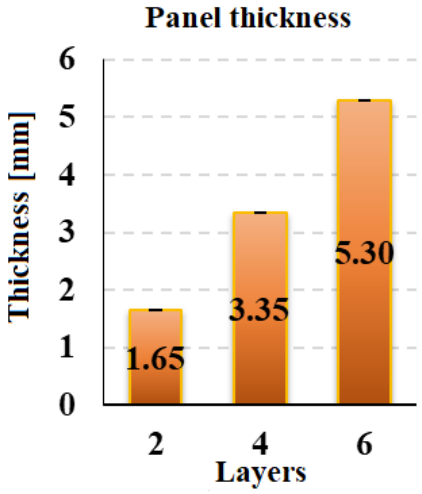

Fig. 5.4. Panel thicknesses (thicknesses measured on panels cut at 60 mm × 60 mm)

a stop. In the case of panels with total penetration, however, the disintegration of the panel does not absorb the entire kinetic energy of the impact.

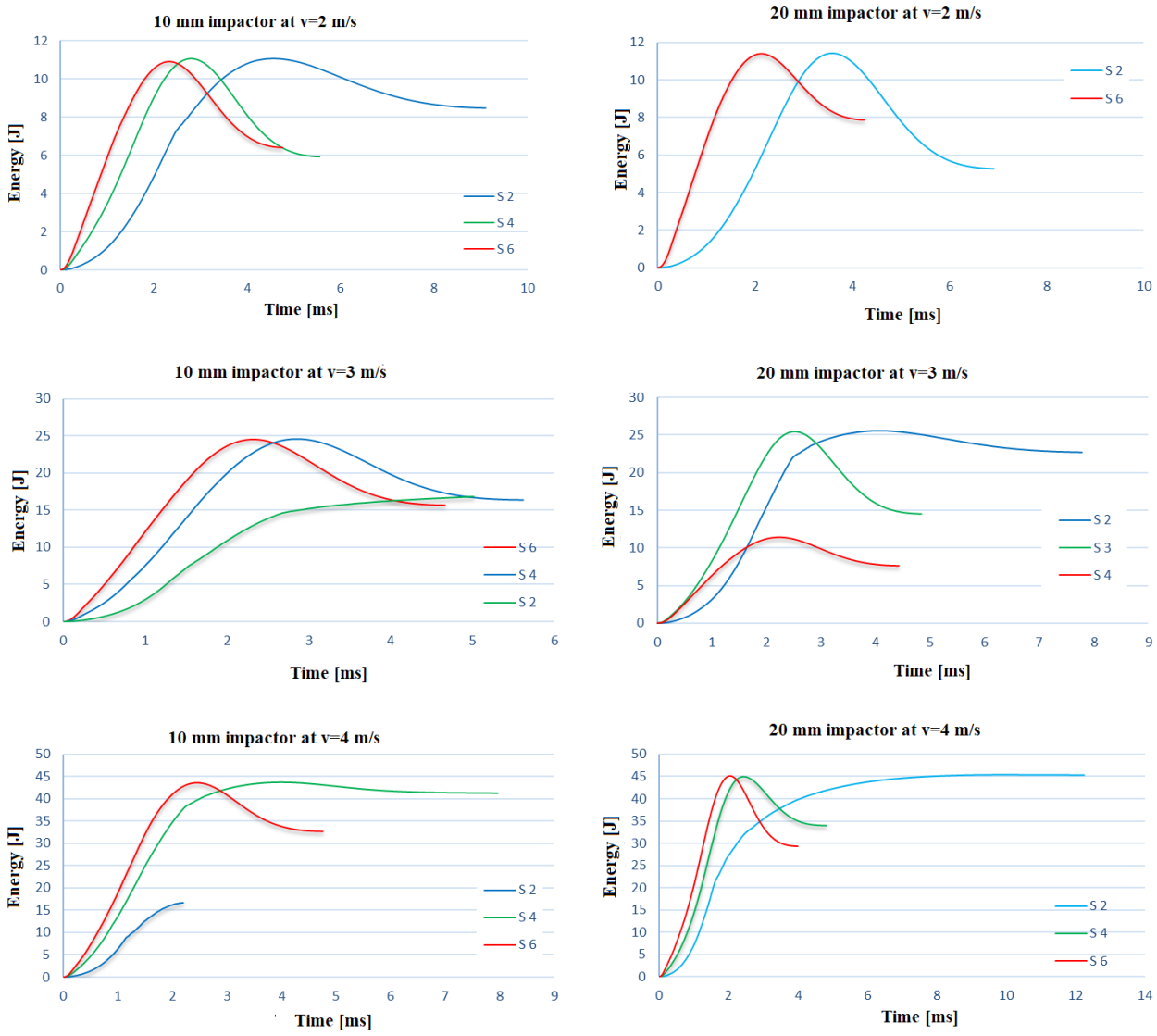

Impactor Ø 10 mm Impactor Ø 20 mm

Fig. 5.5. Influence of the number of layers on the energy-time curve

Figure 5.6 depicts the influence of impact velocity on the number of layers in the analysed composites. These graphs provide insights into how the number of layers in the composite material affects its behaviour under various low-velocity impact.

The destruction of the panel does not absorb all of the kinetic energy of the impact in panels with complete penetration. The energy-time graphs clearly demonstrate which panels exhibit full penetration (the maximum absorbed energy is not close to the impact energy; it has a lower value because the impactor continues its trajectory with a residual velocity) and which exhibit partial penetration (some energy is transferred back to the impactor, causing it to rebound due to elastic deformations).

Total penetration occurs at v_2=3 m/s, for 2-layer panels. The other panels were only partially damaged at this impact velocity, as demonstrated by the energy-time graphs, where the energy passed on to the panel was recorded as 11 J, the established value on the test machine.

Panels of different thicknesses have different gradients of the energy-time curve for the same impactor and impact velocity. The energy absorption gradient is higher for thicker, harder panels. Even with partial and entire penetration, the gradient of energy accumulation maintains the same pattern for the energy-time curve (thinner panels tend to be more elastic).

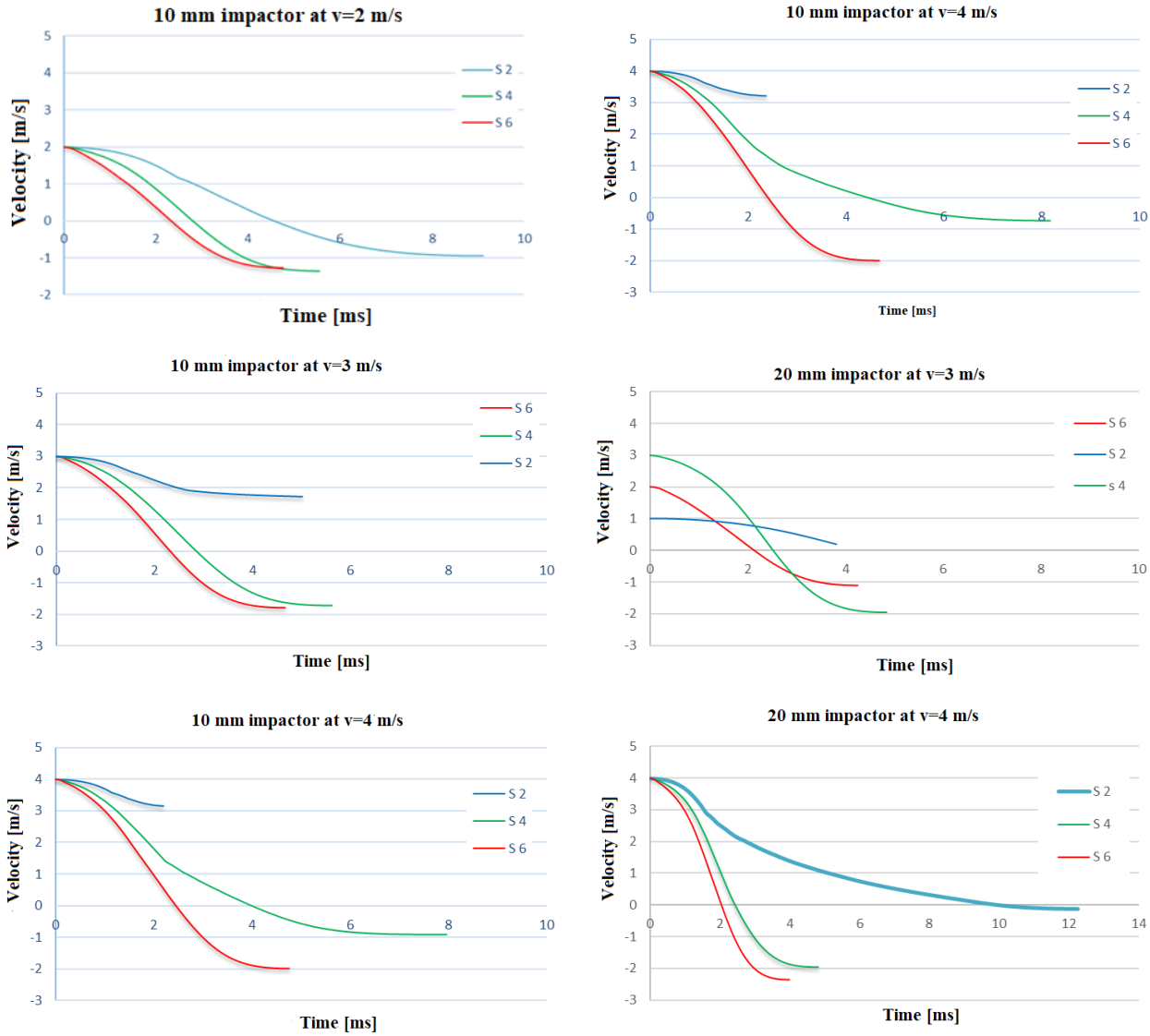

Impactor de Ø 10 mm Impactor de Ø 20 mm

Fig. 5.6. The Influence of Impact Velocity on the Number of Layers

Panels with partial penetration restrict the impactor completely and absorb all of the kinetic energy, whereas panels with total penetration, the panel retains only a fraction of the impact energy and allow the impactor to continue its trajectory with a residual velocity, lower than the impact velocity. The thickness of the panels affects their energy absorption capacity, with thicker panels absorbing greater amounts of energy.

5.3. Investigation of the Failure Mechanisms

In low-velocity impact tests the most critical composite failure mechanisms are yarn/fiber breakage and delamination [25] (Fig. 5.7).

Fibre breaking in composite materials happens as a result of the compressive behavior, which causes fibres to break toward their point of contact and the dispersion of high stress values surrounding the direct contact and under the impactor. Due to the matrix lower mechanical properties, this could also be craked after fibre cracking and delamination. Fibre failure occurs as a result of the low-velocity transverse impact and might result in fibre fragmentation due to high stresses occurring in different locations of the fibre. The significant value of the strain and stress field cause fiber breakage. The impactor also causes tensile stresses and high bending stresses in the zone of the fibre/yarn closer to the impactor direct contact zone.

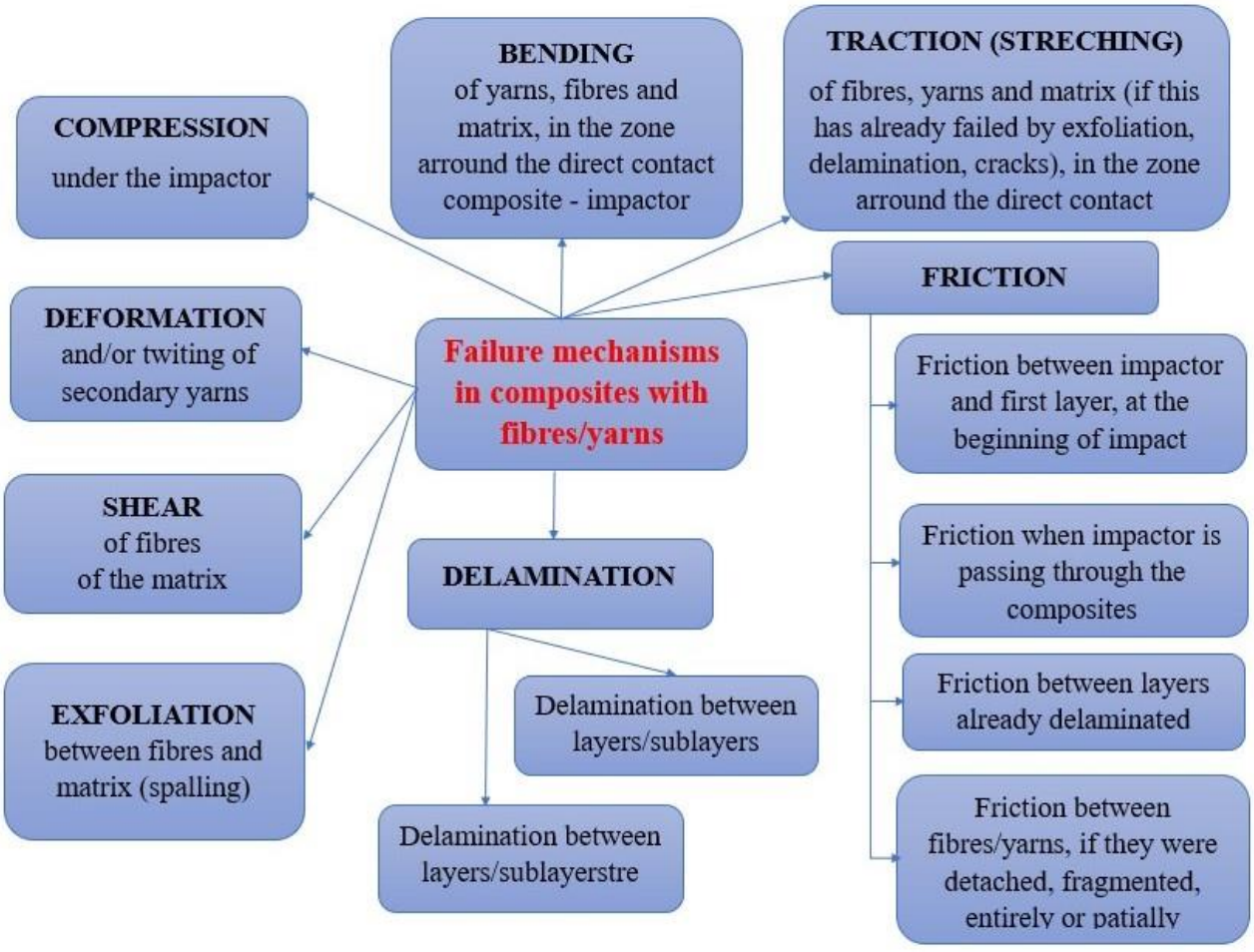

Fig. 5.7. Failure mechanisms in fibre composites

Figure 5.7 shows the different failure mechanisms that may occur in fibre composites.

The penetration mode was also studied macroscopically (Fig. 5.8). Absorption of impact kinetic energy is important in delamination, breakage and elastic and plastic bending of the composite yarns/fibres.

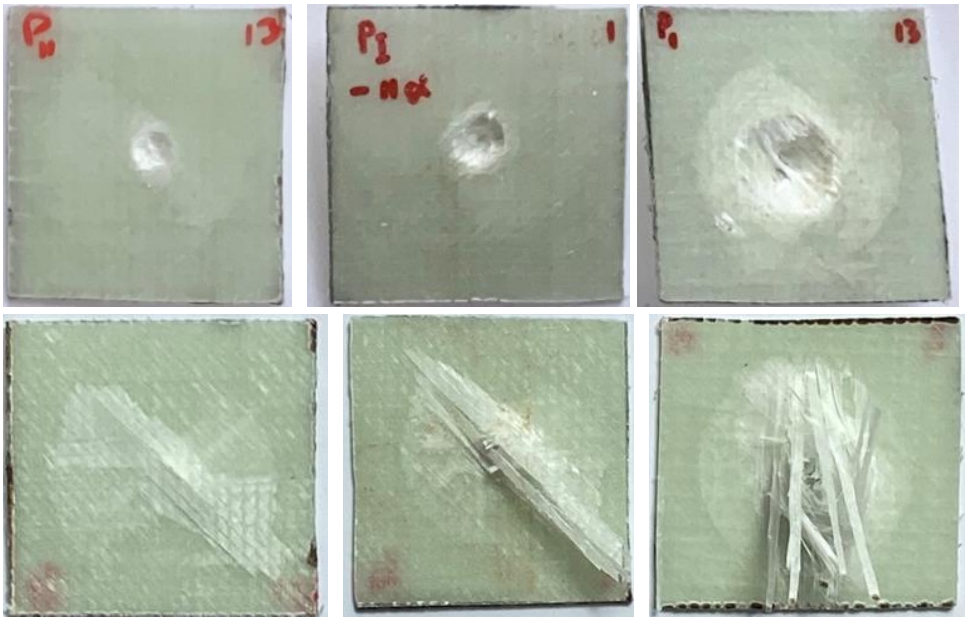

Fig. 5.8. Macroscopic views: front (top) and back (bottom) of 2-layer composites subjected to impact at impact velocities v_1, v_2 and v_3 (from left to right) using the 10 mm impactor (all composite plates are 60 mm × 60 mm) [39]

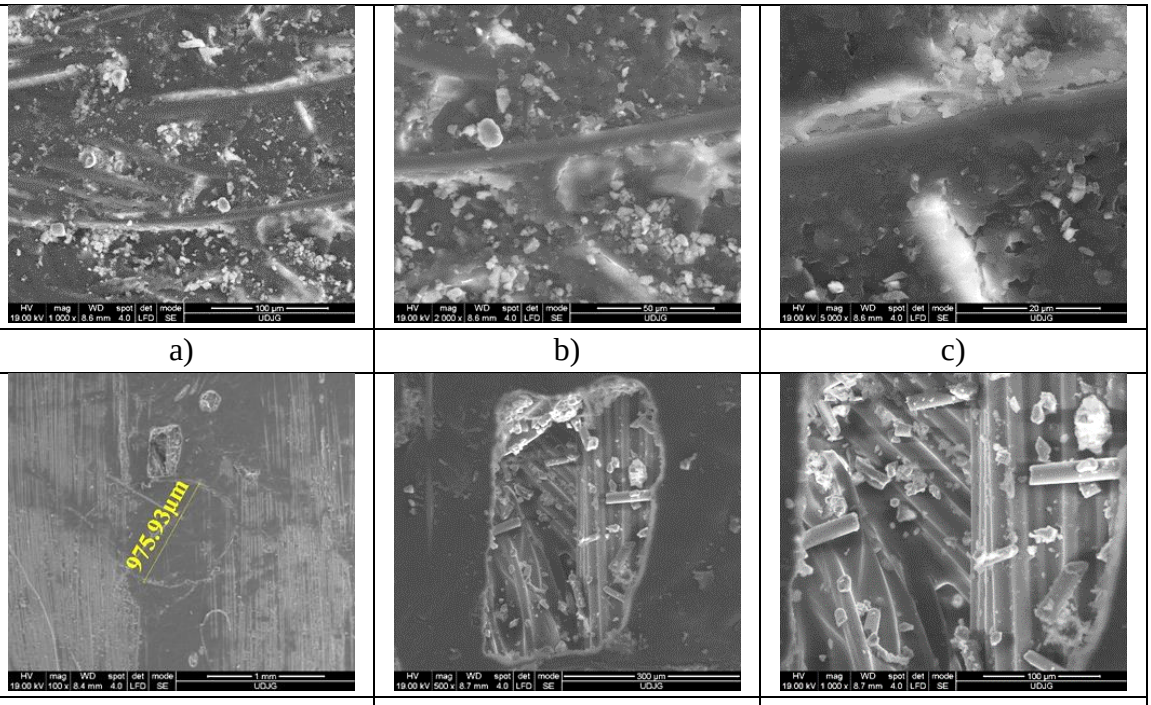

a) b) c)

d) e) f)

Fig. 5.9. SEM images of front (top) and back (bottom) for the 2-layer composite panel, subjected to v_1=2 m/s, after being hit with 10 mm diameter impactor

Analysis of SEM images of 2-layer composites, subjected to impact with v_1=2 m/s and the 10 mm impactor (Fig. 5.9) revealed significant processes, such as matrix cracking and fibre displacement. These observations are of major importance for understanding the behaviour of this type of material under high stress conditions and provide valuable information for improving and optimizing the performance of composite materials used in

impact applications. Thus, SEM images from Fig. 5.9 reveal: a) spalling of the matrix and bending in plane of secondary yarns, near the broken yarns/fibres, b) a details from a) with visible cracks in the matrix and detachment between fibre and matrix, c) same failure (cracks in the matrix and detachment of the fibre from the matrix, but at a higher magnification (×5000), d) cracks in the matrix on the back of the panel, suggesting the circular zone with high values of stress, e) spalling of the matrix, near the impact axis and f) detail of this zone, with several broken fibres, fragments and three of four orientations of the yarns in the fabric.

SEM analysis of 2-layer composites subjected to v3 impact with a 10 mm impactor, shows yarn breaks, which occur at different positions on the fibres, and a shear break (Fig. 5.10). In image (a), it can be clearly observed broken yarns, a process indicating a weakening of the fibre-matrix bond or a stress concentration in that area. Particularly interesting is the fact that the yarn breakage occurs at different positions on the fibre of the composite material, suggesting the variability of fibre characteristics within the material. In image (b), the orientation of the fibres can be clearly seen. This is particularly important in the performance evaluation of composite materials, as fibre orientation can significantly influence the strength and stiffness of the material. In Fig. 5.10c, multiple breakings of fibres are observed, such as fragmental bending breaking and shear breaking. Fragmentary bending fracture indicates that the composite material has been subjected to bending stresses leading to progressive fibre breakage. Shear failure also indicates the exertion of tangential forces on the fibres, resulting in a specific break (almost perpendicular broken section to the fibre length). In pictures (d) and (e), it can be seen how the impactor passes through and disorganizes the yarns and fibres. This disorganisation of the fibres can be caused by the intense stresses generated by the impactor and can lead to an asymmetric breakage of the fibres in the affected area.

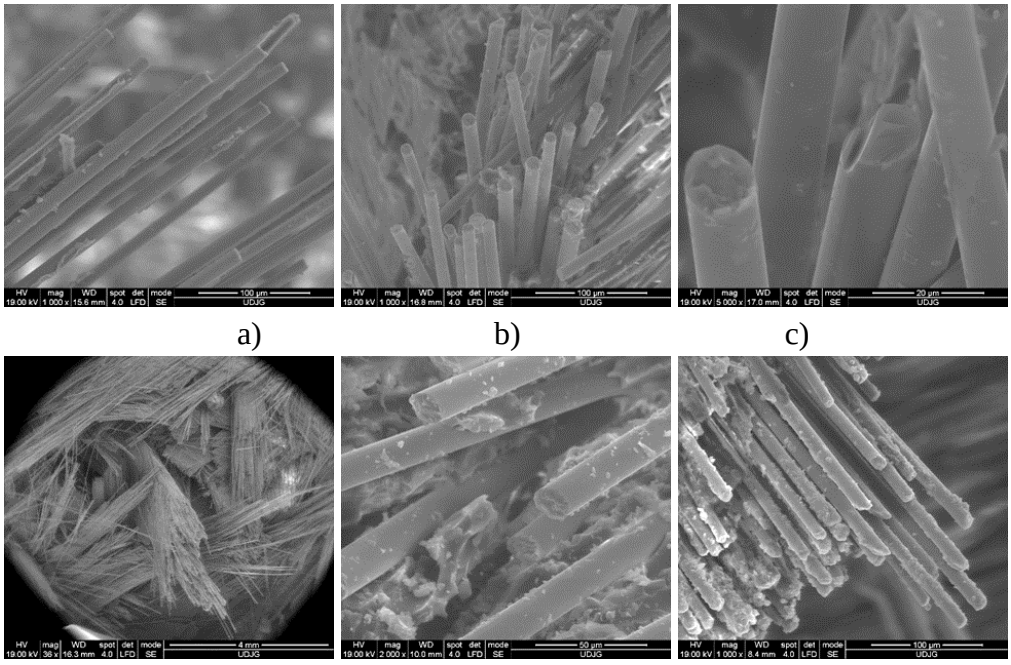

a) b) c)

d) e) f)

Fig. 5.10. SEM images of front (top) and back (bottom) 2-layer composite materials subjected to v_3 impact with 10 mm impactor

Figure 5.11 shows the macroscopic observation of 2-layer composites impacted at different impact velocities (v_1=2 m/s, v_2=3 m/s and v_3=4 m/s), using the 20 mm diameter impactor. The picture presents the visual aspects of the front and back surfaces of the composite material after impact. It is obvious that this panel could be recommended for impact protection only for v1=2 m/s and energy of 11 J. For greater velocities (v2=3 m/s and v3=4 m/s), the panel back reveals severe delamination of the last sublayer and a too deep penetration of the impactor, the main yarns on the last sublayers being broken.

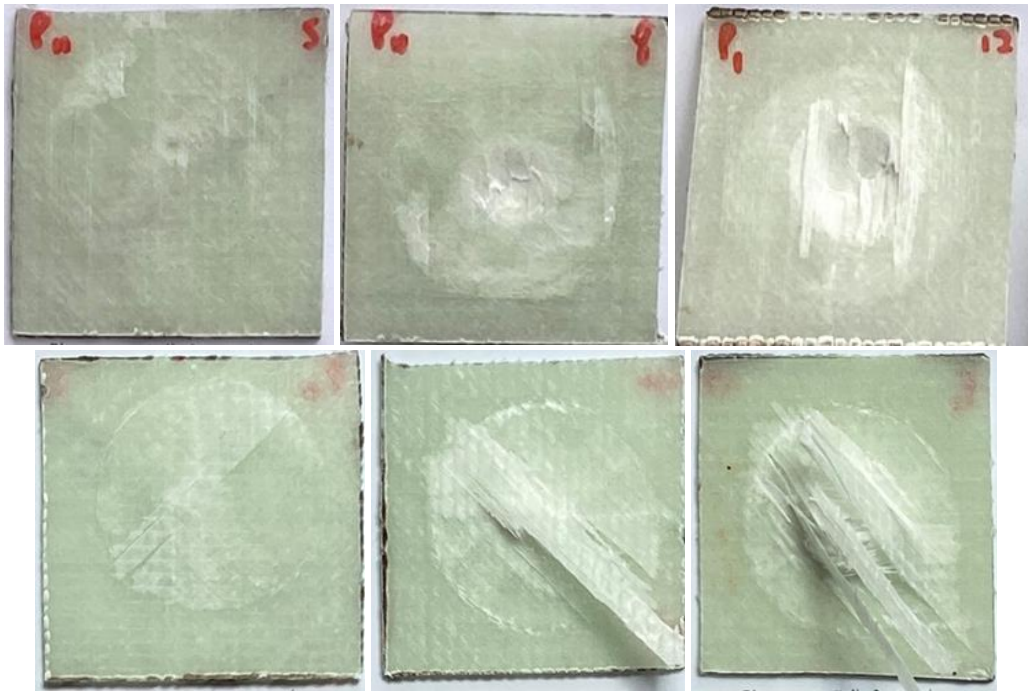

Fig. 5.11. Macroscopic views: front (top) and back (bottom) of 2-layer composites subjected to impact at impact velocities v_1, v_2 and v_3 (left to right) using the 20 mm impactor (all composite plates are 60 mm × 60 mm) [39]

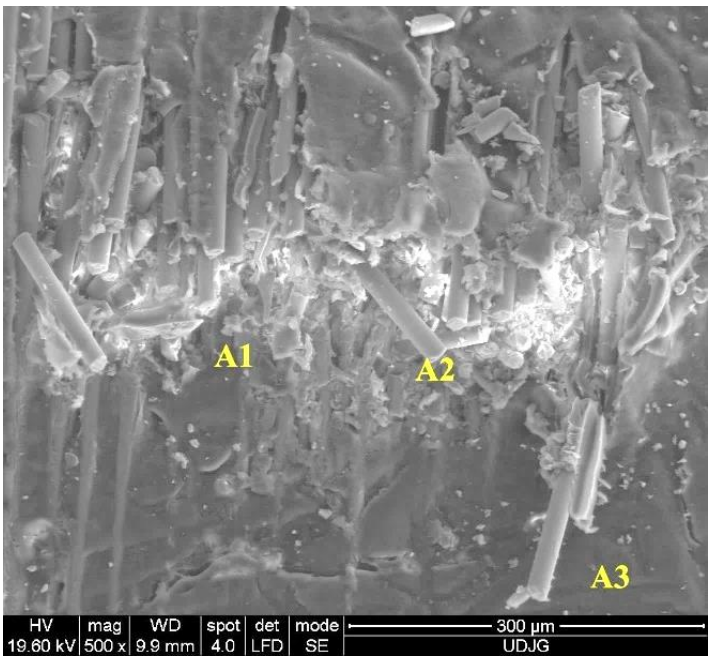

Fig. 5.12. SEM image of 6-layer composite subjected to v_1 impact with Ø 10 mm impactor

Figure 5.12 presents the SEM image for the 6-layer panel at Ø 10 mm impactor at v_1=2 m/s. A1, A2 and A3 represent different fibre orientations and B points out the shape of the matrix after the fibre was detached.

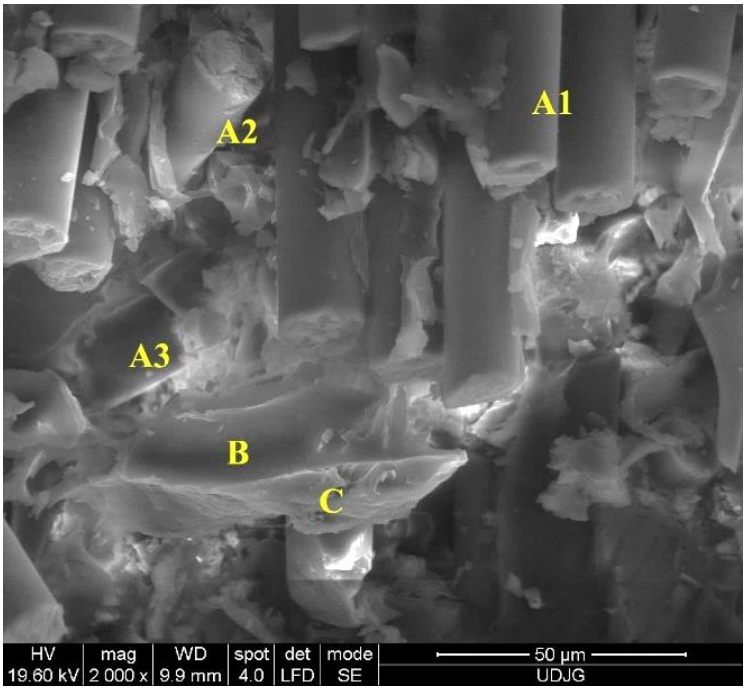

Fig. 5.13. SEM image of 6-layer composite materials subjected to v_1 impact with Ø 10 mm impactor

Fibers can be observed aligned in several orientations in Figure 5.13. With mentions to A1, A2, and A3 as different fiber orientations, it is clear that the materials structure is anisotropic, determined by different fibre orientations.

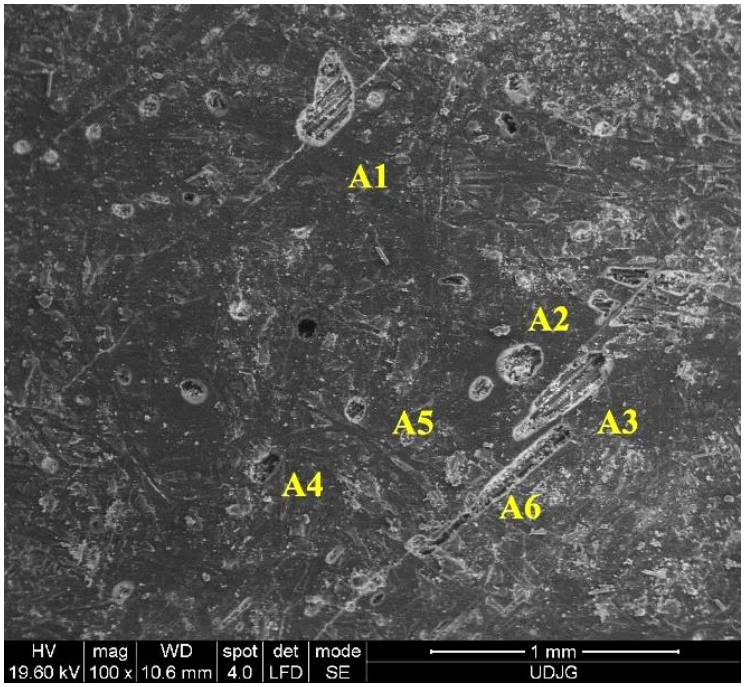

Fig. 5.14. SEM image of 6-layer composite materials subjected to v_1 impact with Ø 10 mm impactor

Exfoliations of various sizes, assigned A1, A2, A3, A4 and A5, may be seen at a larger scale, x100, in Fig. 5.14. The fibres are not damaged in the locations where exfoliation occurred. Small exfoliations indicate that the materials are of outstanding quality, and severe breakdown of the material was not produced for the palte in this figure.

5.4. Synthesis of Experimental Results and Conclusions

The results of this study indicate that the impact velocity and the number of layers in the panels determine the maximum force, F_{max} (Fig. 5.15), and the impact duration, t_f (Fig. 5.17), considered until the force on the panel is canceled, i.e., $F_{(tf)}=0$. At the same velocities and number of layers of quadraxial fabric, the 20 mm diameter impactor generates higher maximum force than the 10 mm diameter impactor.

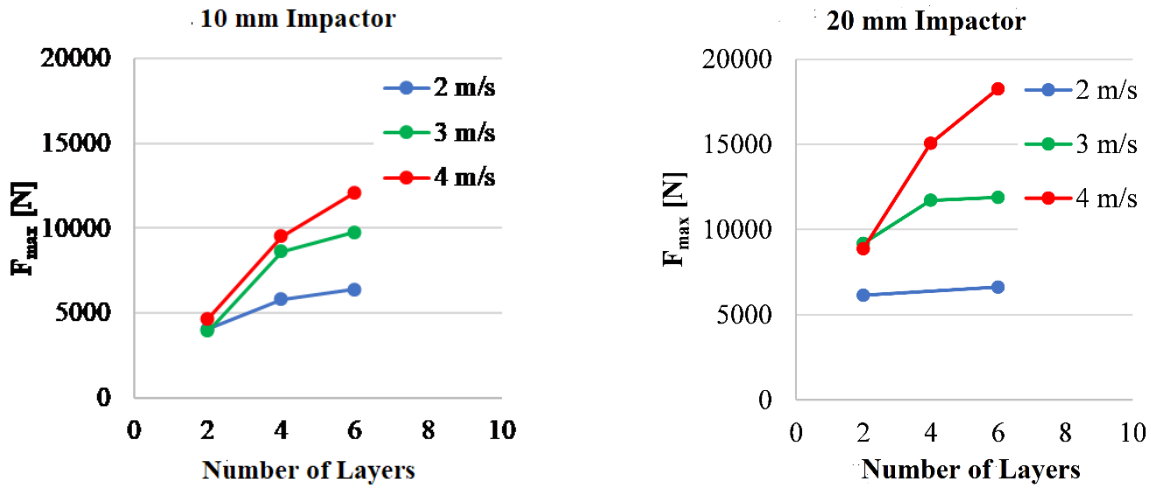

Fig. 5.15. The influence of the obtained F_{max} for the tests conducted with the 10 mm diameter impactor and the 20 mm diameter impactor on the number of layers.

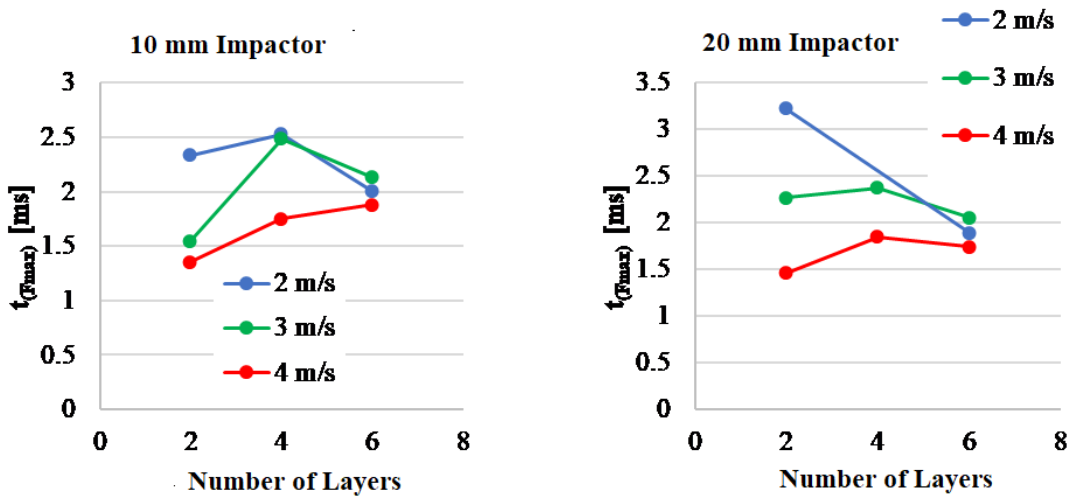

Fig. 5.16. The influence of the number of layers of quadriaxial fabric on the moment when F_{max}, $t_{(Fmax)}$

Impact resistance is higher in panels with more layers, while impact velocity effects both the value of F_{max} and the duration of the impact, t_f. The diameter of the impactor also influences the F_{max}

value and when it occurs. These findings can be used to improve the impact resistance of materials and structures used in a variety of industrial applications.

Figures 5.17, 5.18, 5.19 and 5.20 depict the influence of the number of layers on certain parameters of the impact, in the case of composites subjected to low-velocity impact. The duration until the force is nullified (F=0) decreases with the increase in the number of layers, except for panels impacted by the 10 mm diameter impactor, at v_3=4 m/s. The maximum displacement, d_{max}, decreases with the increase in the number of layers, but for the same panel, it increases with the impact velocity. For impact velocities of 2 m/s and 3 m/s, the graphs of the moments generating the maximum displacement are very close. For the 10 mm impactor, this time is approximately 1 ms longer (the value for the 2-layer panel is not provided as penetration is total).

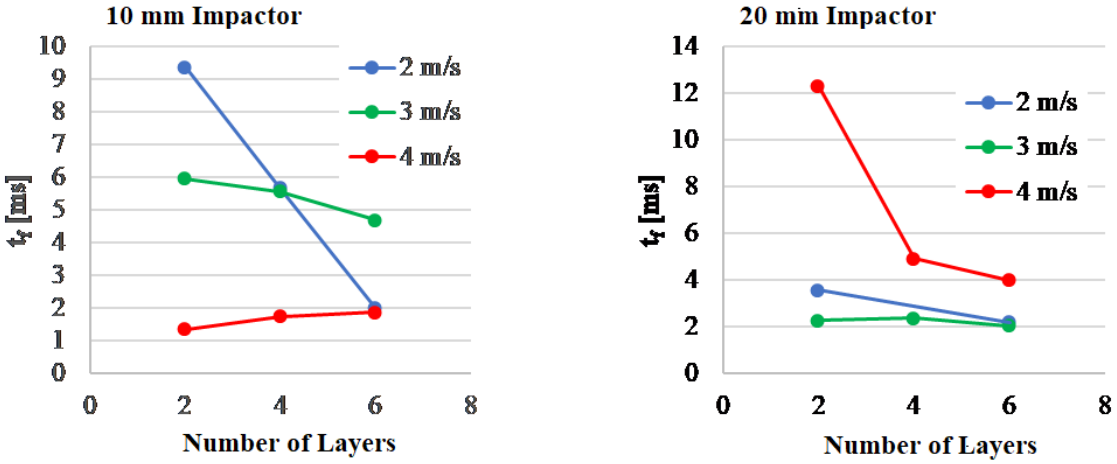

Fig. 5.17. Influence of the number of layers of quadriaxial fabric on the impact duration, t_f, considered from the increase of impact force until its nullification ($F_{(tf)}$=0)

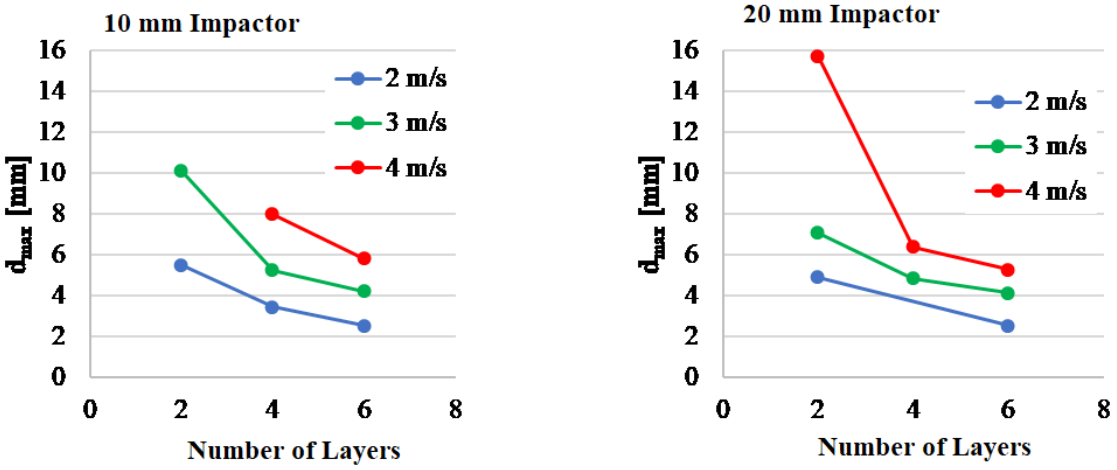

Fig. 5.18. Influence of the number of layers of quadriaxial fabric on the maximum displacement of the impactor, d_{max} (not represented for total penetration)

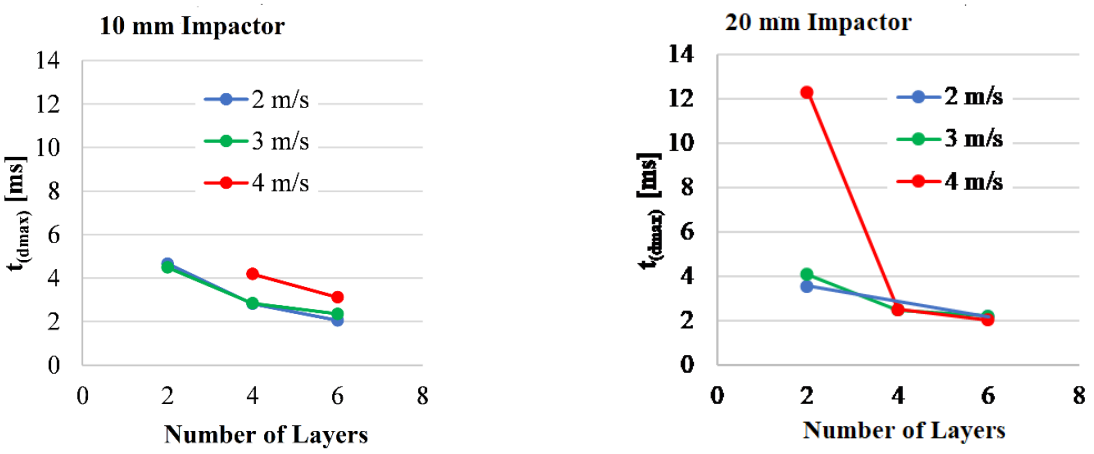

Fig. 5.19. Influence of the number of layers on the duration until the maximum displacement is reached, $t_{(dmax)}$

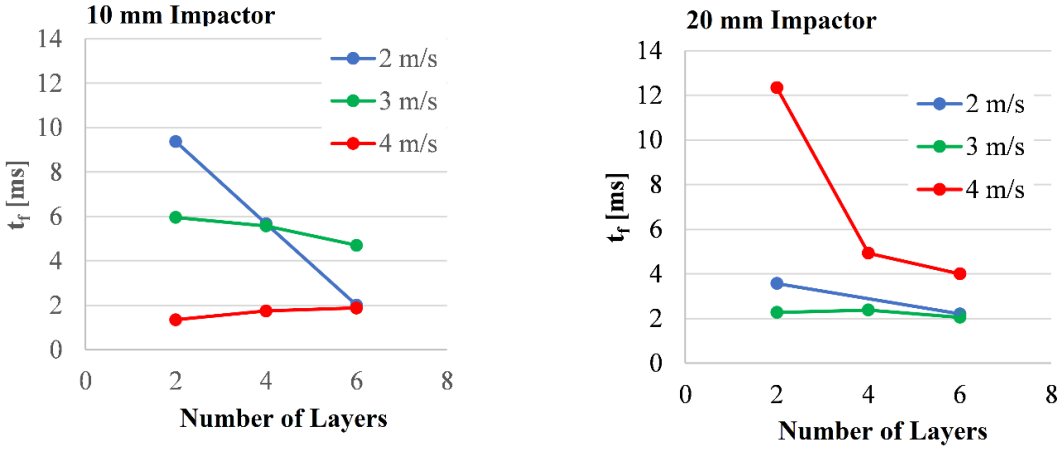

Fig. 5.20. Influence of the number of layers and impact velocity on the duration until the load cancellation moment (F=0), t_f

For the impact duration, considered between the two moments when F=0, noted by t_f, the following conclusions can be made (Fig. 5.20):

- for the Ø 10 mm impactor, for the lowest impact velocity, the duration, t_f, decreases a lot from the 2-layer panel to the 6-layer panel. This means that for multi-layer composites, the impact strength and energy absorption capacity are improved, leading to faster impact completion. The gradient of t_f is greater for the lowest velcity, v_1=2 m/s, but for the other impact velocities, the plot slope is low, decreasing for v_2=3 m/s and increasing for v_3= 4 m/s. This may be influenced by energy absorption and local plastic deformation processes in the composite,

- for the Ø 20 mm impactor, the trend is different. A decrease of t_f characterizes all tests between 2 m/s and 4 m/s, but the impact duration decreases rapidly between the 2-layer panel and 4-layer panel and very slow for the 6-layer panel. This may indicate a different behaviour of the composites under dynamic stresses, where the 4-layer panel may have an increased impact resistance as compared to the 2-layer panel. Once the panel reaches the 4-layer configuration, the impact duration changes when an additional layer is added, that is for the 6-layer panel. This may indicate that, in the case of the larger impactor, adding additional layers may have less influence on impact duration, as the 4-layer panel may already be sufficiently efficient in absorbing energy.

Chapter 6. Personal Contributions and Conclusions

6.1. The Significance of the Thesis

This thesis, titled "The Behaviour of Multiaxial Glass Fibre Fabric Composites under low Velocity Impact", holds long-term significance as technical systems have increased their performance parameters (load, velocity, temperature), consequently raising the risk of impacts involving processed components or elements from other systems.

The thesis objective has been successfully achieved, as the author designed, fabricated, tested, and analysed a class of panels based on glass fibre multiaxial fabrics that offer protection within the range of 1-4 m/s impact velocities and with impact energies up to 45 J.

Several organizations were involved in this research study:

• "Dunarea de Jos" University of Galati, through the laboratory housing the scanning electron microscope (SEM), and the University Library,

• Politehnica University of Bucharest,

• National Institute for Aerospace Research "Elie Carafoli" - INCAS Bucharest,

• INAS Craiova.

The professional experience and competencies of the involved personnel, coupled with available resources and facilities, were crucial elements that contributed to the expansion of individual knowledge and skills, surpassing the initial research boundaries and providing a comprehensive analysis of the addressed topic. This synergistic combination of expertise and resources played a pivotal role in the successful resolution of the proposed subject.

6.2. Final Conclusions on the Low Velocity Impact Resistance of the Panels Realized by the Author

In this study, the author used a 1200 g/m^2, quadriaxial glass fibre fabric with fibre orientations (0º/+45º/90º/-45º), known for its increased strength and intended mainly for ballistic applications. A two-component epoxy resin (Biresin CR82 with Biresin CH80-2 hardener) was used for curing and the process included a stabilising thermal treatment. This combination of materials and treatments contributes to panels with superior properties and potential for improved performance under impact stresses.

The technological process of manufacturing composite panels of different thicknesses involves a series of consecutive steps. These steps include: cutting the fabric (and weighing it in order to make the panel), preparing the mixture of resin and hardener, pressing the composite material, monitoring and controlling the thickness of the panel during pressing, performing a thermal treatment at 60°C for 6 hours, and finally a quality control (which consists of measuring the thickness and calculating the standard deviation for each set of panels).

Table 6.1 shows the damage occurring with the ∅ 10 mm impactor and the 20 mm impactor in preformed panels.

This analysis results in panels that are recommended for certain impact velocity values. Impact values for coloured cells are not recommended.

Table 6.1. Destruction occurring in preformed panels

Ø10 mm Impactor			
Number of layers of quadriaxial fabric	v_1=2 m/s	v_2=3 m/s	v_3=4 m/s
S2	PP	PP*	**TP**
S4	PP	PP*	PP*
S6	PP	PP	PP
Ø20 mm Impactor			
	v_1=2m/s	v_2=3m/s	v_3=4m/s
S2	PP	PP*	**TP**
S4	PP	PP	PP*
S6	PP	PP	PP

TP- total penetration, PP- partial penetration, PP*- partial penetration with extensive damages on the back, not recommended for practical applications

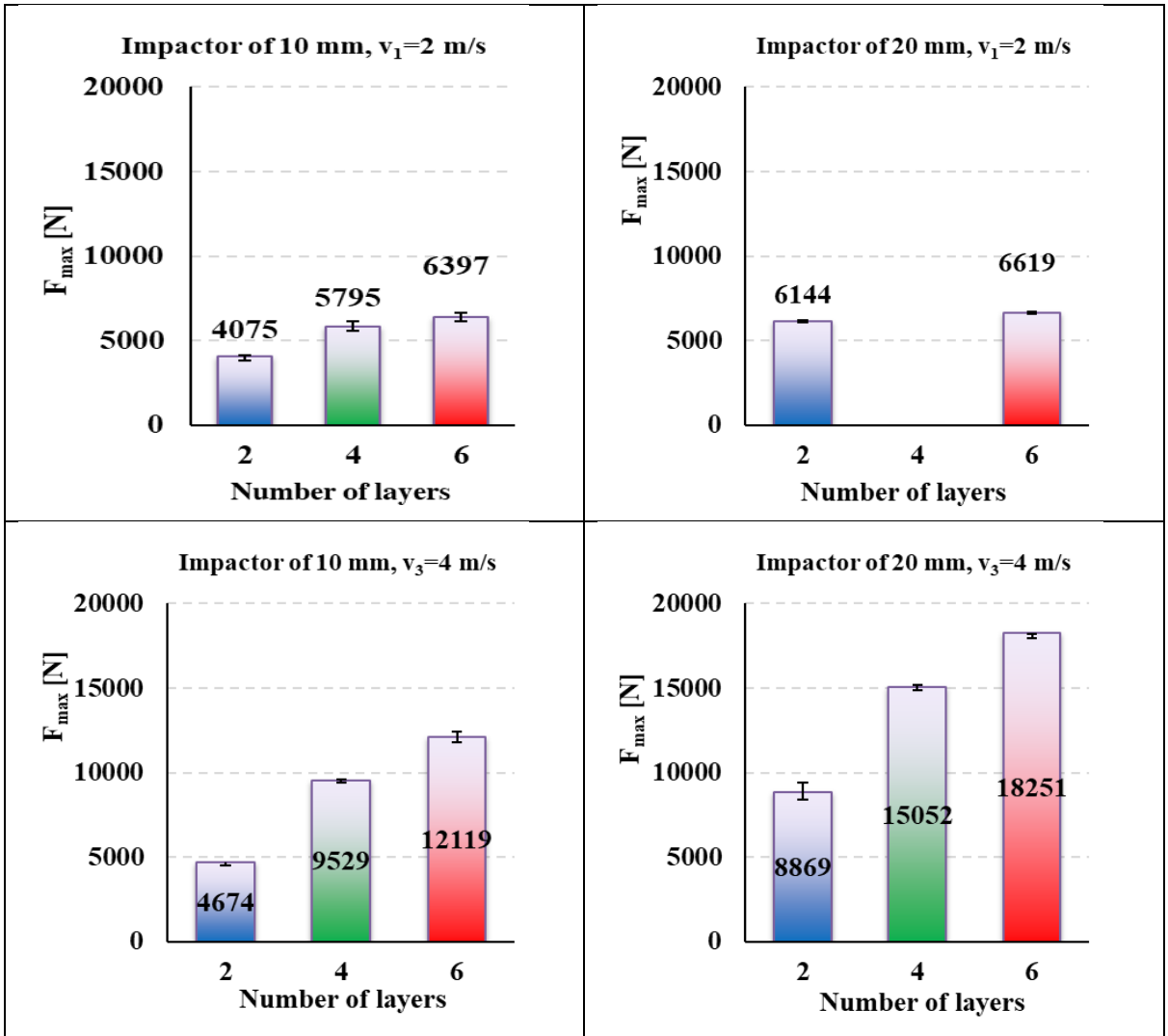

Fig. 6.1. The maximum force, recorded during impact, F_{max}, for the performed tests, as a function of impactor, number of quadriaxial fabric layers and impact velocity

Figure 6.1 illustrates the trend of maximum force, F_{max}, that increases with the increase in the number of layers, as well as with the increase in impact velocity. In the case of the 10 mm diameter impactor, this tendency is more pronounced when transitioning from the 2-layer panel to the 4-layer panel. While the maximum force still grows for the 6-layer panel, the dependency has a more parabolic shape. Furthermore, the increase in maximum force (F_{max}) has a trend that is more closely related to a linear interaction for v_3=4 m/s.

Figure 6.2 shows two macro photographs of composite panels, each with different penetration behaviour.

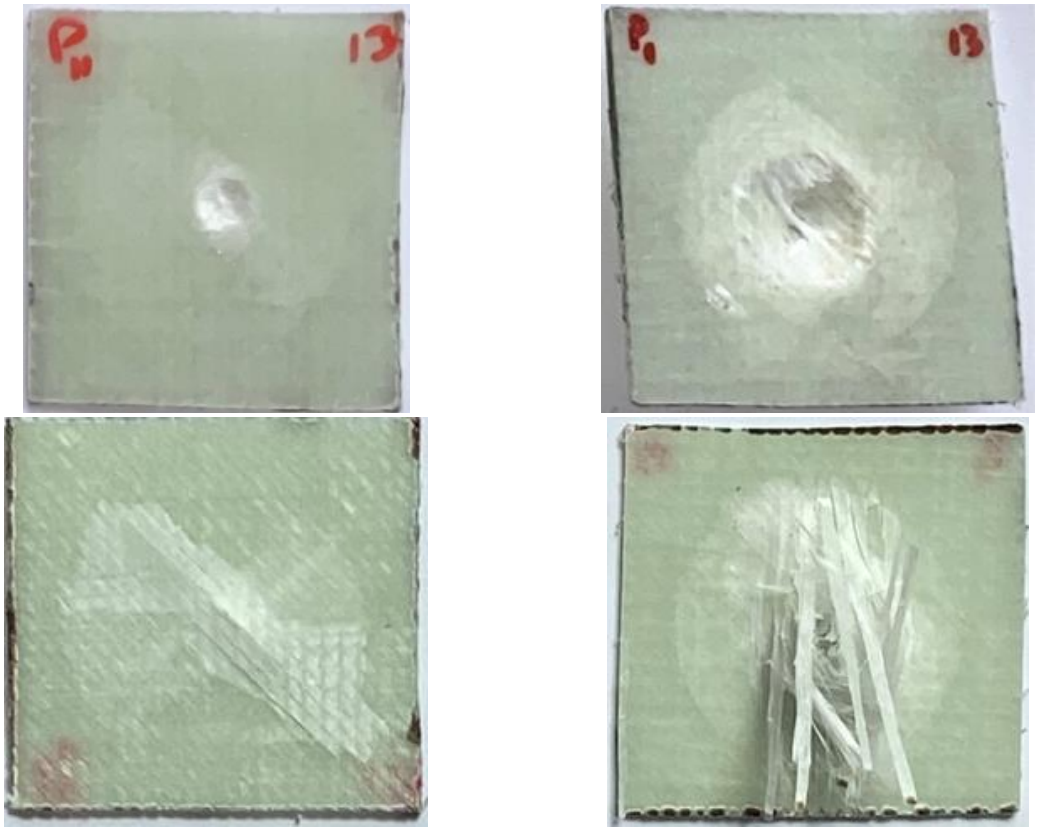

a) partial penetration panel (panel with 2 layers of quadriaxial fabric, 10 mm impactor, v_3=2 m/s)

b) total penetration panel (panel with 2 layers of quadriaxial fabric, 10 mm impactor, v_3=4 m/s)

Fig.6.2. Types of penetrations

Depending on the impact velocity and the diameter of the impactor, adding additional layers to the panels can improve their strength, but the impact may vary depending on the size of the impactor and its velocity.

The fact that the impact testing machine is instrumented with millisecond measuring devices and a precision force cell allowed for comparing parameters that have not been analysed in other works ($t_{(Fmax)}$), the time at which F_{max} occurs, time of completion of impact action, t_f, considered when F=0 again, velocity cancellation time, $t_{(v=0)}$, with the help of which a realistic interpretation of the impact process, in the studied velocity range, could be done and recommendations for the use of composite panels with impact properties could be formulated. The 4-layer panels and 6-layer panels performed well and can be recommended for the impact velocity range of 2-4 m/s.

6.3. Personal Contributions

This research study highlights the following original contributions in the field of material design and testing for low velocity impact through the synergistic approach between experiment and simulation:

• a critical selection was carried out, and an analysis of the existing documentation regarding materials, tests and fabric models, applicable to low-velocity impact, was conducted. This process involved organizing and categorizing the references systematically.

• the research topic, focusing on the use of glass fibre composites, was identified and justified,

• a numerical impact model using the finite element method and a bilinear hardening model for the yarn material, was developed at meso level (by considering the yarns in the fabric as isotropic bodies), which was used to evaluate the impact resistance of a class of composites, with different numbers of quadriaxial fabric layers. This model investigated the influence of impactor size, but may also be used to determine the influence of layer number, impact velocity and matrix quality. In order to validate the simulation results, laboratory tests were also carried out with specific validation criteria, such as the number of broken sublayers,

• the simulations focused on detailing the impact response of the 2-layer panels and were carried out at a speed of 4 m/s.

• panel designing so as to highlight factors influencing the impact process:

- thickness of the panels,
- impact velocity,
- impactor dimension (its diameter), the shape being kept as hemispherical,

• the focus has been on optimizing the composite panel manufacturing process to reduce resin losses and to ensure uniformity of characteristics. Research has focused on the identification and application of new techniques and methods to achieve higher quality of the composite panels.

Based on the experimental results, the author compared the response of the designed panels with other existing solutions reported in the literature. The quality of the manufactured panels was evaluated and reflected by the measured standard deviation for their thickness, which recorded a maximum value of 0.585 mm.

As there were limited time and resource constraints for this research, it was chosen to work on a family of samples with different numbers of layers of quadriaxial fabric (2 layers, 4 layers and 6 layers). This approach allowed for evaluating the quality of the panels in the context of low velocity impact, to analyse the uniformity of the response of panels of the same thickness and opened the possibility of further research on the potential use of this type of panels.

• analysis of panel failure mechanisms as a function of the number of layers, using advanced macrophotography and scanning electron microscopy (SEM). These methods of investigation allow researchers to observe and understand in depth how materials behave under dynamic loading and how failure mechanisms are produced during impact.

• critical analysis of the results and recommendations for the use of 4-layer and 6-layer panels for the tested impact parameters (impact velocity, impact energy, impactor dimension).

By integrating experiments and simulations, this research provides new insights into the materials design and testing to achieve improved low-velocity impact resistance.

For the range of studied parameters (impact velocity, impactor diameter and panel thickness), the author established dependencies between these parameters and the impact parameters, so that these dependencies are useful in the design of real systems (based on the author's proposed recipe for composites).

• dissemination of results was carried out through the publishing and presentation of articles containing experimental and simulation data, at national and international conferences: RoTrib19, the Leading International Conference on Tribology, 2019, Cluj-Napoca; UgalMat 2020, December 8-9, Galati; Doctoral Schools Conference at the "Dunarea de Jos" University of Galati, June 10-11, 2021, Galați; Innovative Manufacturing Engineering & Energy, IManEE2022, November 17-19, Iași; 9th International Conference on Materials Science and Technologies – RoMat 2022, Polytechnic University of Bucharest; Serbiatrib ’23, 18th International Conference on Tribology, Kragujevac, Serbia, May 17–19, 2023; TurkeyTrib 2023 (4rd International Conference on Tribology), May 25-27, 2023; The 29th edition of the International Scientific Conference "The Knowledge - Based Organization," KBO 2023, Sibiu.

6.4. Research Perspectives

Future research perspectives in the field of materials performance under impact and testing for low-velocity impact resistance may be very exciting and promising, given the original contributions of this study. Here are some possible research directions that could be explored further:

- designing and testing low-velocity impact behaviour of other types of composites, such as those with carbon or aramid fibres, to assess the differences in material properties on impact resistance,

- optimising structural configurations to provide the best low velocity impact resistance using simulation,

- in future studies, the impact of other loading parameters on material behaviour, such as impact angle, could be investigated,

- based on the results obtained in this research, it is possible to contribute to the development of tests and performance standards for composite materials used in applications exposed to low-velocity impact. These standards could ensure that materials are evaluated and certified according to specific requirements for their use in various fields,

- this research could evolve towards the practical application of composite materials with low-velocity impact resistance in various industries, such as the automotive sector, railway transportation, the maritime industry, protective equipment, and many others. These materials can contribute to enhancing the performance and safety of products and infrastructure.

This PhD thesis opens multiple directions of exploration and development in the field of materials design and testing for low-velocity impact resistance, providing a solid platform for future studies that can make significant contributions to the field of advanced materials and their practical applications.

List of published and presented works by Iulian Păduraru

Published scientific articles

1. **Păduraru, I.,** Săracu, G., Bogdan, M., Graur, I., Munteniţă, C., & Cîrciumaru, A. (2020). Effects of organic compounds and nickel nitrate on friction coefficient of thermosetting. In *IOP Conference Series: Materials Science and Engineering*, Vol. 724, No. 1, 012016). IOP Publishing. Prezentată la RoTrib'19, The Leading International Conference on Tribology, 2019, Cluj-Napoca, Romania, https://minas.utcluj.ro/assets/files/ROTRIB'19-Conference-Program-(updated-16-09-2019).pdf, doi:10.1088/1757-899X/724/1/012016, WOS:000619349400016
2. Iulia, P. G., Dragomir, C. M. B., & **Păduraru, I**. (2023). Importance of the basic reactions in the manufacture of synthetic resins. *Acta Technica Napocensis-Series: Applied Mathematics, Mechanics and Engineering*, *65*(4S), https://atna-mam.utcluj.ro/index.php/Acta/article/view/2043/1623, prezentată oral la Innovative Manufacturing Engineering & Energy, IManEE2022 17-19 Noiembrie, Iași, https://imane.ro/program/, WOS:000969679100024
3. **Păduraru, I.,** Bria, V., Cîrciumaru, A. (2021). Manufacturing Technology of Some Impact Resistant Materials. *The Annals of "Dunarea de Jos" University of Galati. Fascicle IX, Metallurgy and Materials Science*, *44*(1), 54-58. doi: https://doi.org/10.35219/mms.2021.1.08, prezentată și poster la UgalMat 2020, December 8-9, Galati, Romania, https://www.ugalmat.ugal.ro/images/2020/UGALMAT_2020_PROGRAMME_1.pdf
4. Apareci, T., Dănăilă, I., **Păduraru, I**., Cîrciumaru, A., Gorovei, M. C. (2022). Trends on Reinforced Polymer Composites–A Review. *The Annals of "Dunarea de Jos" University of Galati. Fascicle IX, Metallurgy and Materials Science*, *45*(4), 62-71. https://www.gup.ugal.ro/ugaljournals/index.php/mms/article/view/5821/5063
5. Drăghici, S. M., Dănăilă, I., Apareci, T., Săracu, G., **Păduraru, I**., Bria, V., & Gorovei, M. C. (2022). Modified Thermosets–A Review. *The Annals of "Dunarea de Jos" University of Galati. Fascicle IX, Metallurgy and Materials Science*, 45(4), 72-80.

   https://gup.ugal.ro/ugaljournals/index.php/mms/article/view/5822/5064
6. Dănăilă, I., Apareci, T., Drăghici, S. M., **Păduraru, I.,** Săracu, G., Cîrciumaru, A., & Gorovei, M. C. (2022). A Review on Modified Polymers and Their Composites. *The Annals of "Dunarea de Jos" University of Galati. Fascicle IX, Metallurgy and Materials Science*, 45(4), 114-125, https://www.gup.ugal.ro/ugaljournals/index.php/mms/article/view/5830/5071
7. **Păduraru, I.,** P. Graur, I., Deleanu, L., *Tribology of electric vehicles - a review*, SerbiaTrib '23, 18th International Conference on Tribology17–19 May 2023, Kragujevac, Serbia, Proceedings, ISBN: 978-86-6335-103-5, pp: 629-634, 2023.
8. **Păduraru, I.,** Ojoc, G. G., P.-Graur, I., Petrescu, H., & Deleanu, L. (2023). Analyzing Impact Behaviour of Glass Fiber Epoxy Composites for Higher Safety Systems. In *International Conference Knowledge-Based Organization*, 29(3), pp. 56-64, DOI: https://doi.org/10.2478/kbo-2023-0076

Papers presented at international scientific conferences

1. **Păduraru, I.,** Bria, V., Cîrciumaru, A., Development of Some Modern Composite Materials Used for Ballistic Protection, *Scientific Conference of Doctoral Schools „Perspectives and challenges in doctoral research"*, "Dunarea de Jos" University of Galati, Romania, 10th and 11th of June 2021. https://ro.scribd.com/document/523467062/Program-detaliat-al-conferintei-2021.
2. Săracu, G., **Păduraru, I.,** Drăghici, S.M., Cîrciumaru, *A.*, Electric Properties of Inorganic Agents Modified Epoxy Resin, *9 th International Conference on Materials Science and Technologies – RoMat 2022*, Universitatea Politehnica din București. https://romat2022.ro/wp-content/uploads/2022/11/RoMAT-2022_Conference-Program-Book-of-Abstracts_v3.pdf
3. Apareci (Gîrneț), T., Săracu, G., **Păduraru, I**., Dănăilă (Țîcău), I.. Cîrciumaru, *A.*, An Analysis of Mechanical Properties of Fabric Reinforced Materials with Stratified Polymer Matrix, *9 th International Conference on Materials Science and Technologies – RoMat 2022*, Universitatea Politehnica din București. https://romat2022.ro/wp-content/uploads/2022/11/RoMAT-2022_Conference-Program-Book-of-Abstracts_v3.pdf
4. Dănăilă (Țîcău), I., **Păduraru**, **I.,** Săracu, G., Apareci (Gîrneț), T., Drăghici, S.M., Cîrciumaru*, A., Thermoset Polymer Blends – A Mechanical Analysis, 9 th International Conference on Materials Science and Technologies – RoMat 2022*, Universitatea Politehnica din București https://romat2022.ro/wp-content/uploads/2022/11/RoMAT-2022_Conference-Program-Book-of-Abstracts_v3.pdf
5. **Păduraru, I.,** Graur P. I., Bălănică Dragomir, C. M., Applying Eco-Tribology Principles for Sustainable Management of Natural Resources and Ecosystem Services, *TurkeyTrib 2023 (4rd International Conference on Tribology)*, 25-27 May 2023, http://turkeytribconference.com/index.php/en/

Books

1. Graur, I., **Păduraru, I**., *Modelarea și simularae sistemelor de producție*, suport de curs, Editura Fundaţiei Universitare „Dunărea de Jos" Galaţi, 2023, ISBN 978-973-627-684-2.

2. Graur, I., **Păduraru, I.**, *Modelarea și simularae sistemelor de producție*, îndrumar de laborator, Editura Fundaţiei Universitare „Dunărea de Jos" Galaţi , 2023, ISBN 978-973-627-685-9.

3. Graur, I., **Păduraru, I.,** *Polymeric Composite Materials*, Ed. Lambert, ISBN 978-620-5-52898-3, 2023.

Courses completed during the PhD

1. English for scientific and engineering purposes
2. Scientific research ethics and academic integrity
3. Damage to mechanical systems. Experimental methods of investigation

Postgraduate training and professional development programmes

1. Bibliographic references management

2. Quality management in higher education

References

[1] Abrate, S. (2016). *Damage in laminates from low-velocity impacts*. In Dynamic Deformation, Damage and Fracture in Composite Materials and Structures, 35-69. Woodhead Publishing.

[2] Abtew, M. A., Boussu, F., Bruniaux, P., Loghin, C., Cristian, I. (2019). Ballistic impact mechanisms–a review on textiles and fibre-reinforced composites impact responses. *Composite structures*, **223**, https://doi.org/10.1016/j.compstruct.2019.110966

[3] Aktaş, M., Atas, C., İçten, B. M., Karakuzu, R. (2009). An experimental investigation of the impact response of composite laminates. *Composite Structures*, 87(4). https://doi.org/10.1016/j.compsturct.2008.02.003

[4] Andrianov, I. V., Awrejcewicz, J., Danishevskyy, V. V. (2018). *Asymptotical mechanics of composites*. Cham, Springer, Germany,

[5] Ansari, M. M., Chakrabarti, A., Iqbal, M. A. (2017). An experimental and finite element investigation of the ballistic performance of laminated GFRP composite target. *Composites Part B: Engineering*, 125, https://doi.org/10.1016/j.compositesb.2017.05.079

[6] Balasubramaniam, K., Ziaja, D., Jurek, M., Fiborek, P., Malinowski, P. (2021). Experimental and numerical analysis of multiple low-velocity impact damages in a glass fibered composite structure. *Materials*, 14(23), https://doi.org/10.3390/ma14237268

[7] Bejan, L. (2000). *Introducere în micromecanica materialelor compozite armate cu ţesături*. Editura Gh. Asachi.

[8] Bencomo-Cisneros, J. A., Tejeda-Ochoa, A., García-Estrada, J. A., Herrera-Ramírez, C. A., Hurtado-Macías, A., Martínez-Sánchez, R., Herrera-Ramírez, J. M. (2012). Characterization of Kevlar-29 fibers by tensile tests and nanoindentation. *Journal of Alloys and Compounds*, **536,** https://doi.org/10.1016/j.jallcom.2011.11.031

[9] Chib, A. (2006). *Parametric study of low velocity impact analysis on composite tubes* (Doctoral dissertation), Graduate School of Wichita State University, https://soar.wichita.edu/bitstream/handle/10057/267/t06004.pdf;sequence=3

[10] Chowdhury, U., Wu, X. F. (2021). Cohesive zone modeling of the elastoplastic and failure behavior of polymer nanoclay composites. Journal of Composites Science, 5(5), 131. https://doi.org/10.3390/jcs5050131

[11] Cormos, R., Petrescu, H., Hadar, A., Adir, G. M., Gheorghiu, H. (2017), Finite Element Analysis of the Multilayered Honeycomb Composite Material Subjected to Impact Loading, *Materiale plastice*, 54(1), 180-185

[12] Courant, R., Hilbert, D. (2008). *Methods of mathematical physics: partial differential equations*. John Wiley & Sons.

[13] Dogan, U., Sunbuloglu, E. (2023). A novel simplified ballistic impact theory for woven composites. *International Journal of Impact Engineering*, 177, 104530. https://doi.org/10.1016/j.ijimpeng.2023.104530

[14] Endruweit, A., Zeng, X., Matveev, M., Long, A. C. (2018). Effect of yarn cross-sectional shape on resin flow through inter-yarn gaps in textile reinforcements. *Composites Part A: Applied Science and Manufacturing*, *104*, 139-150. https://doi.org/10.1016/j.compositesa.2017.10.020

[15] Ess, J. W., Hornsby, P. R. (1986). Characterisation of distributive mixing in thermoplastics compositions. *Polymer testing*, 6(3), 205-218https://doi.org/10.1016/0142-9418(86)90063-2

[16] Gao, J., Kedir, N., Hernandez, J. A., Gao, J., Horn, T., Kim, G., Chen, W. (2022). Dynamic fracture of glass fiber-reinforced ductile polymer matrix composites and loading rate effect. *Composites Part B: Engineering*, 235, 109754. https://doi.org/10.1016/j.compositesb.2022.109754

[17] Guedes, R. M. (Ed.). (2019). Creep and fatigue in polymer matrix composites. Woodhead publishing. https://doi.org/10.1016/B978-0-08-102601-4.00009-6

[18] Hadăr, A., Baciu, F., Voicu, A.D., Vlasceanu, D., Tudose, D.I., Adetu, C. (2022) Mechanical Characteristics Evaluation of a Single Ply and Multi-Ply Carbon Fiber-Reinforced Plastic Subjected to Tensile and Bending Loads, *Polymers*, 14(15), DOI 10.3390/polym14153213

[19] Harper, P. W., Sun, L., Hallett, S. R. (2012). A study on the influence of cohesive zone interface element strength parameters on mixed mode behaviour. *Composites Part A: Applied Science and Manufacturing*, 43(4), 722-734. https://doi.org/10.1016/j.compositesa.2011.12.016

[20] Hasan, K. F., Al Hasan, K. N., Ahmed, T., György, S. T., Pervez, M. N., Bejó, L., Alpár, T. (2023). Sustainable bamboo fiber reinforced polymeric composites for structural applications: A mini review of recent advances and future prospects. *Case Studies in Chemical and Environmental Engineering*, 100362. https://doi.org/10.1016/j.cscee.2023.100362

[21] Hosseini, A., Raji, A. (2023). Improved double impact and flexural performance of hybridized glass basalt fiber reinforced composite with graphene nanofiller for lighter aerostructures. *Polymer Testing*, 108107. https://doi.org/10.1016/j.polymertesting.2023.108107

[22] Huang, Z. C., Li, H. Z., Jiang, Y. Q. (2023). Low-velocity impact response of self-piercing riveted carbon fiber reinforced polymer-AA6061T651 hybrid joints. *Composite Structures*, 315, 116983. https://doi.org/10.1016/j.compstruct.2023.116983

[23] Jiang, T. (2006). Impact and penetration studies: Simplified models and materials design from ab initio methods. Georgia Institute of Technology. https://www.proquest.com/openview/68d196bcf906459f723c682505553ea3/1?pq-origsite=gscholar&cbl=18750&diss=y

[24] Khan, Z., Naik, M. K., Al-Sulaiman, F., Merah, N. (2016). Low velocity impact of filament-wound glass-fiber reinforced composite pipes. Journal of Material Sciences and Engineering, 5(253), 2169-0022. doi:10.4172/2169-0022.1000253

[25] Kim J.-K., Mai Y.-W. (1998) Engineered Interfaces in Fiber Reinforced Composites, Elsevier Science Ltd, Oxford U.K.

[26] Kim, E. H., Rim, M. S., Lee, I., Hwang, T. K. (2013). Composite damage model based on continuum damage mechanics and low velocity impact analysis of composite plates. *Composite Structures*, 95, 123-134. https://doi.org/10.1016/j.compstruct.2012.07.002

[27] Lei, Z. X., Ma, J., Sun, W. K., Yin, B. B., Liew, K. M. (2023). Low-velocity impact and compression-after-impact behaviors of twill woven carbon fiber/glass fiber hybrid composite laminates with flame retardant epoxy resin. *Composite Structures*, 117253. https://doi.org/10.1016/j.compstruct.2023.117253

[28] Li, S., Thouless, M. D., Waas, A. M., Schroeder, J. A., Zavattieri, P. D. (2005). Use of a cohesive-zone model to analyze the fracture of a fiber-reinforced polymer–matrix composite. Composites Science and Technology, 65(3-4), 537-549. https://doi.org/10.1016/j.compscitech.2004.08.004

[29] Liu, D. (1988). Impact-induced delamination—a view of bending stiffness mismatching. *Journal of Composite Materials*, 22(**7),** 674-692. https://doi.org/10.1177/002199838802200706

[30] Lu, X., Bardet, J. P., Huang, M. (2012). Spectral analysis of nonlocal regularization in two-dimensional finite element models. *International Journal for Numerical and Analytical Methods in Geomechanics*, 36(2), 219-235, https://doi.org/10.1002/nag.1006

[31] Ma, D., dos Santos Cougo, C. M., Amico, S. C., Giglio, M., Manes, A. (2023). A novel numerical method for stochastic study of fiber-reinforced composites with nanoparticles under impact loading. *International Journal of Impact Engineering*, 104662. https://doi.org/10.1016/j.ijimpeng.2023.104662

[32] Mars, J., Chebbi, E., Wali, M., Dammak, F. (2018). Numerical and experimental investigations of low velocity impact on glass fiber-reinforced polyamide. *Composites Part B: Engineering*, 146, 116-123. https://doi.org/10.1016/j.compositesb.2018.04.012

[33] Mathivanan, N. R., Jerald, J. (2010). Experimental investigation of low-velocity impact characteristics of woven glass fiber epoxy matrix composite laminates of EP3 grade. *Materials & Design*, 31(9), 4553-4560. https://doi.org/10.1016/j.matdes.2010.03.051

[34] Múgica, J. I., Aretxabaleta, L., Ulacia, I., Aurrekoetxea, J. (2016). Rate-dependent phenomenological model for self-reinforced polymers. *Composites Part A: Applied Science and Manufacturing*, 84, 96-102. https://doi.org/10.1016/j.compositesa.2016.01.002

[35] Naresh, K., Shankar, K., Rao, B. S., Velmurugan, R. (2016). Effect of high strain rate on glass/carbon/hybrid fiber reinforced epoxy laminated composites. *Composites Part B: Engineering*, 100, 125-135. https://doi.org/10.1016/j.compositesb.2016.06.007

[36] Năstăsescu, V. (2004). *Finite element method* (in Romanian). Military Technical Academy Publishing, Bucharest.

[37] Ojoc, G. G. (2022). Un studiu teoretic și experimental al pachetelor de protecție balistică pentru blindaje pe bază de fibre de sticlă (A Theoretical and Experimental Study of Ballistic Protection Packages Made of Glass Fibers) (Doctoral dissertation, Universitatea „Dunărea de Jos" din Galați).

[38] Patil, S., Reddy, D. M., Reddy, M. (2018, April). Low velocity impact analysis on composite structures–A review. *In AIP conference proceedings* 1943 (1), 020009. AIP Publishing LLC. https://doi.org/10.1063/1.5029585

[39] Păduraru, I., Ojoc, G. G., P.-Graur, I., Petrescu, H., Deleanu, L. (2023). Analyzing Impact Behaviour of Glass Fiber Epoxy Composites for Higher Safety Systems. *International Conference Knowledge-Based Organization*, 29 (3), 56-64. https://doi.org/10.2478/kbo-2023-0076

[40] Radeş, M. (2007). *Rezistența materialelor*. Printech.

[41] Rajan, B. G., Padmanabhan, S., Ganesh, R. L., Chandana, K. M., Lavanya, E. (2021). Low velocity impact analysis of carbon/glass/epoxy hybrid composite pipes. *Materials Today: Proceedings*, 47, 4181-4188. https://doi.org/10.1016/j.matpr.2021.04.454

[42] Ratna, D., Chongdar, T. K., Chakraborty, B. C. (2004). Mechanical characterization of new glass fiber reinforced epoxy composites. *Polymer composites*, 25(2), 165-171. https://doi.org/10.1002/pc.20013

[43] Reddy, T. S., Mogulanna, K., Reddy, K. G., Reddy, P. R. S., Madhu, V. (2019). Effect of thickness on behaviour of E-glass/epoxy composite laminates under low velocity impact. *Procedia Structural Integrity*, 14, 265-272. https://doi.org/10.1016/j.prostr.2019.05.034

[44] Sadighi, M., Alderliesten, R. C., Benedictus, R. (2012). Impact resistance of fiber-metal laminates: A review. *International Journal of Impact Engineering*, 49, 77-90. https://doi.org/10.1016/j.ijimpeng.2012.05.006

[45] Seydibeyoglu M. O., Mohanty A. K., Misra M. (editori), (2017) *Fiber Technology for Fiber-Reinforced Composites*, Elsevier Ltd

[46] Titire, L. C., Musteata, A. E., Ceoromila, A., Cristea, G. C., Ojoc, G. G., Deleanu, L. (2021). Characterization of Blend PA6+ EPDM (60/40) by Tensile Tests. *Materiale Plastice*, 58(3), 51-63. https://doi.org/10.37358/MP.21.3.5503

[47] Titire, L. C., Rusu, V. T., Sandu, S. (2022, October). Influence of material characteristics on impact response for fabrics made of glass and aramid fibers. *IOP Conference Series: Materials Science and Engineering*, 1262 (1), 012045. IOP Publishing. DOI 10.1088/1757-899X/1262/1/012045

[48] Wang, Z. W., Zhao, J. P., Wang, S. (2019). Low velocity impact responses of glare hybrid laminates based on simplified finite element model. *Key Engineering Materials*, 795, 109-115. https://www.scientific.net/KEM.795.109

[49] Xiao, H., Liu, T., Li, T., Duan, Y. (2023). Design of damage-resistant hybrid lay-up structures for fiber-reinforced composites based on interface properties. Composite Structures, 117210. https://doi.org/10.1016/j.compstruct.2023.117210

[50] *** ANSYS Explicit Dynamics Analysis Guide (2021). ANSYS, Inc., USA

[51] *** 1200 g/m^2 Quadriaxial Stitched Glass Fabric (0º/+45º/90º/-45º), 127 cm wide (accesat 12.01.2022). https://www.castrocompositesshop.com/en/fibre-reinforcements/1204-1200-gm2-quadriaxial-stitched-glass-fabric-0%C2%BA45%C2%BA90%C2%BA-45%C2%BA-127-cm-wide.html

[52] *** Biresin® CR82. Composite Resin System, (accesat 4.10.2020). https://industry.sika.com/dms/getdocument.get/93a3a9b1-7291-47ce-8ca7-18ae3f458043/Biresin-CR82-New.pdf

[53] *** Sika Group. About us (accesat 3.10.2021), https://www.sika.com/en/home.html

[54] *** Uses of Fiberglass [Accessed: 2022-02-22]. 2017. Available from: https://www.thoughtco.com/uses-offiberglass-820412

[55] *** High Strength Glass Fibers (accesat 12.03.2022). https://www.agy.com/wp-content/uploads/2022/03/AGY_HighStBro_HR.pdf., AGY [Internet]. (2017). http://www.agy.com/wp-content/uploads/2014/03/High_Strength_Glass_Fibers-Technical.pdf.

[56] *** Technical Design Guide for FRP Composite Products and Parts [Internet]. (2022). [accessat: 20.03.2022]. https://www.moldedfiberglass.com/?s=Technical+design+guide+for+FRP+Composite+products+and+Parts

[57] *** Handbook INSTRON CEAST 9340, https://www.instron.us/-/media/literature-library/products/2010/02/ceast-9300-series.pdf?la=en-US